[redacted]

NATIONAL ADVISORY COMMITTEE FOR AERONAUTICS

TECHNICAL NOTE

No. 929

ANALYSIS OF CIRCULAR SHELL-SUPPORTED FRAMES

By J. E. Wignot, Henry Combs, and A. F. Ensrud
Lockheed Aircraft Corporation

Washington
May 1944

NATIONAL ADVISORY COMMITTEE FOR AERONAUTICS

TECHNICAL NOTE NO. 929

ANALYSIS OF CIRCULAR SHELL-SUPPORTED FRAMES

By J. E. Wignot, Henry Combs, and A. F. Ensrud

SUMMARY

In the past it has been customary to analyze shell-supported frames on the basis of the assumption that frame bending distortion does not affect the character of the shear resistance in the skin. This assumption has been found to be considerably in error for a majority of practical cases.

In order to obtain results more nearly representing the actual case, it is essential that the deformation of the frame and the deformation of the shell be consistent with each other. While this principle of "consistent deformations" is already well known and appreciated, its application to fuselage frame analysis and similar problems has not been extensively developed.

This paper deals with the single problem of circular shell-supported frames subjected to concentrated loadings. A mathematical attack is developed and presented in the form of nondimensional-coefficient curves. These curves, while they are developed for circular frames only, may, by means of approximations, be used for nearly any practical frame which has curvature in the region of applied loading.

INTRODUCTION

When shell-supported rings are externally loaded, the applied loading is resisted primarily by a system of shearing forces within the shell.

The VQ/I and T/2A shear-flow distribution, which has been used frequently in past analyses, is consistent with the assumption that the ring being loaded is rigid. For small-diameter shells with sturdy rings, this distribution has proved reasonably satisfactory for design

purposes. However, as the size of airplanes increases, the rings become relatively more flexible so that the assumption of infinite ring stiffness may sometimes introduce errors of several hundred percent in ring design. Therefore, the necessity for a more accurate analysis becomes apparent. Such an analysis must consider the finite stiffness of the ring.

Because of the added complexity involved in evaluating the effect of finite ring stiffness, it is desirable to present the results in the form of coefficient curves calculated for typical cases. Then the bending moment, axial load and transverse shear in a ring, and the corresponding shear flow acting on the ring from the supporting shell may be readily obtained from these curves by proper interpolation and superposition.

This report is but the start of the contemplated ring study and covers only the case of a complete circular frame subjected to a system of coplanar loadings. The method will, in later reports, be extended to more general applications which include the following problems:

(1) Analysis of wing-fuselage intersection including design data for the main frames, deflection of the main frames, skin shear flows, and modification of axial stresses (in the vicinity of the main frames) as a result of ring flexibility

(2) Analysis of fuselage cut-outs including design data and deflections for the end frames, skin shear flows, and stringer axial stress modification

(3) Mutual influence of adjacent frames

(4) Analysis of rings involving floor support problems

(5) Analysis of rings indirectly attached to skin

SYMBOLS

a internal axial load acting on ring cross section, pounds

C_n arbitrary constant of integration

C_{mm}, C_{mr}, C_{mt}
C_{sm}, C_{sr}, C_{st}
C_{am}, C_{ar}, C_{at}
C_{qm}, C_{qr}, C_{qt} — final internal load coefficients, where first subscript designates type of internal load or shear flow (m for moment, s for shear, a for axial load, and q for shear flow) second subscript designates type of external applied loading (m for moment, r for radial load, t for tangential load)

d relative-stiffness parameter $\left(\frac{KR^3}{EI}\right.$; approximately equal to $\left.\frac{tR^3}{\mu I}\right)$

dF element of skin shear force

Δx, Δy, $\Delta\phi'$ horizontal, vertical, and angular displacements, respectively, for entire ring (without distortion)

ΔT, ΔR, $\Delta\phi$ final deflection components of any point on distorted ring, tangential, radial, and rotational, respectively

δx, δy, $\delta\phi$ final relative displacements between faces of "cut"

E Young's modulus of elasticity for ring, pounds per square inch

G modulus of shear rigidity of skin, pounds per square inch

H_A internal continuity axial force at cut, pounds

I moment of inertia of ring cross section, inches^4

K skin resisting force per unit tangential deflection, pounds per inch

L distance along shell to a section which is not distorted from a circle

K_{mn}, K_{mn}'	final moment constants	n designates position of term in general expression. prime designates antisymmetry
K_{qn}, K_{qn}'	final shear-flow constants	
K_{sn}, K_{sn}'	final shear constants	
K_{an}, K_{an}'	final axial-load constants	

m internal bending moment acting on ring, inch-pounds

M applied moment acting in plane of frame, inch-pounds

M_A internal continuity moment at cut, inch-pounds

P_r applied radial load acting in plane of frame, pounds

P_t applied tangential load acting in plane of frame, pounds

P_A internal continuity shearing force at cut, pounds

q_i	induced shear flow	expressed in pounds per radian (q as used in final curves is divided by radius to give lb/in.)
q_o	conventional shear flow	
q	resultant shear flow	

R radius of ring, inches

S transverse "beam shear" in fuselage

s internal shearing load acting on ring cross section, pounds

t_e average effective skin thickness supporting ring $\left[0.5\left(t_F + t_A\right)\right]$

t_F effective skin thickness forward of frame

t_A effective skin thickness aft of frame

μ ratio of E of frame to G of skin

ϵ_F relative "shape" stiffness of shell forward of ring

ϵ_A relative "shape" stiffness of shell aft of ring

β, γ damping parameters

σ frequency parameter

$\alpha = \beta^2 + \sigma^2 + 1$

ψ variable angle while θ remains constant

θ angular displacement from cut (may be used alone or as subscript)

$\pm\Phi$ integration limits ($\pm\pi$ for complete circle)

DISCREPANCIES BETWEEN THEORY AND TESTS

A few ring tests on the Constellation fuselage test section have been conducted by Lockheed Aircraft Corporation. Observations based on these tests (unpublished) include the following:

(1) The maximum moments, actually measured, ranged from 5 percent to 50 percent of values obtained by assuming infinite ring stiffness.

(2) The moment pattern for each test indicated that the load affected the ring only locally instead of entirely around the fuselage.

(3) For radial loading the maximum axial load was at the location of the radial load instead of 45° away, as indicated by assuming a very stiff ring. The maximum axial load, as measured, exceeded the calculated values by approximately four times.

(4) For tangential loading the axial-load curve reaches the same maximum as the calculated curve but dies away more rapidly.

The Boeing Aircraft Company has also made some ring tests on the XB-29 fuselage test section. Two equal vertical loads were applied, each at 32½° from top center. The ring stresses, as measured, corresponded in nature to the Constellation ring tests. The following comparison with conventional analysis was taken directly from the Boeing report (unpublished):

> It may be seen that the maximum measured stress . . . is only 20.3 percent of the corresponding theoretical stress, with even greater variation at other points on the frame. Hence this method of analysis is an extremely conservative one.

As a result of these tests, it is evident that the assumption of infinite ring stiffness leads to excessive conservatism for any airplane with rings that are similar to those of the Lockheed Constellation or Boeing XB-29.

GENERAL DEVELOPMENT

Preliminary Discussion

In the general ring analyses that have been developed (reference 1), it has been customary to assume that the resisting skin shear flow follows simple VQ/I and T/2A distribution. As long as the ring remains perfectly rigid, this assumption is reasonably close to the actual conditions. However, in the case of rings of large diameter used in aircraft structures, the assumption of perfect rigidity is often far from the truth.

In the actual case, the ring will always experience some distortion as a consequence of being loaded. This distortion will induce shearing forces in the skin which tend to oppose the ring deflections and, therefore, effectively change the manner in which the applied forces are resisted by the skin. Figure 1 shows the deflected positions of a rigid ring and a flexible ring. Note that the difference in tangential deflection in the two cases would induce additional forces in the skin which oppose the deflections of the flexible ring. A very light ring would tend to deflect until the external moments causing the deflections were neutralized by the sum of the resisting moments in the ring and the resisting moments due to the deflection-induced skin shear flow. Now, if the resistance of the skin to deflection is increased, say by doubling the skin thickness, and the ring is loaded as before, then the skin will resist the deflections of the ring more strongly and will provide a greater proportion of the resisting moment than before.

However, since it is chiefly the moment in the ring that determines the deflection of the ring, the distribution

of the shear flow in the skin has been altered by changing the relative stiffness of the skin and ring. It is then apparent that, in the actual case, the distribution of the skin shear flow depends upon the relative stiffnesses of the skin and ring. It is now possible to consider the skin shear flow as consisting of two parts: the VQ/I and $T/2A$ distribution upon which is superimposed the induced shear flow.

The VQ/I and $T/2A$ distribution may be realized by assuming the shear flow to be proportional to the tangential deflection of the skin with respect to a reference ring which is assumed to be rigidly fixed in space. If a horizontal and vertical force and a moment are applied to the ring, they will produce a horizontal displacement Δx, a vertical displacement Δy, and a rotation $\Delta\phi'$, respectively, of the ring as a unit. The shear flow at any point is then given by

$$q_o = K(\Delta x \cos \theta + \Delta y \sin \theta + \Delta\phi')$$

where K is the ratio of tangential shear force per radian to tangential deflection.

The induced shear flow is proportional to the relative tangential deflection of a point due to the bending moment in the ring.

$$q_i = K \Delta T_m$$

The resultant shear flow acting on the ring is then given by

$$\begin{aligned} q &= \frac{dF}{d\theta} \\ &= q_o + q_i \\ &= K(\Delta x \cos \theta + \Delta y \sin \theta + \Delta\phi' + \Delta T_m) \end{aligned} \qquad (1)$$

The moments produced in the ring by this load system may now be determined.

Development of General Differential Equation

Figure 2 shows a portion of a fuselage ring that has been cut at point A and the forces required to produce continuity have been applied at the cut. An element of skin shear force acting on the ring is represented by dF. The bending moment at any point θ in the ring will then be given by

$$m = M_A + H_A R(1 - \cos\theta) - P_A R \sin\theta - R\int_0^\theta \left[1 - \cos(\theta - \psi)\right] dF \qquad (2)$$

Expanding $\cos(\theta - \psi)$ and differentiating m with respect to θ yields

$$\frac{dm}{d\theta} = H_A R \sin\theta - P_A R \cos\theta + R\frac{dF}{d\theta}(\cos^2\theta + \sin^2\theta) - R\frac{dF}{d\theta} - R\sin\theta\int_0^\theta \cos\psi\, dF + R\cos\theta\int_0^\theta \sin\psi\, dF \qquad (3)$$

Differentiating again with respect to θ yields

$$\frac{d^2m}{d\theta^2} = H_A R\cos\theta + P_A R\sin\theta - R\cos\theta\int_0^\theta \cos\psi\, dF - R\sin\theta\int_0^\theta \sin\psi\, dF \qquad (4)$$

The third derivative yields

$$\frac{d^3m}{d\theta^3} = -H_A R\sin\theta + P_A R\cos\theta - R(\cos^2\theta + \sin^2\theta)\frac{dF}{d\theta} + R\sin\theta\int_0^\theta \cos\psi\, dF - R\cos\theta\int_0^\theta \sin\psi\, dF$$

If the similarity between alternate derivatives is noted, it may be seen that adding the first and third derivatives yields

$$\frac{dm}{d\theta} + \frac{d^3m}{d\theta^3} = -R\frac{dF}{d\theta} \tag{5}$$

Since m is the moment at any point in the ring, the tangential deflection at D (fig. 2) due to a moment at C acting over an elementary length of the ring $R\,d\theta$ will be given by

$$d(\Delta T) = \frac{-mR\,d\theta\,b}{EI} \tag{6}$$

From figure 2 it is evident that

$$b = R[1 - \cos(\theta - \psi)]$$

By substituting for b and integrating, equation (6) becomes

$$\Delta T = -\frac{R^2}{EI}\int_0^\theta m[1 - \cos(\theta - \psi)]d\theta$$

Substituting for ΔT in equation (1) yields

$$\frac{dF}{d\theta} = K\,\Delta\Phi' + K\,\Delta y \sin\theta + K\,\Delta x\cos\theta - \frac{KR^2}{EI}\int_0^\theta m[1 - \cos(\theta - \psi)]d\theta \tag{7}$$

Noting the similarity between equations (2) and (7), it is evident by comparison that

$$\frac{d^2F}{d\theta^2} + \frac{d^4F}{d\theta^4} = -\frac{KR^2}{EI}m \tag{8}$$

$$\frac{dq}{d\theta} + \frac{d^3q}{d\theta^3} = -\frac{KR^2}{EI}m \tag{9}$$

Adding the first and third derivatives of equation (5) gives

$$\frac{d^6m}{d\theta^6} + 2\frac{d^4m}{d\theta^4} + \frac{d^2m}{d\theta^2} = -R\left(\frac{d^2F}{d\theta^2} + \frac{d^4F}{d\theta^4}\right) \tag{10}$$

Substituting equation (8) in equation (10) gives

$$\frac{d^6m}{d\theta^6} + 2\frac{d^4m}{d\theta^4} + \frac{d^2m}{d\theta^2} - \frac{KR^3}{EI}m = 0 \tag{11}$$

Equation (11) is the differential equation defining the moment distribution in a skin-supported ring subjected to any loading. It is interesting to note that the distribution depends only upon the value of KR^3/EI, hereinafter called the "relative-stiffness parameter d," because K is a factor denoting the stiffness of the skin and EI/R^3 is a factor denoting the stiffness of the ring.

The general solution (see appendix) of equation (11) yields

$$m = C_1e^{\gamma\theta} + C_2e^{-\gamma\theta} + C_3e^{\beta\theta}\cos\sigma\theta + C_4e^{-\beta\theta}\cos\sigma\theta$$

$$+ C_5e^{\beta\theta}\sin\sigma\theta + C_6e^{-\beta\theta}\sin\sigma\theta \tag{12}$$

where the values of γ, β, and σ are as plotted in figure 3 for different values of KR^3/EI. Inasmuch as there are six independent constants in equation (12), six independent conditional equations are needed for a complete solution. These are the three equations of equilibrium and the three equations of continuity.

Considering only symmetrical or antisymmetrical loadings reduces the number of independent constants to three, and the general solution reduces to

$$m = K_{m_1} \cosh \gamma\theta + K_{m_2} \cosh \beta\theta \cos \sigma\theta + K_{m_3} \sinh \beta\theta \sin \sigma\theta \tag{13}$$

for symmetrical loading and to

$$m' = K_{m_1}' \sinh \gamma\theta + K_{m_2}' \sinh \beta\theta \cos \sigma\theta + K_{m_3}' \cosh \beta\theta \sin \sigma\theta \tag{14}$$

for antisymmetrical loading.

The expressions for the shearing force, axial force, and skin shear flow at any point θ may be shown to be given by (see appendix)

$$s = \frac{1}{R} \frac{dm}{d\theta} \tag{15}$$

$$a = -\frac{1}{R} \frac{d^2m}{d\theta^2} \tag{16}$$

$$q = -\frac{1}{R} \left(\frac{dm}{d\theta} + \frac{d^3m}{d\theta^3} \right) \tag{17}$$

where m is given by equation (13) or (14).

The components of absolute deflection (that is, with respect to "fixed structure") may be shown to be given by (see appendix)

$$\Delta T = -\frac{1}{RK} \left(\frac{dm}{d\theta} + \frac{d^3m}{d\theta^3} \right) \tag{18}$$

$$\Delta R = \frac{1}{RK} \left(\frac{d^2m}{d\theta^2} + \frac{d^4m}{d\theta^4} \right) \tag{19}$$

$$\Delta\phi = \frac{1}{R^2K} \left(\frac{dm}{d\theta} + 2\frac{d^3m}{d\theta^3} + \frac{d^5m}{d\theta^5} \right) \tag{20}$$

Examination of equations (13) and (14) and their derivatives reveals that the derivatives of m are alternately symmetric and antisymmetric and the alternate derivatives differ only in the numerical value of the three coefficients. Inasmuch as all the preceding quantities are proportional to derivatives of m or sums of even or odd derivatives of m, they will also differ from the similar quantities only in the numerical value of the three coefficients. Therefore, the interrelation between these coefficients may be conveniently shown in tabular form. (See table I.)

The six conditional equations may be represented as

$$\sum V = 0 \tag{21a}$$

$$\sum \Delta\Phi = 0 \tag{21b}$$

$$\sum \Delta x = 0 \tag{21c}$$

$$\sum H = 0 \tag{21d}$$

$$\sum M = 0 \tag{21e}$$

$$\sum \Delta y = 0 \tag{21f}$$

The first three conditions are automatically satisfied by conditions of antisymmetrical loading and the last three are satisfied for symmetrical loading. Therefore, for symmetrical loading, equations (21a) to (21c) become

$$\int_{-\Phi}^{\Phi} q \sin\theta \, d\theta = P_r \tag{22a}$$

$$\int_{-\Phi}^{\Phi} \frac{mR}{EI} d\theta = \delta\Phi \tag{22b}$$

$$\int_{-\Phi}^{\Phi} \frac{mR^2}{EI}(\cos\theta - \cos\Phi) \, d\theta = \delta x \tag{22c}$$

where

$$q = K_{q_1} \sinh \gamma\theta + K_{q_2} \sinh \beta\theta \cos \sigma\theta + K_{q_3} \cosh \beta\theta \sin \sigma\theta$$

$$m = K_{m_1} \cosh \gamma\theta + K_{m_2} \cosh \beta\theta \cos \sigma\theta + K_{m_3} \sinh \beta\theta \sin \sigma\theta$$

For antisymmetrical loading, equations (21d) to (21f) become

$$\int_{-\Phi}^{\Phi} q \cos \theta \, d\theta = P_t \qquad (22d)$$

$$\int_{-\Phi}^{\Phi} q(1 - \cos \Phi \cos \theta)R \, d\theta = M \qquad (22e)$$

$$\int_{-\Phi}^{\Phi} \frac{MR^2}{EI} \sin \theta \, d\theta = \delta y \qquad (22f)$$

where

$$q = K_{q_1}' \cosh \gamma\theta + K_{q_2}' \cosh \beta\theta \cos \sigma\theta + K_{q_3}' \sinh \gamma\theta \sin \sigma\theta$$

$$m = K_{m_1}' \sinh \gamma\theta + K_{m_2}' \sinh \beta\theta \cos \sigma\theta + K_{m_3}' \cosh \beta\theta \sin \sigma\theta$$

All integrals to be evaluated for equation (22) come under one of the seven general types given in general form in the appendix. The numerical evaluation of these integrals is accomplished on computation form 3. (See appendix.)

The coefficients, evaluated in accordance with computation form 5, are used as shown in the following table:

FINAL FORMULAS

	Radial load	Tangential load	Moment load
Bending moment	$m = C_{mr}P_rR$	$m = C_{mt}P_tR$	$m = C_{mm}M$
Shearing force	$s = C_{sr}P_r$	$s = C_{st}P_t$	$s = C_{sm}\frac{M}{R}$
Axial force	$a = C_{ar}P_r$	$a = C_{at}P_t$	$a = C_{am}\frac{M}{R}$
Shear flow	$q = C_{qr}\frac{P_r}{R}$ (lb/in.)	$q = C_{qt}\frac{P_t}{R}$ (lb/in.)	$q = C_{qm}\frac{M}{R^2}$ (lb/in.)
Tangential deflection	$\Delta T = \frac{R}{K}q = -C_{\Delta T_r}\frac{P_r}{K}$	$\Delta T = \frac{R}{K}q = -C_{\Delta T_t}\frac{P_t}{K}$	$\Delta T = \frac{R}{K}q = -C_{\Delta T_m}\frac{M}{KR}$
Radial deflection	$\Delta R = -\frac{R}{K}\frac{dq}{d\theta} = C_{\Delta R_r}\frac{P_r}{K}$	$\Delta R = -\frac{R}{K}\frac{dq}{d\theta} = C_{\Delta R_t}\frac{P_t}{K}$	$\Delta R = -\frac{R}{K}\frac{dq}{d\theta} = C_{\Delta R_m}\frac{M}{KR}$
Sectional rotation	$\Delta\phi = -\frac{1}{K}\left(q + \frac{d^2q}{d\theta^2}\right) = C_{\Delta\phi_r}\frac{P_r}{KR}$	$\Delta\phi = -\frac{1}{K}\left(q + \frac{d^2q}{d\theta^2}\right) = C_{\Delta\phi_t}\frac{P_t}{KR}$	$\Delta\phi = -\frac{1}{K}\left(q + \frac{d^2q}{d\theta^2}\right) = C_{\Delta\phi_m}\frac{M}{KR^2}$

DISCUSSION OF PHYSICAL CONCEPTS

Effect of Ring Flexibility on Shear-Flow Pattern

The shape of the shear-flow pattern, for a given external load applied to the ring, depends entirely upon the stiffness of the ring relative to the shell. This statement has been substantiated mathematically in this report. However, in order to establish nonmathematical concepts of the general phenomena involved, the following paragraphs will be devoted to a study of the effects encountered with each loading case.

Before the character of the shear-flow pattern may be determined, it is first necessary to realize fully that the shear-flow intensity is proportional to the tangential deflection imposed on the skin by the loaded ring. This statement is apparent since shear force in the plane of the skin is certainly necessary to produce tangential deflection of the skin, and the magnitude of this shear force is proportional to the deflection which causes it. With this fact clearly in mind, consider a shell section loaded radially as shown in figure 4.

First, assume that the ring is very stiff and remains circular throughout the loading process. Under these conditions, it is evident that the ring will undergo a pure translation displacement in the direction of the load P_r. This translation will impose the maximum tangential deflection on the skin at points 90° away from the loading P_r. In other words, the skin shear-flow pattern assumes the VQ/I (or sine) wave form as illustrated in figure 5.

Now, if the ring distorts, as shown in figure 4, the point of maximum tangential deflection is no longer 90° away from the loading. Instead, it moves to the region indicated in figure 4, due primarily to the tangential deflection induced in this region by straightening the top portion of the ring. (The ring axial loads do not ordinarily cause sufficient axial deformation to affect appreciably the general problem.) Therefore, when the ring is somewhat flexible, as it is for most practical cases, the shear-flow pattern takes a form similar to that shown in figure 6. The extent to which the shear flow is localized in this manner depends entirely upon the stiffness of the ring relative to the stiffness of

the shell. However, this shear flow is inconsistent in one respect. If the ring is flexible, as it must be for this type of shear flow, the points b (fig. 6) on the ring will deflect downward excessively due to the relative "opening" action of the shear flow acting against P_r. Therefore, the shear-flow pattern, indicated in figure 6, must be modified so as to incorporate secondary waves (as shown in fig. 7), which restrain this downward deflecting tendency.

In summarizing the case of a radially loaded ring, it may be stated that when the ring is infinitely stiff the shear-flow pattern follows a VQ/I wave (fig. 5) but, as the ring becomes finitely flexible, the shear flow gradually changes from a sine wave to a pattern similar to that shown in figure 7.

Now consider the study of a fuselage ring loaded with a single tangential load.

If the ring is extremely stiff, the shear-flow pattern resisting the tangential load is as shown in figure 8. This pattern may be obtained by applying the customary VQ/I and $T/2A$ distribution. Note that the chief function of the secondary wave is to offset the moment induced by the primary wave about point A.

If the ring is not extremely stiff, the shear-flow pattern cannot form as shown in figure 8, since the ring is not capable of distributing the loading entirely around the section. Instead, it distorts under the loading P_t and tends to localize the shear flow. Therefore, the shear flow assumes a pattern similar to that shown in figure 9.

Since the primary wave for a flexible ring, as shown in figure 9, produces less moment about point A than it does for a rigid ring (fig. 8), the secondary waves become less significant as the ring becomes more flexible.

For the last type loading, consider a single applied concentrated moment.

If the ring is infinitely rigid, the resisting shear flow, for moment loading, is a constant of $T/2A$ entirely around the section.

When the ring is not extremely stiff, the shear-flow pattern cannot remain constant since the ring is not capable of distributing the loading entirely around the section. Instead, it distorts, under the moment loading, and tends to localize the shear flow, as shown in figure 10 where the primary waves resist the applied moment and the secondary wave compensates for the horizontal components induced by the primary waves. It is observed that the intensity of the secondary shear flow becomes quite severe for very flexible rings and entirely disappears when the ring becomes infinitely stiff.

Relative-Stiffness Parameter

On the preceding pages, the shear-flow patterns obtained with various relative ring stiffnesses have been described in some detail. However, the exact parameter which measures relative stiffnesses has not been mentioned. It is a natural product of the mathematical analysis. However, the terms included in it are reasonably self-explanatory when considered from a deflection standpoint. This parameter, which defines the shear-flow distribution in every case, is given as

$$d = \frac{KR^3}{EI}$$

where

$\frac{R^3}{EI}$ factor which is proportional to tangential deflection of ring

K factor which, by definition, is inversely proportional to tangential deflection of skin, pounds per inch

This term KR^3/EI is used throughout the mathematical derivation. However, its exact evaluation depends upon the accurate determination of K, for which further development, supplemented by tests, is clearly needed. Therefore, until a better means is made available, K may be approximated as

$$K = \frac{RtG}{L}$$

where L is the distance along the shell to a section which is not distorted from a circle. At this section a VQ/I shear-flow pattern may be considered to exist; R/L is assumed to be never less than unity (except for the case of adjacent rings similarly loaded). This approximation for K seems justified for any large fuselage comparable with that of the Lockheed Constellation or Boeing Model XB-29 since it gives good test agreement for those airplanes. Then, by substituting in the expression for d,

$$d = \frac{t_e R^3}{\mu I}$$

where

t_e average effective skin thickness supporting ring $\left(\frac{R}{L}t\right)$

R radius of ring (suggest that R be mean radius between skin and ring neutral axis)

I mean effective moment of inertia of ring cross section including effective skin

μ ratio of E of ring to G of skin

t actual skin thickness

APPLICATION OF METHOD AND USE OF CURVES

General.- The curves, as presented in figures 11 to 43, are derived for the ideal case of a continuous circular shell-supported frame of constant EI with any system of applied loads in the plane of the frame.

However, rings which vary considerably from the ideal case may be handled with reasonable accuracy by approximating "equivalent ideal conditions."

The coefficients for (1) bending moment, (2) axial load, (3) shearing load, and (4) shear flow are plotted against angular location for various values of the relative-stiffness parameter d. There is an independent

set of curves for each type of loading (radial, tangential, moment, and rotation) and a separate plot for each coefficient.

The value of the relative-stiffness parameter may be determined from the relation $d = t_e R^3/\mu I$ as previously discussed.

The details for using the curves to find bending moments, axial loads, and so forth for a given single loading become evident by examination of the curves.

The results for any system of loadings may be obtained by breaking the system down into a series of individual radial, tangential, and moment components and superimposing the individual results.

Shear flow in skin.- The shear flow as obtained from the curves is the total shear flow acting on the ring. This shear flow (see section entitled "Preliminary Discussion") is composed of (1) a VQ/I (or $d = 0$) shear flow which provides equilibrium and (2) "induced" shear flow, not affecting equilibrium, induced by ring distortion. The VQ/I portion is resisted from the fore-and-aft sides of the ring in proportion to the total shear and torsion on each side. The so-called induced portion of the shear flow acting on the ring is supplied by the skin from the fore-and-aft sides of the ring in proportion to the relative "shape" stiffness of the shell on each side. The shape stiffness refers to the resistance of the adjacent shell structure to distortion from a circular shape. It depends upon the number of rings, ring spacing, ring stiffnesses, skin thickness, skin shearing modulus, and the distance from the loaded ring to a section in the shell which undergoes no distortion. It is hoped that further development and test data will provide a simple method for obtaining this shape-stiffness factor fairly accurately. However, at present the following approximation, involving only the skin thicknesses and the distances to undistorted sections are suggested since it is felt that they are perhaps the most important factors for the usual case. The relative shape stiffness of the shell forward of the ring is assumed to be

$$\epsilon_F = \frac{t_F}{t_F + t_A}$$

and aft of the ring to be

$$\epsilon_A = \frac{t_A}{t_F + t_A}$$

where

t_F effective skin thickness forward of ring $\left(\frac{R}{L}\,t\right)$

t_A effective skin thickness aft of ring $\left(\frac{R}{L}\,t\right)$

(For significance of R/L, see discussion under Relative-Stiffness Parameter.)

Cases 1, 2, and 3 are given as illustrations of the skin shear flow on either side of the ring.

Case 1: General case of a loaded ring in any cylinder

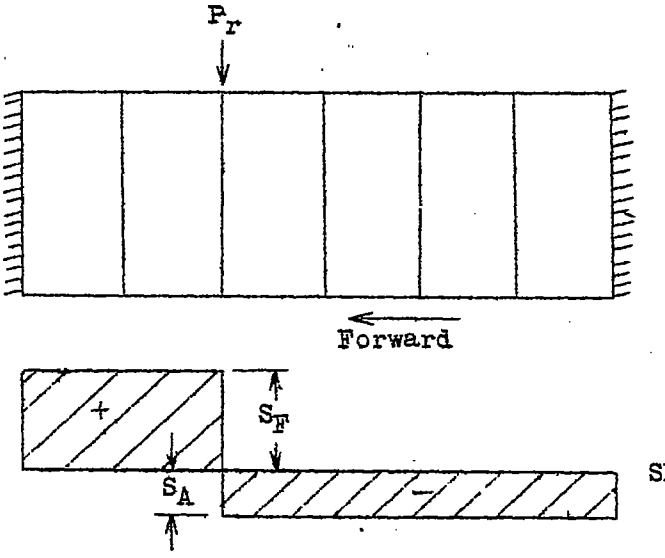

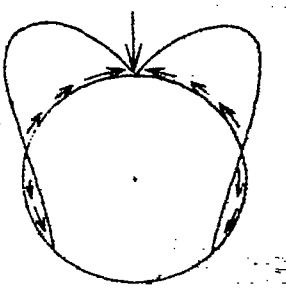

View of forces acting on ring

The skin shear flow fore and aft of the loaded ring may be given as

$$q_F = -\epsilon_F \left[\begin{pmatrix}\text{Shear flow as}\\ \text{obtained from}\\ \text{curves, using}\\ \text{actual d}\end{pmatrix} - \begin{pmatrix}\text{Shear flow}\\ \text{as obtained}\\ \text{for d = 0}\end{pmatrix}\right] - \frac{S_F}{P_r}\begin{pmatrix}\text{Shear flow}\\ \text{as obtained}\\ \text{for d = 0}\end{pmatrix}$$

$$q_A = \epsilon_A \left[\text{——————do——————}\right] - \frac{S_A}{P_r}\left(\text{——do——}\right)$$

where the first terms represent the shear flow induced by ring distortion, and the second terms represent the loading (or equilibrium) shear flow. Positive skin shear flow is considered to be acting clockwise on the section "ahead" when viewed looking forward.

Case 2: Loaded ring in a cantilevered cylinder

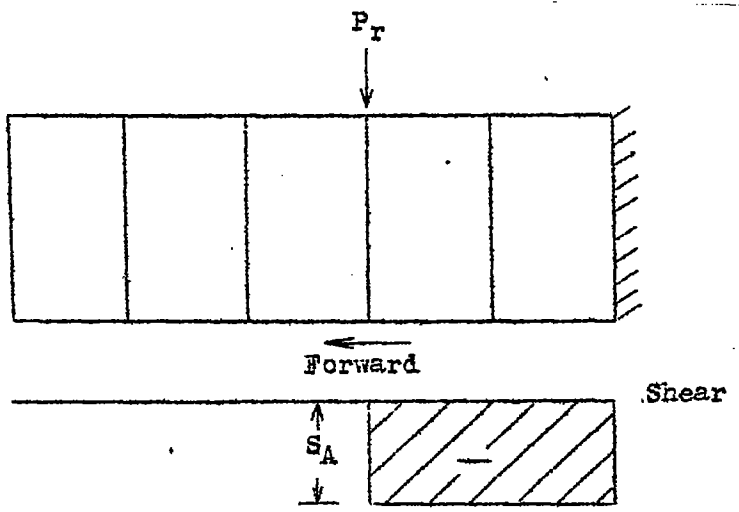

The shear flow fore and aft of the loaded ring may be determined using the same expressions as for case 1, The only difference is that S_F is zero. (See shear diagram.)

Case 3: Loaded ring at the free end of a cantilevered cylinder

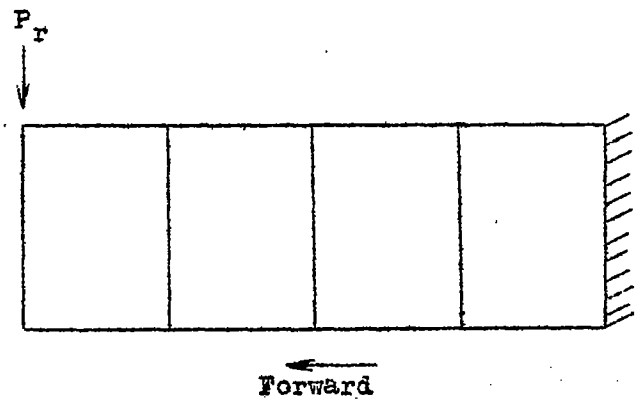

The shear flow in the skin aft of the ring is the same as the shear flow acting on the ring. It is noted that, if the general expressions from case 1 are applied, ϵ_F and S_F are both zero and ϵ_A is unity, so that q_A becomes

q_A = Shear flow as obtained from curves using actual d

Approximation involved when t, R, or I does not remain constant.- When the curves are to be applied to an actual ring which is not associated with entirely constant values of t, R, and I, approximate "effective" properties may be obtained which will give reasonable results. Therefore, the following paragraphs are devoted to a discussion of these approximations.

The relative importance of the skin thickness at any point is proportional to the intensity of the shear flow acting on the ring at that point. It is suggested, for the purpose of simplification, that the skin thickness be considered only over approximately the first major wave of shear flow. A trial, using an assumed thickness, may be necessary in order to locate approximately the first major shear flow wave. Then the average effective skin thickness may be obtained as follows:

(1) Obtain the actual weighted average of skin thickness over approximately the first major wave of shear flow for both the fore-and-aft sides of the ring.

(2) Note the distance L each way from the loaded ring to the section that cannot undergo any distortion in sympathy with the loaded ring. Examples of such points are points of fixed shell support and points of antisymmetry halfway between two separate rings which are loaded so as to cause opposite shell deflections.

(3) If this distance L either way from the ring is less than the radius of the shell, the effective thickness on that side of the ring should be increased by the ratio R/L.

(4) Then t_e is the average of the effective thicknesses on each side of the ring as found in accordance with steps (1), (2), and (3).

The ring radius R and the moment of inertia I need be constant only from the loading point around through the region of appreciable bending moment. If, in this region of appreciable bending moments, R and I vary slightly, satisfactory results may be obtained by using the average values of R and I. However, if R varies considerably, it is recommended that overlapping assumptions be applied.

If I varies considerably, the following means for finding the approximate equivalent moment of inertia is suggested:

$$I' = \frac{\text{Length of arc}}{\sum \frac{ds}{I}}$$

where the length of arc and $\sum \frac{ds}{I}$ is continued over only the region of appreciable bending moment. This region of appreciable bending moment may be approximately located by using an estimated relative-stiffness parameter d.

The curves are set up for coefficients at definite angular positions. These positions are measured from the point of load application with respect to the center of the circle. For a case of varying curvature the approximate point on the actual ring, for which the coefficients apply, may be obtained by laying out around the ring a distance of $R\theta\frac{\pi}{180}$ inches, where R is the assumed equivalent radius and θ is the angle (in deg) from the loading to any point on the assumed equivalent circle.

The effective width of skin acting with the ring is not constant even though the structure is perfectly uniform throughout the circumference. However, the final results are not very sensitive to the value of d, especially when d is large. Therefore, the following effective-width assumptions are recommended:

(1) For determining the section properties needed for d, use an effective width approximately equal to the depth of the ring

(2) For determining the section properties needed

for the margin of safety of the ring, base the effective width upon the stress condition (tension or compression in the skin)

Effect of adjacent rings being similarly loaded.- Further development, supplemented by tests, is clearly needed in order to predict accurately the effect of loading adjacent rings simultaneously. In view of available data, the following approximations are recommended:

(1) For the design of a ring where one adjacent ring of approximately the same flexural proportions is similarly loaded, use

$$d = \frac{\frac{1}{2}t_c R^3}{\mu I}$$

(2) For the design of a ring where at least both adjacent rings are loaded similarly, use

$$d = \frac{\frac{1}{4}t_c R^3}{\mu I}$$

These adjustments in d may be considered as adjustments in the $\frac{R}{L}$ -value used in the expression $t_e = \frac{R}{L}t$. (See section entitled "Relative-Stiffness Parameter.")

Analysis of a ring containing a pin joint.- A pin joint in a ring simply permits enough angular rotation at the pin joint to relieve completely the bending that would exist there if the ring were continuous. Therefore a ring with one pin joint may be readily analyzed in two steps:

(1) Find the results which would exist if the ring were continuous instead of pin jointed

(2) Superimpose the results for a "rotation loading" applied at the pin joint where the amount of rotation is determined so as to require "end" couples exactly equal and opposite to the bending moment found at the pin-joint

location in step (1). Examination of the formula for bending moment due to rotation loading, as given in figure 35,

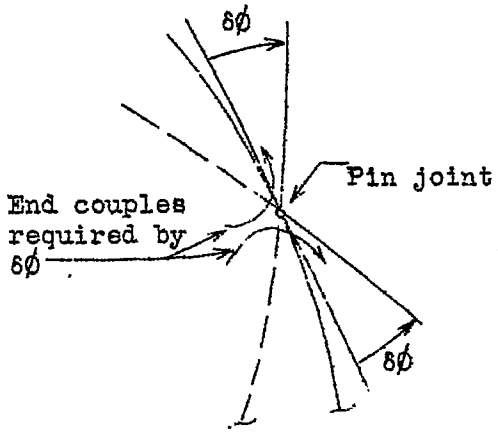

indicates that the required rotation to each side of the joint would be

$$\delta\phi = -\frac{R}{EI}\frac{\text{(Moment as found in step (1))}}{(C_{m\delta\phi} \quad \text{at} \quad \theta = 0 \quad \text{for proper value of} \quad d)}$$

(Note that when this expression for $\delta\phi$ is inserted in the formulas for bending moment, axial load, transverse shear, and shear flow, the EI-term cancels out.)

Analysis of free rings.- The term "free ring" is used to indicate any circular ring for which the complete loading system is independent of the relative flexibility of the ring. The "complete loading system" includes both the applied and the resisting forces.

Primarily this report has been concerned with flexible rings externally loaded and supported by shell structure. It has already been shown that the supporting portion of the complete loading system on such a ring is dependent upon the stiffness of the ring relative to the shell structure. Therefore any shell-supported ring other than an infinitely rigid one is not classed as a free ring.

However, the analysis of free rings may be readily accomplished through the utilization of the $d = 0$ results for ordinary shell-supported rings.

Consider a free ring in equilibrium and loaded as shown in the accompanying sketch. By superimposing the shear-flow patterns as obtained for both loadings, by using the $d \neq 0$ curves, the net shear flow is found to be zero. This same phenomenon is true regardless of the number of applied loadings, their positions, or their type as long as the complete loading system is in equilibrium and remains coplanar.

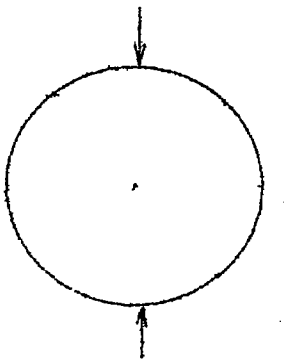

Therefore, ring bending moments, axial loads, and transverse shears for any free ring may be readily obtained by application of the $d = 0$ curves.

However, the problem of free-ring deflections requires additional development. For example, consider the $d = 0$ curve for radial deflections due to radial loads. (See fig. 15.) From the expression for d (see section entitled "Relative-Stiffness Parameter"), it is seen that in order for d to be zero one of the two conditions must exist:

(1) The ring must be infinitely rigid.

(2) The thickness of the supporting skin must be zero.

If the skin thickness becomes zero it is noted that K also becomes zero. Since K is in the denominator of the expression for ΔR, the value of ΔR becomes infinite. Such a value has no significance in free-ring analysis. Therefore, the $d = 0$ curve in figure 15 is of use only

in case the ring is infinitely rigid (for example, a solid plate) and would then give pure translation deflections.

Thus it is apparent that the deflections for free rings must be obtained in a manner which bypasses this tendency to become indeterminate. Basically the entire mathematical analysis is indeterminate for $d = 0$. Therefore all $d = 0$ values for bending-moment coefficients, and so forth, are obtained by using $d = 0.010201$ which approaches $d = 0$ very closely for all practical purposes. The regular calculated deflections consist of (1) pure translation deflection of the ring as a whole, and (2) the distortion deflection of the ring itself. When d becomes zero, the distortion deflection also becomes zero. When $d = 0.010201$, some distortion deflection still remains but is very small relative to the translation deflection. For any free ring which is in equilibrium, the total translation deflections are zero since there is no tendency for the ring to shift in space. Therefore, it is not necessary to evaluate any translation deflections, and the distortion deflections become the desired results. Since the bending moments in a free ring may be found quite accurately by using $d = 0.010201$ instead of $d = 0$, the distortion deflections for $d = 0.010201$ are satisfactory for free-ring deflections.

Reasonably accurate values for distortion deflection coefficients have been obtained by using six to ten significant figures throughout the numerical solution for deflection coefficients (when $d = 0.010201$) and then subtracting the pure translation deflection coefficients which are obtained by simple geometry.

The formulas for actual deflections of free rings are the same as the formulas for the deflections of shell-supported rings except for the following considerations:

(1) The value of K is obtained as follows:

$$d = \frac{KR^3}{EI}$$

Then

$$K = 0.010201 \frac{EI}{R^3}$$

The value 0.010201 has been combined with the distortion deflections and the resulting values are plotted as deflection coefficients for free rings. (See figs. 18, 25, 34, and 67.) The formulas for the coefficients to be used to find actual deflections are presented with the curves.

Lockheed Aircraft Corporation,
Burbank, Calif., December 16, 1943.

APPENDIX

SUMMARY OF ASSUMPTIONS

The assumptions upon which the mathematical derivation is based are

(1) The frame is of constant initial curvature and constant flexural rigidity

(2) The supporting skin is of constant thickness and continuously attached to the frame

(3) The skin shear flow is proportional to the tangential deflection of the ring with respect to "rigid structure"

(4) The frame complies with the assumptions for the flexure theory of curved beams with uniform rectangular cross sections

(5) All loading is in the plane of the frame

(6) The distortion of the frame, under loading, alters the skin shear-flow distribution but does not alter the geometry of the frame

(7) The skin shear flow acts along the elastic axis of the frame

(8) The frame undergoes no axial deformations

(9) The structure is loaded within the elastic limit

Solution of Differential Equation

The solution of the differential equation

$$\frac{d^6m}{d\theta^6} + 2\frac{d^4m}{d\theta^4} + \frac{d^2m}{d\theta^2} - \frac{KR^3}{EI}m = 0 \qquad (11)$$

may be readily obtained by writing it in symbolic form as

$$(D^6 + 2D^4 + D^2 - d)m = 0$$

and noting that the associated equation is of a quadra-cubic form with one pair of real roots and two pairs of imaginary roots.

The roots, as determined algebraically, are

$$r = \pm\gamma$$

and

$$r = \pm\beta \pm i\sigma$$

where $i = \sqrt{-1}$ and γ, β, and σ have the values computed on form 1 and plotted in figure 3 for various values of the relative-stiffness parameter d.

The general solution is then given by

$$m = C_1e^{\gamma\theta} + C_2e^{-\gamma\theta} + C_3e^{(\beta+i\sigma)\theta} + C_4e^{(\beta-i\sigma)\theta}$$

$$+ C_5e^{-(\beta+i\sigma)\theta} + C_6e^{-(\beta-i\sigma)\theta}$$

which may be expressed in terms of real functions as

$$m = C_1e^{\gamma\theta} + C_2e^{-\gamma\theta} + C_3e^{\beta\theta}\cos\sigma\theta + C_4e^{-\beta\theta}\cos\sigma\theta$$

$$+ C_5e^{\beta\theta}\sin\sigma\theta + C_6e^{-\beta\theta}\sin\sigma\theta \qquad (12)$$

where $C_1 \ldots C_6$ are arbitrary independent constants, to be determined by the conditions of continuity and equilibrium.

Expressions for Shearing Force and Axial Force Acting on a Ring X-Section

By rewriting equation (3) in the form

$$\frac{dM}{d\theta} = R\left(H_A \sin\theta - P_A \cos\theta - \sin\theta \int_0^\theta \cos\psi \, dF + \cos\theta \int_0^\theta \sin\psi \, dF\right)$$

and noting that the shearing force on a ring cross section is given by the expression in the brackets, it may be concluded that

$$s = \frac{1}{R}\frac{dm}{d\theta} \tag{15}$$

Similarly, equation (4) yields the expression for axial force

$$a = -\frac{1}{R}\frac{d^2m}{d\theta^2} \tag{16}$$

the minus sign resulting from a tension force being considered positive.

Expression for Skin Shear Flow q

The expression for the skin shear flow q comes from the equation

$$q = \frac{dF}{d\theta} = -\frac{1}{R}\left(\frac{dm}{d\theta} + \frac{d^3m}{d\theta^3}\right) \tag{17}$$

where q is expressed in pounds per radian.

Expressions for Component Deflections

The tangential deflection is obtained directly from the third assumption.

$$\Delta T = \frac{1}{K} q$$

Substituting equation (17) yields the alternate form

$$\Delta T = -\frac{1}{KR}\left(\frac{dm}{d\theta} + \frac{d^3 m}{d\theta^3}\right) \tag{18}$$

The radial deflection of a ring cross section is given by

$$\Delta R = \Delta x \sin \theta + \Delta y \cos \theta + \int_0^\theta \frac{mR^2}{EI} [\sin (\theta - \psi)]\, d\theta$$

whence

$$\Delta R + \frac{d^2(\Delta R)}{d\theta^2} = \frac{mR^2}{EI}$$

Substituting equation (9) yields

$$\Delta R + \frac{d^2(\Delta R)}{d\theta^2} = -\frac{1}{K}\left(\frac{dq}{d\theta} + \frac{d^3 q}{d\theta^3}\right)$$

whence

$$\Delta R = -\frac{1}{K}\frac{dq}{d\theta}$$

or substituting the derivative of equation (17) gives

$$\Delta R = \frac{1}{KR}\left(\frac{d^2 m}{d\theta^2} + \frac{d^4 m}{d\theta^4}\right) \tag{19}$$

The rotation of a ring cross section is given by

$$\Delta\phi = \int_0^\theta \frac{mR}{EI}\, d\theta$$

Substituting equation (9) for m yields

$$\Delta\phi = -\int_0^\theta \frac{1}{RK}\left(\frac{dq}{d\theta} + \frac{d^3q}{d\theta^3}\right) d\theta$$

whence

$$\Delta\phi = -\frac{1}{RK}\left(q + \frac{d^2q}{d\theta^2}\right) + \frac{1}{RK}\left(q_o + \frac{d^2q_o}{d\theta^2}\right)$$

But $\frac{1}{RK}\left(q_o + \frac{d^2q_o}{d\theta^2}\right)$ is initial rotation at point A with respect to rigid structure; therefore, $\Delta\phi = -\frac{1}{RK}\left(q + \frac{d^2q}{d\theta^2}\right)$ "absolute" rotation in radians or, by substituting equation (17) in its second derivative,

$$\Delta\phi = \frac{1}{R^2K}\left(\frac{dm}{d\theta} + 2\frac{d^3m}{d\theta^3} + \frac{d^5m}{d\theta^5}\right) \qquad (20)$$

Hyperbolic Trigonometric Integrals

$$\int \sinh ax \sin bx \sin x\, dx$$

$$= \frac{1}{\alpha^2 - 4b^2}\left\{a \cosh ax\,(\alpha \sin bx \sin x + 2b \cos bx \cos x)\right.$$

$$\left. + \sinh ax\left[(2-\alpha)b \cos bx \sin x + (2b^2 - \alpha)\sin bx \cos x\right]\right\}$$

$$\int \sinh ax \sin bx \cos x \, dx$$

$$= \frac{1}{\alpha^2 - 4b^2}\left\{a \cosh ax \, (\alpha \sin bx \cos x - 2b \cos bx \sin x)\right.$$

$$\left. + \sinh ax \left[(2 - \alpha)b \cos bx \cos x - (2b^2 - \alpha) \sin bx \sin x\right]\right\}$$

$$\int \sinh ax \cos bx \sin x \, dx$$

$$= \frac{1}{\alpha^2 - 4b^2}\left\{a \cosh ax \, (\alpha \cos bx \sin x - 2b \sin bx \cos x)\right.$$

$$\left. + \sinh ax \left[(2b^2 - \alpha) \cos bx \cos x - (2 - \alpha)b \sin bx \sin x\right]\right\}$$

$$\int \sinh ax \cos bx \cos x \, dx$$

$$= \frac{1}{\alpha^2 - 4b^2}\left\{a \cosh ax \, (\alpha \cos bx \cos x + 2b \sin bx \sin x)\right.$$

$$\left. - \sinh ax \left[(2b^2 - \alpha) \cos bx \sin x + (2 - \alpha)b \sin bx \cos x\right]\right\}$$

It should be noted that

(1) $\alpha = a^2 + b^2 + 1$

(2) e^{ax} may be substituted for sinh ax and cosh ax

(3) sinh ax and cosh ax may be used interchangeably in these formulas as long as work is consistent

$$\int \sinh ax \sin bx \, dx = \frac{1}{a^2 + b^2}(a \cosh ax \sin bx - b \sinh ax \cos bx)$$

$$\int \sinh ax \cos bx \, dx = \frac{1}{a^2 + b^2}(a \cosh ax \cos bx + b \sinh ax \sin bx)$$

$$\int \sinh ax \, dx = \frac{\cosh ax}{a}$$

Discussion of Computation Forms

The computation forms used in order to obtain data for plotting the curves contained in this report are listed as follows:

Form 1: Solution of Auxiliary Equation

Form 2: Hyperbolic and Natural Functions of θ for a Given Value of d

Form 3: Evaluation of Integrals for a Given Value of Φ

Form 4: Final Constants for Type of Applied Loading

Form 5: Final Coefficients for Type of Applied Loading

The primary function of form 1 is, as the title indicates, to evaluate the auxiliary equation which is associated with the symbolic form used for solving the general differential equation (11). The relation between the various stiffnesses d and the damping and frequency parameters are obtained on this form. In fact, the plot of the damping and frequency parameters against d (see fig. 3) is based upon the results from this form.

Form 2 serves to evaluate the various hyperbolic and natural trigonometric functions of θ which are needed in the conditional equations of continuity and equilibrium. (See equations (21) and (22).) Since the damping and frequency parameters γ, β, and σ depend upon the relative-stiffness parameter d, a separate form 2 must be used for each value of d.

Form 3 is used to evaluate the integrals which are involved in the conditional equations of continuity and equilibrium. The angle Φ, referred to on the form, is specifically intended to cover the case of partial rings as well as the complete rings with which this paper deals. For a complete ring, Φ is 180° and remains at that value as far as this report is concerned. The data for form 3 are obtained from the form 2 for each value of d being considered.

Form 4 is used to obtain, from the conditional equations of continuity and equilibrium, the coefficients of

the hyperbolic functions which are used in the equations for the final load coefficients. Form 4 differs slightly for each type of loading that is applied and is so designated by subscripts V, R, X, and so forth.

Form 5 is used to determine the final nondimensional load coefficients which are plotted against θ for each value of d, thus yielding the curves in figures 11 to 31.

REFERENCE

1. Wise, Joseph A.: Analysis of Circular Rings for Monocoque Fuselages. Jour. Aero. Sci., vol. 6, no. 11, Sept. 1939, pp. 460-463.

BIBLIOGRAPHY

Frocht, Max M.: Photoelastic Investigation of Shear and Bending Stresses in Centrally Loaded Simple Beams. Eng. Bull., Carnegie Inst. Tech., 1937.

Newell, Joseph S.: The Use of Symmetric and Anti-Symmetric Loadings. Jour. Aero. Sci., vol. 6, no. 6, April 1939, pp. 235-239.

Ruffner, Benjamin F.: Stress Analysis of Monocoque Fuselage Bulkheads by the Photoelastic Method. T.N. No. 870, NACA, 1942.

Form 1

SOLUTION OF AUXILIARY SYMBOLIC EQUATION

(1)	(2)	(3)	(4)	(5)	(6)	(7)	(8)	(9)	(10)
	γ^2	γ^4	γ^6	$1+\frac{a}{2}\gamma^2$	$1+.75\gamma^2$	$\sqrt{1+.75\gamma^2}$	$b\sqrt{1+.75\gamma^2}$	TAN θ b/a	θ
γ	(1)^2	(2)^3	(2) (3)	1+.5(2)	1+.75(2)	$\sqrt{(6)}$	(1) (7)	(8)/(5)	
.1	.01	.0001	.000001	1.005	1.0075	1.003743	.1003743	.0998749	5.703494
2.0	4.0000	16.0000	64.0000	3.0000	4.0000	2.0000	4.0000	1.33333	53°7'45"
1.7364	3.0151	9.09074	27.4095	2.50755	3.26132	1.80591	3.13578	1.25054	51°21'10"
1.25	1.5625	2.4416	3.81493	1.78125	2.17188	1.47372	1.84815	1.03419	45°57'49"
1.992	3.9681	15.7455	62.4792	2.98405	3.97608	1.99401	3.97207	1.33110	53°5'0"
2.46	6.0516	36.62186	221.6208	4.02580	5.53870	2.35344	5.78946	1.43809	55°11'13"
2.5	6.2500	39.0625	244.141	4.1250	5.6875	2.3848	5.9618	1.44588	55°19'12"
3.0	9.0000	81.0000	729.000	5.5000	7.7500	2.7839	8.3517	1.51849	56°37'59"
*3.052	9.3147			5.6574	7.9860	2.8260	8.6250	1.52455	56°44'15"
3.2	10.2400	104.8576	1073.74	6.1200	8.6800	2.9463	9.4278	1.54049	57°0'39"
3.4	11.5600	133.6336	1544.80	6.7800	9.6700	3.1097	10.5730	1.55944	57°19'44"
*3.452	11.9163			6.9582	9.9372	3.1524	10.8821	1.56392	57°24'13"
3.6	12.9600	167.9616	2176.78	7.4800	10.7200	3.2741	11.7868	1.57578	57°36'14"
*3.685	13.5792			7.7896	11.1844	3.3443	12.3237	1.58207	57°42'15"
3.8	14.4400	208.5136	3010.94	8.2200	11.8300	3.4395	13.0701	1.59004	57°50'2"
*3.900	15.2100			8.6050	12.4075	3.5224	13.7374	1.59644	57°56'14"
4.0	16.0000	256.0000	4096.00	9.0000	13.0000	3.6056	14.4224	1.60249	58°3'5"
*4.060	16.4800			9.2400	13.3600	3.6553	14.8401	1.60607	58°5'31"
4.2	17.6400	311.1696	5489.03	9.8200	14.2300	3.7723	15.8437	1.61341	58°12'33"
4.4	19.3600	374.8096	7256.31	10.6800	15.5200	3.9395	17.3338	1.62301	58°21'39"
4.6	21.1600	447.7456	9474.30	11.5800	16.8700	4.1073	18.8936	1.63157	58°29'43"
4.8	23.0400	530.8416	12230.6	12.5200	18.2800	4.2755	20.5224	1.63917	58°36'52"
5.0	25.0000	625.0000	15625.0	13.5000	19.7500	4.4441	22.2205	1.64598	58°43'9"
5.367	28.8047	829.7107	23899.6	15.4024	22.6035	4.7543	25.5163	1.65664	58°53'7"
6.765	45.7652	2094.4535	95853.1	23.8826	35.3239	5.9434	40.2071	1.68353	59°17'84"

Do not follow operations but were read from curve of other values.

Form 1 (cont'd)

(11)	(12)	(13)	(14)	(15)	(16)	(17)	(18)	(19)	(20)	(21)
$\theta/2$	sin $\theta/2$	cos $\theta/2$	a^2+b^2	$\sqrt{a^2+b^2}$	$\sqrt[4]{a^2+b^2}$	σ	β	d		
.5 (10)			(5)^2+(8)^2	$\sqrt{(14)}$	$\sqrt{(15)}$	(13)(16)	(12)(16)	(2)+2(3)+(4)		
2.851747	.0497518	.998763	1.020100	1.01000	1.00498756	1.0037444	.05	.010301		
26°33'28"	.44710	.89448	25.0000	5.0000	2.23607	2.00012	.99975	100.		
25°40'35"	.43328	.90125	16.12092	4.01509	2.00377	1.80590	.86820	48.61		
22°58'54"	.39043	.92064	6.56637	2.56249	1.60078	1.47374	.62500	10.2606		
26°32'30"	.44685	.89460	24.68189	4.96809	2.22897	1.99404	.99600	97.9383		
27°35'36"	.46315	.88628	49.72491	7.05159	2.65548	2.35350	1.23000	300.9162		
27°39'36"	.46423	.88572	52.5587	7.2497	2.69253	2.38483	1.24995	329		
28°19'	.47434	.88034	100.0009	10.0000	3.16228	2.78388	1.50000	900		
28°22'8"	.47514	.87991	106.3968	10.3149	3.21168	2.82599	1.52600	*1000		
28°30'20"	.47734	.87877	126.3378	11.2400	3.35261	2.94617	1.60000	1294		
28°39'52"	.47968	.87745	157.7567	12.5601	3.54401	3.10969	1.70000	1824		
28°42'6"	.48025	.87714	166.8366	12.9165	3.59395	3.15240	1.72599	*2000		
28°48'2"	.48176	.87631	194.8791	13.9599	3.73630	3.27416	1.80000	2528		
28°51'8"	.48255	.87587	213.5514	14.5791	3.81826	3.34430	1.84250	*3000		
28°55'1"	.48354	.87532	238.3959	15.4401	3.92939	3.43947	1.90000	3443		
28°58'7"	.48433	.87488	262.7622	16.2099	4.02615	3.52340	1.95000	*4000		
29°1'2.5"	.48507	.87447	289.0056	17.0002	4.12313	3.60555	2.00001	4624		
29°2'46"	.48551	.87423	305.6062	17.4816	4.18110	3.65524	2.03997	*5000		
29°6'16"	.48641	.87373	347.4552	18.6401	4.31742	3.77226	2.10004	6129		
29°10'50"	.48757	.87309	414.5230	20.3598	4.51218	3.93954	2.20000	8025	Assumed	8000
29°14'51"	.48858	.87252	491.0645	22.1600	4.70744	4.10734	2.29996	10391		
29°18'36"	.48949	.87201	577.9193	24.0399	4.90305	4.27551	2.39999	13315		
29°21'34"	.49029	.87156	676.0006	26.0000	5.09901	4.44409	2.49999	16900		
29°26'34"	.491554	.870847	888.3155	29.8046	5.45935	4.75426	2.68357	35588		
29°38'42"	.494625	.869107	3186.9895	46.7653	6.83851	5.94340	3.38350	100088		

*Do not follow operations but were read from curve of other values.

Form B

HYPERBOLIC AND NATURAL FUNCTIONS OF θ FOR d = 1000

$\beta = 1.526 \quad \gamma = 5.052 \quad K = \beta(.0075798675) = .01156688 \quad \sigma = 2.826$

① θ IN DEG.	② βθ IN RAD. K ①	③ $e^{\beta\theta}$ ANTILOG ②	④ $e^{\gamma\theta}$ ③^2	⑤ $e^{2\gamma\theta}$ ④^2	⑥ $2e^{\beta\theta}$ 2 ③	⑦ $2e^{\gamma\theta}$ 2④	⑧ Sinh βθ (④ − 1)/⑥	⑨ Cosh βθ (④ + 1)/⑥	⑩ Tanh βθ (④ − 1)/(④ + 1)
0	0	1.000000	1.00000	1.00000	2.00000	2.00000	.000000	1.00000	.00000
5	.0578344	1.14244	1.30517	1.70347	2.28488	2.61034	.13356	1.00888	.13239
10	.1156688	1.30518	1.70349	2.90188	2.61036	3.40698	.26950	1.03568	.26022
15	.173503	1.49109	2.22335	4.94329	2.98218	4.44670	.410220	1.08087	.37953
20	.231338	1.70348	2.90184	8.42068	3.40696	5.80368	.55822	1.14528	.48742
25	.289172	1.94613	3.78742	14.34455	3.89226	7.57484	.71614	1.22998	.58224
30	.347006	2.22334	4.94324	24.43562	4.44668	9.88648	.88678	1.33656	.66348
35	.404841	2.54004	6.45180	41.62572	5.08008	12.90360	1.07317	1.46687	.73181
40	.462675	2.90180	8.42044	70.90381	5.80360	16.84088	1.27859	1.62321	.78770
45	.520510	3.31521	10.99062	120.79373	6.63042	21.98124	1.50679	1.808435	.83320
50	.578344	3.78743	14.34463	205.76841	7.57486	28.68926	1.76170	2.02573	.86966
55	.636178	4.32691	18.72215	350.51890	8.65382	37.44430	2.04790	2.27901	.89859
60	.694013	4.94325	24.43572	597.10441	9.88650	48.87144	2.37048	2.57277	.92137
65	.751847	5.64738	31.89290	1017.15707	11.29476	63.78580	2.73515	2.91223	.93920
70	.809682	6.45182	41.62598	1732.72221	12.90364	83.25196	3.14841	3.30341	.95308
75	.867516	7.37685	54.32913	2951.65437	14.74166	108.65826	3.61758	3.75385	.96385
80	.925350	8.42074	70.90886	5028.06643	16.84148	141.81772	4.15099	4.26975	.97219
85	.983185	9.62022	92.54863	8565.24891	19.24044	185.09726	4.75614	4.86208	.97862
90	1.041019	1.09903×10	1.20787×10^2	1.45895×10^4	2.19806×10	2.41574×10^2	.54497×10	.55407×10	.98358
95	1.098854	1.25561×10	1.57656×10^2	2.48554×10^4	2.51123×10	3.15313×10^2	.623824×10	.63179×10	.98739
100	1.156688	1.43446×10	2.05768×10^2	4.23405×10^4	2.86892×10	4.11536×10^2	.71375×10	.72072×10	.99033
105	1.214522	1.63879×10	2.68563×10^2	7.21261×10^4	3.27758×10	5.37126×10^2	.81634×10	.82245×10	.99256
110	1.272357	1.87222×10	3.50581×10^2	12.28650×10^4	3.74444×10	7.01042×10^2	.93344×10	.93878×10	.99431
115	1.330191	2.13899×10	4.57528×10^2	20.93319×10^4	4.27798×10	9.15056×10^2	1.06716×10	1.07183×10	.99564
120	1.388026	2.44358×10	5.97106×10^2	35.65580×10^4	4.88716×10	11.94216×10^2	1.21974×10	1.22384×10	.99666
125	1.445860	2.79164×10	7.79385×10^2	60.73475×10^4	5.58328×10	15.58650×10^2	1.39403×10	1.39761×10	.99744
130	1.503694	3.18929×10	10.17157×10^2	103.46064×10^4	6.37858×10	20.34314×10^2	1.59306×10	1.59621×10	.99804
135	1.561529	3.64359×10	13.27575×10^2	176.24554×10^4	7.28718×10	26.55150×10^2	1.82042×10	1.82317×10	.99849
140	1.619363	4.16254×10	17.32674×10^2	300.21592×10^4	8.32508×10	34.65348×10^2	2.08007×10	2.08247×10	.99885
145	1.677198	4.75551×10	22.61488×10^2	511.43280×10^4	9.51102×10	45.22976×10^2	2.37670×10	2.37881×10	.99913
150	1.735032	5.43290×10	29.51840×10^2	871.21787×10^4	10.86580×10	59.03680×10^2	2.71553×10	2.71737×10	.99938
155	1.792866	6.20678×10	38.52412×10^2	1484.10782×10^4	12.41356×10	77.04824×10^2	3.10858×10	3.10420×10	.99948
160	1.850701	7.09088×10	50.28058×10^2	2528.13673×10^4	14.18176×10	100.56116×10^2	3.54473×10	3.54615×10	.99960
165	1.908538	8.10099×10	65.62604×10^2	4306.77713×10^4	16.20198×10	131.25208×10^2	4.04988×10	4.05111×10	.99970
170	1.966370	9.25487×10	85.65963×10^2	7336.37131×10^4	18.50974×10	171.30534×10^2	4.62689×10	4.62796×10	.99977
175	2.024204	1.05736×10^2	1.11799×10^4	1.24990×10^8	2.11470×10^2	2.23598×10^4	.52863×10^2	.52872×10^2	.99982
180	2.082038	1.20792×10^2	1.45907×10^4	2.12899×10^8	2.41584×10^2	2.91814×10^4	.60392×10^2	.60400×10^2	.99986

Form 2 (cont'd)

HYPERBOLIC AND NATURAL FUNCTIONS OF θ FOR d = 1000

$\beta = 1.526$ $\gamma = 3.052$ $K = \beta(.0075798675) = .01156688$ $\sigma = 2.826$

①	⑪	⑫	⑬	⑭	⑮	⑯	⑰	⑱	⑲	⑳
θ IN DEG.	Tanh γ θ	σ θ	Sin σ θ	Cos σ θ	Sinh γ θ	(Sinh βθ) (Cos σθ)	(Cosh βθ) (Sin σ θ)	Cosh γ θ	(Cosh βθ) (Cos σθ)	(Sinh βθ) (Sin σ θ)
	(⑤ − 1)/(⑤ + 1)	①	Sin ⑫	Cos (12)	(⑤ − 1)/⑦	⑧ ⑭	⑨ ⑬	(⑤ + 1)/⑦	⑨ ⑭	⑧ ⑬
0	.00000	.00000	.00000	1.00000	.00000	.00000	.00000	1.00000	1.00000	.00000
5	.25021	14.130	.24412	.96974	.26949	.12952	.24629	1.03568	.97835	.03260
10	.48743	28.260	.47347	.88081	.55823	.23738	.49036	1.14526	.91224	.12760
15	.66349	42.390	.67417	.73857	.89679	.30298	.72869	1.33656	.79630	.27656
20	.78770	56.520	.83408	.55165	1.27862	.30794	.95524	1.62323	.63178	.46560
25	.86968	70.650	.94351	.33134	1.76169	.23729	1.16050	2.02573	.40754	.67569
30	.92137	84.780	.99586	+.09098	2.37047	.08068	1.33103	2.57277	.12160	.88311
35	.95308	98.910	.98793	−.15488	3.14840	−.16621	1.44916	3.30340	−.22719	1.06022
40	.97219	113.040	.92024	−.39137	4.15084	−.50040	1.49374	4.26960	−.63528	1.17661
45	.98358	127.170	.79684	−.60418	5.44982	−.91037	1.44102	5.54080	−1.09262	1.20067
50	.99033	141.300	.62524	−.78043	7.13746	−1.37488	1.25651	7.20717	−1.58094	1.10149
55	.99431	155.430	.41580	−.90945	9.33437	−1.86246	.94761	9.38778	−2.07265	.85152
60	.99666	169.560	+.18121	−.98345	12.19740	−2.33185	+.46621	12.23832	−2.53019	+.48955
65	.99804	183.690	−.06436	−.99793	15.93077	−2.72949	−.18743	15.96213	−2.90620	−.17603
70	.99885	197.820	−.30605	−.95202	20.80098	−2.99735	−1.01094	20.82500	−3.14491	−.96351
75	.99932	211.950	−.52918	−.84851	27.15536	−3.06965	−1.98614	27.17577	−3.18467	−1.92435
80	.99960	226.080	−.72031	−.69365	35.44738	−2.87933	−3.07554	35.46148	−2.96171	−2.99000
85	.99977	240.210	−.86765	−.49682	46.26891	−2.36394	−4.21956	46.27972	−2.41558	−4.12935
90	.99986	254.340	−.96288	−.26993	.60389×10^2	−.14710×10	−.53350×10	.60398×10^2	−.14956×10	−.52474×10
95	.99992	268.470	−.99964	−.02670	.78825×10^2	−.01666×10	−.63156×10	.78831×10^2	−.01687×10	−.62360×10
100	.99995	282.600	−.97592	+.21814	1.02882×10^2	+.15570×10	−.70337×10	1.02887×10^2	+.15722×10	−.69656×10
105	.99997	296.730	−.89314	.44979	1.34280×10^2	.36718×10	−.73456×10	1.34283×10^2	.36993×10	−.72911×10
110	.99998	310.860	−.75631	.65421	1.75259×10^2	.61067×10	−.71001×10	1.75262×10^2	.61416×10	−.70597×10
115	.99999	324.990	−.57372	.81908	2.28763×10^2	.87409×10	−.61493×10	2.28765×10^2	.87791×10	−.61225×10
120	.99999	339.120	−.35641	.93433	2.98553×10^2	1.13964×10	−.43619×10	2.98555×10^2	1.14347×10	−.43473×10
125	1.00000	353.250	−.11754	.99307	3.89662×10^2	1.38437×10	−.16428×10	3.89663×10^2	1.38792×10	−.16385×10
130	1.00000	367.380	+.12846	.99172	5.08578×10^2	1.57989×10	+.20503×10	5.08579×10^2	1.58299×10	+.20463×10
135	1.00000	381.510	.36666	.93035	6.63787×10^2	1.69363×10	.66848×10	6.63788×10^2	1.69619×10	.66748×10
140	1.00000	395.640	.58269	.81269	8.66337×10^2	1.69045×10	1.21343×10	8.66337×10^2	1.69240×10	1.21204×10
145	1.00000	409.770	.76346	.64586	11.30744×10^2	1.53502×10	1.81613×10	11.30744×10^2	1.53638×10	1.81452×10
150	1.00000	423.900	.89803	.43994	14.75820×10^2	1.19467×10	2.44028×10	14.75820×10^2	1.19548×10	2.43863×10
155	1.00000	438.030	.97826	+.20740	19.26206×10^2	.64348×10	3.03671×10	19.26206×10^2	+.64381×10	3.03513×10
160	1.00000	452.160	.99929	−.03769	25.14029×10^2	−.13360×10	3.54363×10	25.14029×10^2	−.13365×10	3.54221×10
165	1.00000	466.290	.95985	−.28050	32.81302×10^2	−1.13599×10	3.88846×10	32.81302×10^2	−1.13634×10	3.88728×10
170	1.00000	480.420	.86234	−.50633	42.82631×10^2	−2.34273×10	3.99069×10	42.82631×10^2	−2.34329×10	3.98995×10
175	1.00000	494.550	.71264	−.70153	.55899×10^4	−.37085×10^2	.37679×10^2	.55899×10^4	−.37091×10^2	.37672×10^2
180	1.00000	508.680	.51982	−.85428	.72954×10^4	−.51592×10^2	.31397×10^2	.72954×10^4	−.51599×10^2	.31393×10^2

Form 5

EVALUATION OF INTEGRALS FOR $\phi = 180^{\circ}$

	①	②	③	④	⑤	⑥	⑦	⑧	⑨	⑩
		β	α	σ	2σ		$\cos\phi$	$\cosh \beta\phi \cos \sigma\phi$	$\frac{\cosh \beta\phi \cos \sigma\phi}{\cos\phi}$	$\cosh \gamma\phi \cos\phi$
d			㉘ + 1		2④				⑦⑧	⑦㉗
1000		1.52600	11.31495	2.82600	5.65200		-1.00000	$-.61599\times10^{2}$	$+.61599\times10^{2}$	$-.72954\times10^{4}$
2000		1.72600	13.91418	3.15200	6.30400		-1.00000	-1.005472×10^{2}	1.005472×10^{2}	-2.58325×10^{4}
3000		1.84250	15.57714	3.34400	6.68800		-1.00000	$-.76841\times10^{2}$	$.76841\times10^{2}$	-5.32966×10^{4}
4000		1.95000	17.20698	3.52200	7.04400		-1.00000	15.80273	$-.158027\times10^{2}$	-10.47218×10^{4}
5000		2.03000	18.47993	3.65500	7.31000		-1.00000	1.37669×10^{2}	-1.37669×10^{2}	-17.31161×10^{4}
6000		2.20000	21.36360	3.94000	7.88000		-1.00000	4.92985×10^{2}	-4.92985×10^{2}	-50.37569×10^{4}
	⑪	⑫	⑬	⑭	⑮	⑯	⑰	⑱	⑲	⑳
	$\tan\phi$	$\tan\sigma\phi$	$\tan\phi \tan\sigma\phi$	$\tanh\beta\phi$	$\frac{1}{2n_I}\int_{-\phi}^{\phi}\sinh\beta\theta \sin d\theta\, d\theta$	$\frac{1}{2n_I}\int_{-\phi}^{\phi}\cosh\beta\theta \cos d\theta\, d\theta$	γ	$\tanh\gamma\phi$	$\frac{1}{2n_{II}}\int_{-\phi}^{\phi}\sinh\gamma\theta \sin\theta\, d\theta$	$\frac{1}{2n_{II}}\int_{-\phi}^{\phi}\cosh\gamma\theta \cos\theta\, d\theta$
d			⑪⑫		②⑫ − ④⑭	⑨⑭ + ④⑬			⑪⑰ − ⑱	⑰⑱ + ⑪
1000	0	-.60849	0	.99998	-3.75418	-.193808	3.05300	1.00000	-1.00000	3.05300
2000	0	+.51748	0	.99998	-3.35674	+3.35696	3.45300	1.00000	-1.00000	3.45300
3000	0	1.87438	0	.99998	.10961	8.11039	3.68500	1.00000	-1.00000	3.68500
4000	0	-14.44555	0	.99999	-31.89079	-48.92725	3.90000	1.00000	-1.00000	3.90000
5000	0	-1.88888	0	.99999	-7.48898	-4.87315	4.06000	1.00000	-1.00000	4.06000
6000	0	-.19076	0	1.00000	-4.35967	+1.44941	4.40000	1.00000	-1.00000	4.40000
	㉑	㉒	㉓	㉔	㉕	㉖	㉗	㉘	㉙	㉚
	$(2-\alpha)\sigma$	$\alpha - 2\sigma^2$	$\beta\alpha \tanh\beta\phi$	$2\sigma\beta \tanh\beta\phi$	$\frac{1}{2n_I}\int_{-\phi}^{\phi}\cosh\beta\theta \sin d\theta \sin\theta\, d\theta$	$\frac{1}{2n_I}\int_{-\phi}^{\phi}\cosh\beta\theta \cos d\theta \cos\theta\, d\theta$	$\cosh\gamma\phi$	$\beta^2 + \sigma^2$	$\alpha^2 - 4\sigma^2$	$\gamma^2 + 1$
d	−③④+⑤	−④⑤+③	⑭㉛	⑭㉜	⑪㉑ − ⑫㉒ + ⑬㉓ + ㉔	⑪㉒ − ⑫㉑ + ⑬㉔ + ㉓		③² + ④²	③² − ⑤²	⑰² + 1
1000	-36.32405	-4.85760	17.26419	8.62374	5.78984	1.24837	$.72954\times10^{4}$	10.31495	98.06399	10.31470
2000	-37.55350	-5.95603	24.01491	10.88026	13.96227	43.44734	2.56326×10^{4}	13.91418	183.86399	13.91630
3000	-45.40196	-6.78753	28.70031	12.32239	25.04480	113.80084	5.32966×10^{4}	15.57714	197.91795	14.57922
4000	-53.55898	-7.60199	33.55327	13.73556	-96.07937	-740.13565	10.47218×10^{4}	18.20698	248.48222	16.21000
5000	-60.23414	-8.32812	37.51388	14.83915	-.72002	-76.24914	17.31161×10^{4}	17.47993	296.07171	17.49360
6000	-76.29856	-9.98360	46.99992	17.33600	18.48875	32.44635	50.37569×10^{4}	20.36360	394.20800	20.36000
	㉛	㉜	㉝	㉞	㉟	㊱	㊲	㊳	㊴	㊵
	$\beta\alpha$	$2\sigma\beta$	$(2-\alpha)\sigma \tanh\beta\phi$	$(\alpha-2\sigma^2)\tanh\beta\phi$	$\frac{1}{2n_I}\int_{-\phi}^{\phi}\sinh\beta\theta \cos d\theta \sin\theta\, d\theta$	$\frac{1}{2n_I}\int_{-\phi}^{\phi}\sinh\beta\theta \sin d\theta \cos\theta\, d\theta$	$\sinh\gamma\phi$	n_I	n	n_{II}
d	②③	②⑤	⑭㉑	⑭㉒	⑪㉛ − ⑫㉜ − ⑬㉝ − ㉞	−⑪㉜ + ⑫㉛ + ⑬㉞ + ㉝		⑧ / ㉘	⑨ / ㉙	⑩ / ㉚
1000	17.26861	8.62495	-26.32035	-4.85895	9.90515	-36.63498	$.72954\times10^{4}$	-5.00836	+.83703	$-.070728\times10^{4}$
2000	23.01567	10.88070	-37.55200	-5.95579	+.32546	-85.12475	2.56326×10^{4}	-7.78580	.65548	$-.198451\times10^{4}$
3000	28.70088	12.32264	-45.40105	-6.78739	-16.30992	+8.39531	5.32966×10^{4}	-5.27133	.38825	$-.36557\times10^{4}$
4000	33.55361	13.73560	-53.55644	-7.60191	206.03210	-538.35879	10.47218×10^{4}	+.97506	-.084118	$-.645032\times10^{4}$
5000	37.51426	14.83930	-60.23364	-8.32804	36.26473	-131.08597	17.31161×10^{4}	7.87563	-.47790	$-.990183\times10^{4}$
6000	46.99992	17.33600	-76.29356	-9.98360	18.99062	-68.25826	50.37569×10^{4}	24.30913	-1.25025	-2.474248×10^{4}

Form 3 (cont'd)

COEFFICIENTS OF BOUNDARY

CONDITION EQUATIONS FOR $\phi = 180^0$

	(41)	(42)	(43)	(44)	(45)	(46)	(47)	(48)	(49)	(50)
	$\frac{1}{2}\int_{-\phi}^{\phi} \cosh \gamma\theta \cos\theta\, d\theta$	$\frac{1}{2}\int_{-\phi}^{\phi} \cosh \beta\theta \cos\delta\theta \cos\theta\, d\theta$	$\frac{1}{2}\int_{-\phi}^{\phi} \sinh \beta\theta \sin\delta\theta \cos\theta\, d\theta$	A^*	B	$\gamma + \gamma^3$				
d	(20)(40)	(36)(39)	(38)(39)	(32)(2) + (33)(4)	-(38)(5) + (31)	(17)(30)				
1000	$-.215863\times10^4$	+.66928	-19.77716	$-.07039\times10^{-5}$	-31.48161	31.48046				
2000	$-.683053\times10^4$	28.39197	-16.41852	$.66816\times10^{-5}$	-44.57606	44.58707				
3000	-1.34712×10^4	44.18318	3.28948	$.69639\times10^{-5}$	-53.71294	53.72443				
4000	-2.51952×10^4	47.45803	34.51208	1.06018×10^{-3}	-63.30137	63.31900				
5000	-4.03005×10^4	38.43948	82.64599	1.34504×10^{-3}	-70.98103	70.98342				
8000	-10.88669×10^4	-40.56805	108.59418	-1.41840×10^{-3}	-89.60776	89.58400				
	(51)	(52)	(53)	(54)	(55)	(56)	(57)	(58)	(59)	(60)
		COEFFICIENTS OF K'S FOR ANTISYMMETRICAL LOADING CASES								
		HORIZ. EQUILIBRIUM EQUATION			MOMENT EQUILIBRIUM EQUATION			VERTICAL DISPLACEMENT EQUA.		
		For K_1	For K_2	For K_3	For K_1	For K_2	For K_3	For K_1	For K_2	For K_3
d		-(46)(41)	-(45)(42) -(44)(43)	+(44)(42) -(45)(43)	-(46)(65) -(7)(53)	-(7)(53)+(44)(67) -(45)(66)	-(7)(54)+(44)(68) -(45)(67)	-(19)(40)	-(35)(39)	-(25)(39)
1000		6.79844×10^4	+21.05809	-628.61731	$-.72965\times10^4$	+51.59043	-31.40532	$-.070738\times10^4$	-5.31936	-3.10931
2000		30.54451×10^4	1385.71183	-731.66327	$-2.5\times317\times10^4$	100.53879	52.06114	$-.198451\times10^4$	-.21868	-9.12406
3000		72.37335×10^4	2373.18581	175.38377	-5.32893×10^4	76.83523	144.05141	$-.36557\times10^4$	+6.33333	-9.78384
4000		159.28153×10^4	3998.91985	3181.71377	-10.47223×10^4	-15.90051	238.25914	$-.646032\times10^4$	13.21037	-6.16041
5000		285.35690×10^4	2584.93866	4445.91346	-17.31314×10^4	-137.75807	259.97933	$-.990163\times10^4$	17.33091	-.34410
8000		976.27324×10^4	-3633.52137	9532.239131	-50.37577×10^4	-492.94470	94.19648	-2.474248×10^4	16.24158	+19.36483
	(61)	(62)	(63)	(64)	(65)	(66)	(67)	(68)	(69)	(70)
		COEFFICIENTS OF K'S FOR SYMMETRICAL LOADING CASES								
		VERTICAL EQUILIBRIUM EQUATION			ROTATION EQUATION			HORIZ. DISPLACEMENT EQUA.		
		For K_1	For K_2	For K_3	For K_1	For K_2	For K_3	For K_1	For K_2	For K_3
d		-(46)(58)	-(45)(59) -(44)(60)	+(44)(59) -(45)(60)	(37)/(17)	(38)(18)	(38)(15)	-(65)+(41)	-(66)+(42)	-(67)+(43)
1000		2.23655×10^4	-167.46421	-97.87919	$.23804\times10^4$	+.96949	+18.77962	$-.45490\times10^4$	-.30021	-38.55678
2000		8.84835×10^4	-9.41949	-406.71607	$.74254\times10^4$	-28.13668	17.58610	-1.42759×10^4	+54.53859	-34.00462
3000		19.64004×10^4	340.19574	-532.24122	1.44631×10^4	-42.75254	-.57779	-2.79343×10^4	86.93572	3.83727
4000		40.84150×10^4	834.92001	-389.20632	2.68517×10^4	-47.70700	-30.90042	-5.20489×10^4	95.16302	85.41350
5000		70.28518×10^4	1329.82388	-24.18458	4.26894×10^4	-38.38010	-58.98193	-8.28399×10^4	74.81956	121.62792
8000		221.65303×10^4	1455.64082	+1735.00784	11.44902×10^4	35.08475	-105.54388	-23.33571×10^4	-75.63080	813.13798

* The algebraic sign for the value of A should be reversed. However, the final results are only affected in the 4th significant figure. Therefore the figures are considered sufficiently accurate to eliminate the necessity of revision.

Form 4V
Ref. code:
(cd)Form

FINAL CONSTANTS FOR UNIT

VERTICAL LOAD

$\phi = 180^{\circ}$

		①	②	③	④	
		VALUE OF DETERMINANTS				
		K_1'	K_2'	K_3'	D	
d		$(66)_3(70)_3 - (67)_3(69)_3$	$(67)_3(68)_3 - (65)_3(70)_3$	$(65)_3(69)_3 - (66)_3(68)_3$	$(1)(62)_3 + (2)(63)_3 + (3)(64)_3$	
1000		-31.74258	$+.673764 \times 10^4$	$+.369259 \times 10^4$	-219.65057×10^4	
2000		-70.17941	$+.14405 \times 10^4$	3.17728×10^4	-1914.57969×10^4	
3000		-113.82245	-3.93587×10^4	6.30977×10^4	-6869.66226×10^4	
4000		-180.05685	-14.81658×10^4	7.22874×10^4	-22537.92225×10^4	
5000		-255.08968	-30.00843×10^4	1.08575×10^4	-54860.356×10^4	
8000		-543.79831	-71.37582×10^4	$-82,70245 \times 10^4$	$-367921.49941 \times 10^4$	

Form 4V (cont'd)

	⑤	⑥	⑦	⑧	⑨	⑩
	MOMENT CONSTANTS			TRANS. SHEAR CONSTANTS		
	K_1	K_2	K_3	$+K_1\gamma$	$K_2\beta+K_3\sigma$	$-K_2\sigma+K_3\beta$
d	$.5\frac{①}{④}$	$.5\frac{②}{④}$	$.5\frac{③}{④}$	$+⑰_3⑤$	$⑧_3⑥+④_3⑦$	$-④_3⑥+②_3⑦$
1000	$.722670\times10^{-5}$	-15.3372×10^{-4}	-8.40560×10^{-4}	2.20528×10^{-5}	-47.1588×10^{-4}	30.5160×10^{-4}
2000	$.183276\times10^{-5}$	$-.376192\times10^{-4}$	-8.39759×10^{-4}	$.632669\times10^{-5}$	-26.80331×10^{-4}	-13.13588×10^{-4}
3000	$.0828443\times10^{-5}$	$+2.86468\times10^{-4}$	-4.59249×10^{-4}	$.305281\times10^{-5}$	-10.07911×10^{-4}	-18.04115×10^{-4}
4000	$.0399453\times10^{-5}$	$+3.28703\times10^{-4}$	-1.60368×10^{-4}	$.155787\times10^{-5}$	$+.761548\times10^{-4}$	-14.70410×10^{-4}
5000	$.0232490\times10^{-5}$	2.73498×10^{-4}	$-.0989558\times10^{-4}$	$.0943909\times10^{-5}$	5.19033×10^{-4}	-10.19723×10^{-4}
8000	$.0073901\times10^{-5}$	$+.969987\times10^{-4}$	$+1.12391\times10^{-4}$	$.0325164\times10^{-5}$	6.56218×10^{-4}	-1.34915×10^{-4}
	⑪	⑫	⑬	⑭	⑮	⑯
	AXIAL LOAD CONSTANTS			SHEAR FLOW CONSTANTS		
	$-K_1\gamma^3$	$-⑨\beta-⑩\sigma$	$-⑩\beta+⑨\sigma$	$-K_1\gamma-K\gamma^3$		
d	$-⑰_3⑧$	$-②_3⑨-④_3⑩$	$-②_3⑩+④_3⑨$	$⑰_3⑪-⑧$	$②_3⑫+④_3(13)-⑨$	$②_3⑬-④_3⑫-⑩$
1000	-6.73051×10^{-5}	-14.2739×10^{-4}	-179.838×10^{4}	-22.74680×10^{-5}	-482.845×10^{-4}	-364.611×10^{-4}
2000	-2.18397×10^{-5}	$+87.66681\times10^{-4}$	-61.81150×10^{-4}	-8.17173×10^{-5}	-16.71362×10^{-4}	-369.57855×10^{-4}
3000	-1.12498×10^{-5}	78.90037×10^{-4}	$-.463725\times10^{-4}$	-4.45078×10^{-5}	$+153.90236\times10^{-4}$	-346.6561×10^{-4}
4000	$-.607569\times10^{-5}$	60.30282×10^{-4}	$+31.35517\times10^{-4}$	-2.54531×10^{-5}	207.76186×10^{-4}	101.31985×10^{-4}
5000	$-.383227\times10^{-5}$	26.73451×10^{-4}	39.67103×10^{-4}	-1.65029×10^{-5}	194.07834×10^{-4}	-6.98531×10^{-4}
8000	$-.143072\times10^{-5}$	-9.12114×10^{-4}	38.82312×10^{-4}	$-.662033\times10^{-5}$	86.93440×10^{-4}	-100.69731×10^{-4}

Form 4H
Ref. code
(cd)Form

FINAL CONSTANTS FOR UNIT

HORIZONTAL LOAD

Page A:13
Model General
Rept 4222

$\phi = 180^\circ$

		①	②	③	④	
			VALUE OF DETERMINANTS			
		K_1'	K_2'	K_3'	D	
d		$(58)_3(60)_3 - (57)_3(59)_3$	$(57)_3(58)_3 - (55)_3(60)_3$	$(55)_3(59)_3 - (58)_3(58)_3$	$(1)(52)_3 + (2)(53)_3 + (3)(54)_3$	
1000		-327.46165	$-.0473996\times10^4$	7.53016×10^4	-6914.652×10^4	
2000		-906.14010	-33.71810×10^4	20.49478×10^4	-85350.69×10^4	
3000		-1659.20185	-104.47747×10^4	-5.65955×10^4	-369018.87×10^4	
4000		-2817.43403	-211.97594×10^4	-148.61427×10^4	-1424625.97×10^4	
5000		-4458.2753	-263.37901×10^4	-436.43907×10^4	-3893388.6×10^4	
8000		-11075.67940	$+742.45277\times10^4$	-2037.84651×10^4	-32965527.10×10^4	
	⑤	⑥	⑦	⑧	⑨	⑩
	MOMENT CONSTANTS			TRANS. SHEAR CONSTANTS		
	K_1	K_2	K_3	$+K_1\gamma$	$K_2\beta+K_3\sigma$	$-K_2\sigma+K_3\beta$
d	$.5\frac{(1)}{(4)}$	$.5\frac{(2)}{(4)}$	$.5\frac{(3)}{(4)}$	$+(17)_3(5)$	$(2)_3(6) + (4)_3(7)$	$-(4)_3(6) + (2)_3(7)$
1000	2.36788×10^{-6}	$+.0342748\times10^{-4}$	-5.44508×10^{-4}	$.722677\times10^{-5}$	-15.33549×10^{-4}	-8.40605×10^{-4}
2000	$.5308335\times10^{-6}$	$+1.975268\times10^{-4}$	-1.200622×10^{-4}	$.183244\times10^{-5}$	$-.37505\times10^{-4}$	-8.29832×10^{-4}
3000	$.2248128\times10^{-6}$	1.415611×10^{-4}	$+.076684\times10^{-4}$	$.0828434\times10^{-5}$	2.86469×10^{-4}	-4.59251×10^{-4}
4000	$.1023930\times10^{-6}$	$.743970\times10^{-4}$	$.521590\times10^{-4}$	$.0399333\times10^{-5}$	3.28778×10^{-4}	-1.60316×10^{-4}
5000	$.0572544\times10^{-6}$	$.338239\times10^{-4}$	$.560487\times10^{-4}$	$.0232453\times10^{-5}$	2.73521×10^{-4}	$-.0984749\times10^{-4}$
8000	$.0167989\times10^{-6}$	$-.1126104\times10^{-4}$	$.309088\times10^{-4}$	$.00739152\times10^{-5}$	$.97006\times10^{-4}$	1.12368×10^{-4}
	⑪	⑫	⑬	⑭	⑮	⑯
	AXIAL LOAD CONSTANTS			SHEAR FLOW CONSTANTS		
	$-K_1\gamma^2$	$-(9)\beta-(10)\sigma$	$-(10)\beta+(9)\sigma$	$-K_1\gamma-K_1\gamma^3$		
d	$-(17)_3(8)$	$-(2)_3(9) - (4)_3(10)$	$-(2)_3(10) + (4)_3(9)$	$(17)_3(11) - (8)$	$(2)_3(12) + (4)_3(13) - (9)$	$(2)_3(13) - (4)_3(12) - (10)$
1000	-2.20561×10^{-5}	47.15746×10^{-4}	-30.51046×10^{-4}	-7.46417×10^{-5}	1.07521×10^{-4}	-171.41989×10^{-4}
2000	$-.638558\times10^{-5}$	26.80364×10^{-4}	13.14074×10^{-4}	-2.36683×10^{-5}	88.05775×10^{-4}	-53.50584×10^{-4}
3000	$-.305878\times10^{-5}$	10.07916×10^{-4}	18.04122×10^{-4}	-1.20778×10^{-5}	76.03600×10^{-4}	4.12875×10^{-4}
4000	$-.155740\times10^{-5}$	$-.76484\times10^{-4}$	14.70572×10^{-4}	$-.64732\times10^{-5}$	47.01433×10^{-4}	32.97308×10^{-4}
5000	$-.0943759\times10^{-5}$	-5.19255×10^{-4}	10.19710×10^{-4}	$-.406411\times10^{-5}$	23.99431×10^{-4}	39.77736×10^{-4}
8000	$-.0325227\times10^{-5}$	-6.56143×10^{-4}	1.34994×10^{-4}	$-.15049\times10^{-5}$	-10.08644×10^{-4}	27.69822×10^{-4}

Form 4M
Ref. code
(cd)Form

FINAL CONSTANTS FOR UNIT MOMENT LOAD PER INCH RADIUS $\phi = 180^{\circ}$

Page A:14
Model General
Rept. 4222

		①	②	③	④	
		VALUE OF DETERMINANTS				
		K_1'	K_2'	K_3'	D	
d		$-(53)_3(60)_3 + (54)_3(59)_3$	$-(54)_3(58)_3 + (52)_3(60)_3$	$-(52)_3(59)_3 + (53)_3(56)_3$	$(1)(55)_3+(2)(56)_3 + (3)(57)_3$	
1000		+3377.39	-651649.3	346581.4	-69148.5×10^3	
2000		+11704.0	-4338932.8	-2446855.7	-853506×10^3	
3000		24186.6	-6396163.8	-13258568.4	-3690189×10^3	
4000		47295.8	+4282174.0	-40415660.4	-14246858×10^3	
5000		77941.2	43039877	-75050054	-38933885×10^3	
8000		225505.4	425205992.3	-68496868.5	-329655286×10^3	
	⑤	⑥	⑦	⑧	⑨	⑩
	MOMENT CONSTANTS			TRANS. SHEAR CONSTANTS		
	K_1	K_2	K_3	$+K_1\gamma$	$K_2\beta+K_3\sigma$	$-K_2\sigma+K_3\beta$
d	$.5(1)_4$	$.5(2)_4$	$.5(3)_4$	$+(17)_3(5)$	$(2)_3(6) + (4)_3(7)$	$-(4)_3(6) + (2)_3(7)$
1000	$-.244220\times10^{-4}$	$+.471209\times10^{-2}$	$-.250614\times10^{-2}$	$-.745359\times10^{-4}$	$.0108298\times10^{-2}$	-1.71407×10^{-2}
2000	-6.856435×10^{-6}	2.483247×10^{-3}	1.433414×10^{-3}	-23.668380×10^{-6}	8.804805×10^{-3}	-5.353122×10^{-3}
3000	-3.277149×10^{-6}	$.866644\times10^{-3}$	1.796462×10^{-3}	-12.076294×10^{-6}	7.604160×10^{-3}	$+.411924\times10^{-3}$
4000	-1.659938×10^{-6}	$-.150291\times10^{-3}$	1.418466×10^{-3}	-6.473758×10^{-6}	4.702770×10^{-3}	3.295334×10^{-3}
5000	-1.000943×10^{-6}	$-.552730\times10^{-3}$	$.963814\times10^{-3}$	-4.06383×10^{-6}	2.40070×10^{-3}	3.97877×10^{-3}
8000	$-.342032\times10^{-6}$	$-.644925\times10^{-3}$	$.103892\times10^{-3}$	-1.504941×10^{-6}	-1.009501×10^{-3}	2.769567×10^{-3}
	⑪	⑫	⑬	⑭	⑮	⑯
	AXIAL LOAD CONSTANTS			SHEAR FLOW CONSTANTS		
	$-K_1\gamma^2$	$-(9)\beta-(10)\sigma$	$-(10)\beta+(9)\sigma$	$-K_1\gamma-K_1\gamma^3$		
d	$-(17)_3(8)$	$-(2)_3(9) - (4)_3(10)$	$-(2)_3(10) + (4)_3(9)$	$(17)_3(11) - (8)$	$(2)_3(12) + (4)_3(13)-(9)$	$(2)_3(13) - (4)_3(12)-(10)$
1000	2.27484×10^{-4}	4.82744×10^{-2}	2.64628×10^{-2}	7.68817×10^{-4}	14.83423×10^{-2}	-7.89005×10^{-2}
2000	81.703248×10^{-6}	$+1.676983\times10^{-3}$	36.990343×10^{-3}	3.057080×10^{-4}	11.088383×10^{-2}	6.391260×10^{-2}
3000	44.501143×10^{-6}	-15.388139×10^{-3}	24.669341×10^{-3}	1.760630×10^{-4}	4.653747×10^{-2}	9.649927×10^{-2}
4000	25.247656×10^{-6}	-20.776568×10^{-3}	10.137255×10^{-3}	1.049396×10^{-4}	$-.951367\times10^{-2}$	8.964739×10^{-2}
5000	16.49915×10^{-6}	-19.40852×10^{-3}	$.701715\times10^{-3}$	71.05038×10^{-6}	-39.23523×10^{-3}	68.38585×10^{-3}
8000	6.621740×10^{-6}	-8.691192×10^{-3}	-10.070481×10^{-3}	$.306406\times10^{-4}$	-5.778882×10^{-2}	$.931867\times10^{-2}$

Form 4A

Page A:15
Model Gen
Report 4822

FINAL DEFLECTION CONSTANTS

$\phi = 180^0$

	d	(17)	(18)	(19)	(20)	(21)	(22)
		RADIAL DEFLECTION CONSTANTS			ROTATIONAL DEFLECTION CONSTANTS		
		$-(17)_3(14)$	$-(2)_3(16)$ $-(4)_3(16)$	$+(4)_3(15)$ $-(2)_3(16)$	$(17)_3(17)-(14)$	$(2)_3(18)$ $+(4)_3(19)-(15)$	$(2)_3(19)$ $-(4)_3(18)-(16)$
Radial load	.010201	.00163526	.31645282	.00840856	.015506	.031572	-.0023088
	10.26	.01734449	.05814348	.31687154	.03555620	.33473182	.22355861
	48.61	.00894524	-.24857180	.20186171	.02068411	.00418771	.55599864
	97.94	.00582730	-.30018183	.03246037	.01453333	-.3235159	.50487138
	300.92	.00241228	.11939904	-.21863955	.00691481	-.6092857	-.06590499
	1000	$.694232\times10^{-3}$	148.4612×10^{-3}	-96.0724×10^{-3}	$.234626\times10^{-2}$	$.333569\times10^{-2}$	-53.9697×10^{-2}
	2000	$.383088\times10^{-3}$	119.4699×10^{-3}	58.5726×10^{-3}	$.105549\times10^{-2}$	39.2497×10^{-2}	-23.8485×10^{-2}
	4000	$.984871\times10^{-4}$	$-.482871\times10^{-2}$	9.29311×10^{-2}	$.409353\times10^{-3}$	.2971112	.208354
	8000	$+.291295\times10^{-4}$	.0588003	.0130987	$+.134790\times10^{-3}$	-90.385232×10^{-3}	248.22059×10^{-3}
	25000	3.50679×10^{-6}	.0166023	-.0164744	13.9310×10^{-6}	-.0396474	-.121977
	100000	$.616501\times10^{-7}$	-.00504980	+.000939435	4.26176×10^{-7}	-.0119821	.0326168
Tangential load	.010201	.01535267	.00730934	.31490873	.15506200	.00385686	.03186234
	10.26	.0138758	-.16770726	.11057848	.0284453	-.04635159	.24678828
	48.61	.00515167	-.14454297	-.06815617	.01191223	-.24917542	.12210611
	97.94	.00292549	-.06918362	-.11595064	.00729620	-.26744898	-.0285443
	300.92	.000980605	.05213880	.07798384	.00281091	-.0842836	-.2148300
	1000	$.227501\times10^{-3}$	48.2792×10^{-3}	26.4625×10^{-3}	$.768875\times10^{-3}$	148.3496×10^{-3}	-78.9133×10^{-3}
	2000	$.081703\times10^{-3}$	1.66687×10^{-3}	36.9909×10^{-3}	$.305707\times10^{-3}$	110.6656×10^{-3}	63.9448×10^{-3}
	4000	$.352455\times10^{-4}$	-20.78091×10^{-3}	10.1287×10^{-3}	1.049306×10^{-4}	-9.5509×10^{-3}	89.6440×10^{-3}
	8000	$.662156\times10^{-5}$	$-.869408\times10^{-2}$	-1.006767×10^{-2}	$.306398\times10^{-4}$	-577.84952×10^{-4}	98.35979×10^{-4}
	25000	$.467018\times10^{-6}$	.00412294	.00116534	3.59350×10^{-6}	.0167899	-.0157117
	100000	$.911293\times10^{-8}$	$-.484681\times10^{-3}$	$-.573806\times10^{-3}$	6.39960×10^{-8}	$-.00501193$	$.836653\times10^{-3}$
Moment load	.010201	-.01550620	-.03157824	.00230822	-.15661360	-.00311865	.000543446
	10.26	-.03555666	-.33472905	-.32356404	-.07289116	-.49084844	.10741177
	48.61	-.0206840	-.00418920	-.5559954	-.0478277	-.7585377	-.5973607
	97.94	-.01453389	.32333819	-.50486014	-.03624764	-.4172368	-1.1190107
	300.92	-.00691506	.6092718	.06592768	-.0198220	.9888337	-1.13799163
	1000	$-.234643\times10^{-2}$	$-.339754\times10^{-2}$	53.961750×10^{-3}	$-.793012\times10^{-2}$	137.14321×10^{-2}	91.19583×10^{-2}
	2000	$-.105530\times10^{-2}$	-39.249275×10^{-3}	23.856319×10^{-3}	$-.394860\times10^{-2}$	-3.61783×10^{-2}	158.49829×10^{-2}
	4000	$-.0409264\times10^{-2}$	-29.718643×10^{-2}	-30.831968×10^{-2}	$-.170107\times10^{-2}$	-130.37018×10^{-2}	55.08198×10^{-2}
	8000	$-.134819\times10^{-3}$	9.04198×10^{-2}	-24.81890×10^{-2}	$-.623844\times10^{-3}$	-721.1523×10^{-3}	-911.58848×10^{-3}
	25000	$-.139309\times10^{-4}$	.0396512	.121980	$-.773073\times10^{-4}$	.642708	.202085
	100000	$-.428117\times10^{-6}$	.0119802	-.0326150	-2.94567×10^{-6}	-.148309	-.182360

(Sym.)
Form 5

FINAL COEFFICIENTS FOR UNIT VERTICAL LOAD

d = 1000 Φ = 180

Page A:16
Model General
Report 4222

Ref. Code:
(Col)Form

θ	(1) Moment coeff. C_m* $(5)_4(18)_2+(6)_4(19)_2+(7)_4(20)_2$	(2) Shear coeff. C_n* $(8)_4(15)_2+(9)_4(16)_2+(10)_4(17)_2$	(3) Axial load coeff. C_t* $(11)_4(18)_2+(12)_4(19)_2+(13)_4(20)_2$	(4) Shear flow coeff. C_q* $(14)_4(15)_2+(15)_4(16)_2+(16)_4(17)_2$
0	-.0015	.0000	-.0015	0
5			-.0021	-.0128
10	-.0015	+.0004	-.0037	-.0246
15				
20	-.0013	.0015	-.0094	-.0404
25				
30	-.0009	.0037	-.0162	-.0397
35				
40	.0000	.0070	-.0205	-.0163
45				
50	+.0016	.0105	-.0180	+.0312
55				
60	.0036	.0127	-.0049	.0975
65				
70	.0058	.0115	+.0204	.1667
75				
80	.0073	+.0049	.0556	.2123
85			.0746	
90	.0071	-.0080		.1985
95			.1071	
100	+.0042	-.0265		+.0875
105			.1168	
110	-.0022	-.0466		-.1468
115			+.0822	
120	-.0117	-.0605		-.5028
125			-.0166	
130	-.0223	-.0570		-.9328
135			-.1889	
140	-.0299	-.0236		-1.3344
145			-.4244	
150	-.0282	+.0507		-1.5583
155			-.6847	
160	-.0096	.1699		-1.4450
165			-.9037	
170	+.0333	.3267	-.9723	-.8990
175				
180	.1055	.4999798	-.9819	-.000784

* → $M = C_m PR$ $P_n = C_n P$ $P_t = C_t P$ $q = C_q \left(\frac{P}{R}\right)$

θ	(1) Moment coeff. C_m* $(5)_4(15)_2+(6)_4(16)_2+(7)_4(17)_2$	(2) Shear coeff. C_n* $(8)_4(18)_2+(9)_4(19)_2+(10)_4(20)_2$	(3) Axial load coeff. C_t* $(11)_4(15)_2+(12)_4(16)_2+(13)_4(17)_2$	(4) Shear flow coeff. C_q* $(14)_4(18)_2+(15)_4(19)_2+(16)_4(20)_2$
0	.0000	-.0015	.0000	.0000
5				
10	-.0003	-.0015	-.0004	-.0022
15				
20	-.0005	-.0013	-.0015	-.0080
25				
30	-.0007	-.0009	-.0037	-.0153
35				
40	-.0008	.0000	-.0070	-.0206
45				
50	-.0007	+.0016	-.0105	-.0196
55				
60	-.0002	.0036	-.0127	-.0085
65				
70	+.0006	.0058	-.0115	+.0146
75				
80	.0017	.0073	-.0050	.0483
85				
90	.0030	.0071	+.0080	.0853
95				
100	.0041	.0042	.0265	.1119
105				
110	.0043	-.0022	.0466	.1086
115				
120	.0031	-.0117	.0605	+.0535
125				
130	+.0001	-.0223	.0570	-.0713
135				
140	-.0046	-.0299	+.0236	-.2705
145				
150	-.0098	-.0282	-.0507	-.5268
155				
160	-.0133	-.0096	-.1699	-.7947
165				
170	-.0117	+.0333	-.3267	-1.0057
175				
180	+.00000188353	+.1055	-.499997	-1.0876

* ⟶ $M = C_m PR$ $P_n = C_n P$ $P_t = C_t P$ $q = C_q\left(\frac{P}{R}\right)$

FINAL COEFFICIENTS FOR UNIT VERTICAL LOAD

d = 1000 $\phi = 180^0$

θ	(1) Radial deflect. coeff., $C_{\Delta R_r}$* $(17)_4(18)_2 + (18)_4(19)_2 + (19)_4(20)_2$	(2) Rotation deflect. coeff., $C_{\Delta\phi_r}$* $(20)_4(15)_2 + (21)_4(16)_2 + (22)_4(17)_2$	(3) Axial load coeff. C_t* $(11)_4(18)_2 + (12)_4(19)_2 + (13)_4(20)_2$	(4) Shear flow coeff. C_q* $(14)_4(15)_2 + (15)_4(16)_2 + (16)_4(17)_2$
0	.1492	.0000		
5				
10	.1240	-.2635		
15				
20	+.0502	-.5115		
25				
30	-.0650	-.7125		
35				
40	-.2044	-.7981		
45				
50	-.3355	-.8714		
55				
60	-.4084	-.8308		
65				
70	-.3599	+.5844		
75				
80	-.1278	1.7334		
85				
90	+.3240	3.0161		
95				
100	.9740	4.0426		
105				
110	1.7117	4.2635		
115				
120	2.3225	3.0926		
125				
130	2.5066	+.1394		
135				
140	1.9496	-4.4598		
145				
150	+.4565	-9.6676		
155				
160	-1.8562	-13.2308		
165				
170	-4.3390	-11.5687		
175				
180	-5.6118	-.0001		

* $\longrightarrow M = C_m PR$ $\quad P_n = C_n P$ $\quad P_t = C_t P$ $\quad q = C_q \left(\frac{P}{R}\right)$

$(17)_4 = .694232(10^{-3})$ $\quad (18)_4 = 148.4612(10^{-3})$

$(19)_4 = -96.0724(10^{-3})$ $\quad (20)_4 = .234626(10^{-2})$

$(21)_4 = .333569(10^{-2})$ $\quad (22)_4 = -53.9697(10^{-3})$

TABLE I.- COEFFICIENTS FOR SYMMETRICAL AND ANTISYMMETRICAL LOADING

[Use K_1' for K_1, etc., for antisymmetry. Numerical subscript refers to term; for example, 1 may refer to values under either sinh $\gamma\theta$ or cosh $\gamma\theta$ while 2 refers to values under either sinh $\beta\theta$ cos $\sigma\theta$ or cosh $\beta\theta$ cos $\sigma\theta$.]

Coefficient of	Symbol	SYMMETRICAL LOADING – COEFFICIENT OF					
		sinh $\gamma\theta$	sinh $\beta\theta$ cos $\sigma\theta$	cosh $\beta\theta$ sin $\sigma\theta$	cosh $\gamma\theta$	cosh $\beta\theta$ cos $\sigma\theta$	sinh $\beta\theta$ sin $\sigma\theta$
Bending moment	C_m				K_1	K_2	K_3
Shearing force	C_s	γK_1	$K_2\beta + K_3\sigma$	$-K_2\sigma + K_3\beta$			
Axial force	C_a				$-\gamma^2 K_1$	$-C_{s_2}\beta - C_{s_3}\sigma$	$-C_{s_3}\beta + C_{s_2}\sigma$
Shear flow	C_q	$-\gamma K_1$ $-\gamma^3 K_1$	$C_{a_2}\beta + C_{a_3}\sigma$ $- C_{s_2}$	$C_{a_3}\beta - C_{a_2}\sigma$ $- C_{s_3}$			
Tangential deflection	$C_{\Delta T}$	C_{q_1}	C_{q_2}	C_{q_3}			
Radial deflection	$C_{\Delta R}$				$-\gamma C_{\Delta T_1}$	$-\beta C_{\Delta T_2}$ $-\sigma C_{\Delta T_3}$	$+\sigma C_{\Delta T_2}$ $-\beta C_{\Delta T_3}$
Sectional rotation	$C_{\Delta\phi}$	$-C_{\Delta T_1}$ $+\gamma C_{\Delta R_1}$	$-C_{\Delta T_2} + \beta C_{\Delta R_2}$ $++\sigma C_{\Delta R_3}$	$-C_{\Delta T_3} - \sigma C_{\Delta R_2}$ $+ \beta C_{\Delta R_3}$			
		cosh $\gamma\theta$	cosh $\beta\theta$ cos $\sigma\theta$	sinh $\beta\theta$ sin $\sigma\theta$	sinh $\gamma\theta$	sinh $\beta\theta$ cos $\sigma\theta$	cosh $\beta\theta$ sin $\sigma\theta$
		ANTISYMMETRICAL LOADING – COEFFICIENT OF					

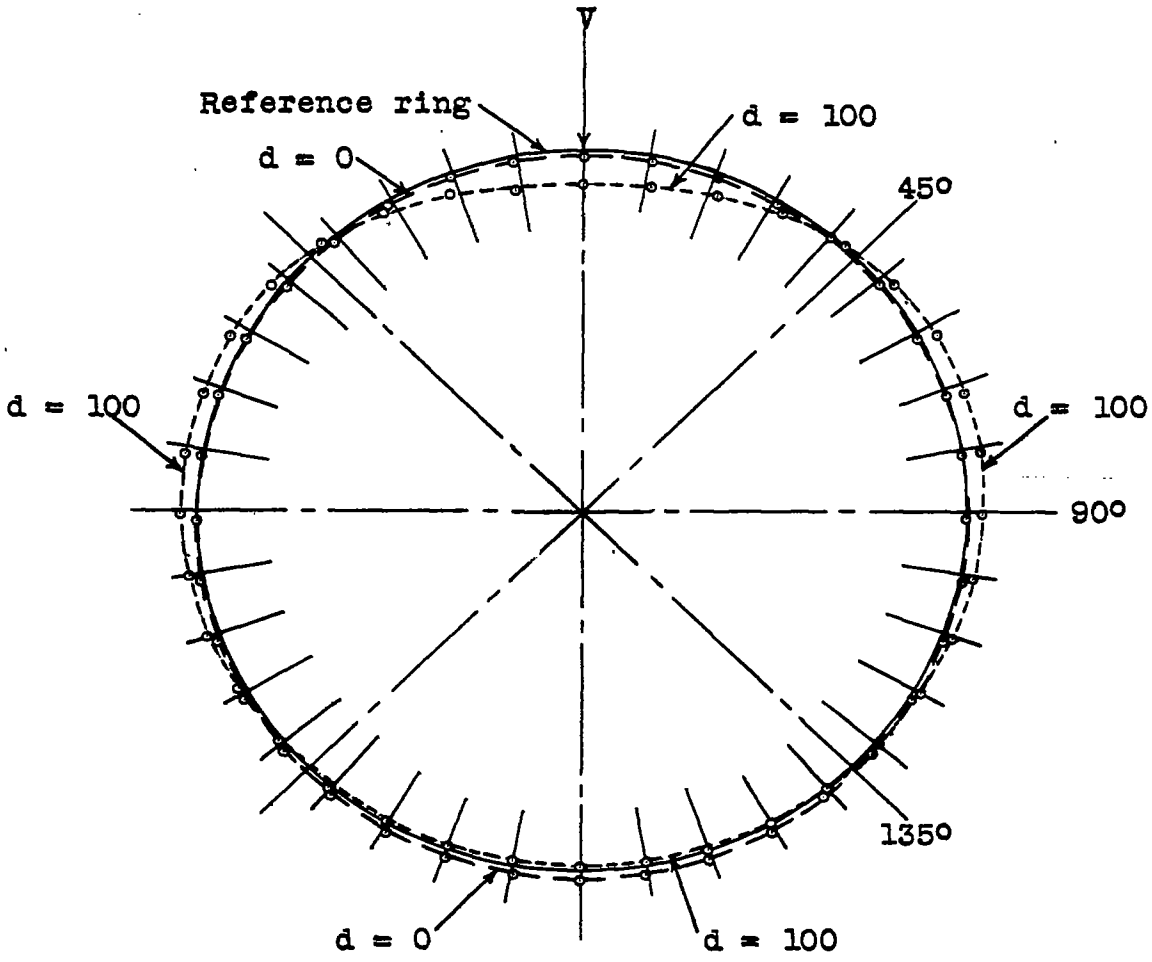

Notes:
Relative stiffness is measured by parameter "d"; d = 0 represents a relatively rigid ring and d = 100 represents a somewhat flexible ring. Deflection scale magnified. Dash lines indicate deflected positions.

Figure 1.- Characteristic deflection curves for a rigid ring and for a flexible ring.

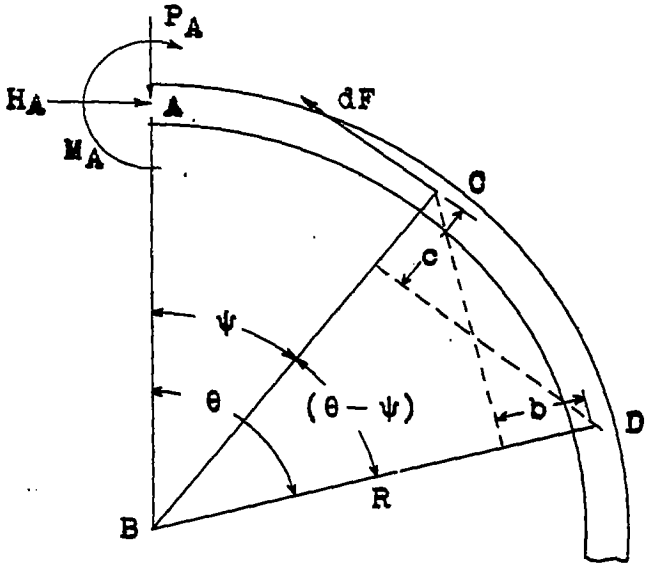

Figure 2

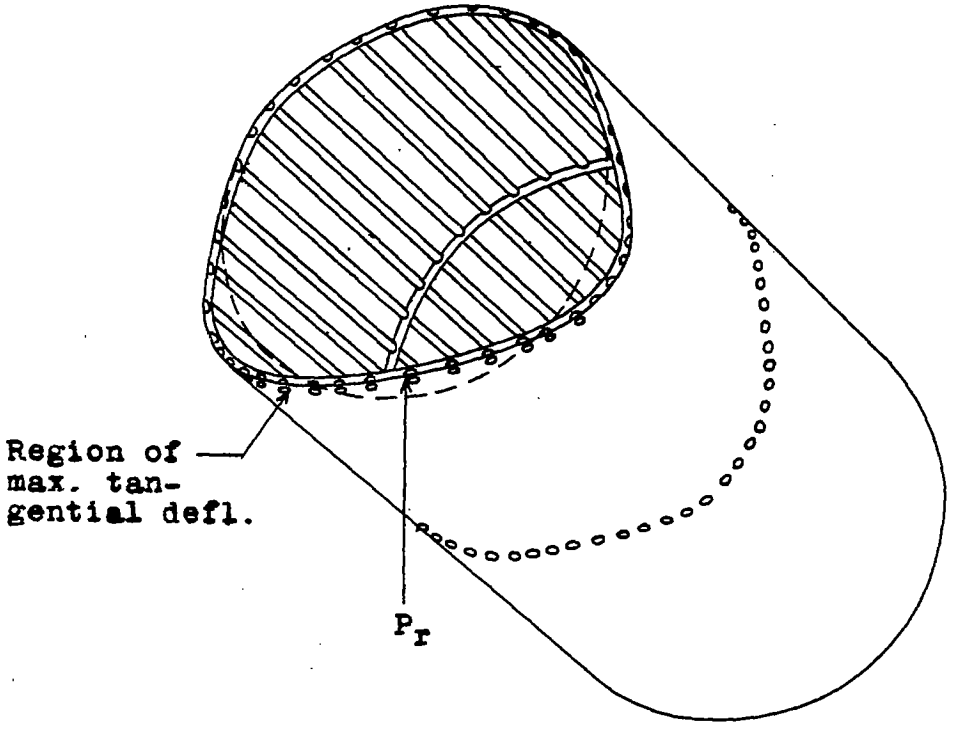

Figure 4

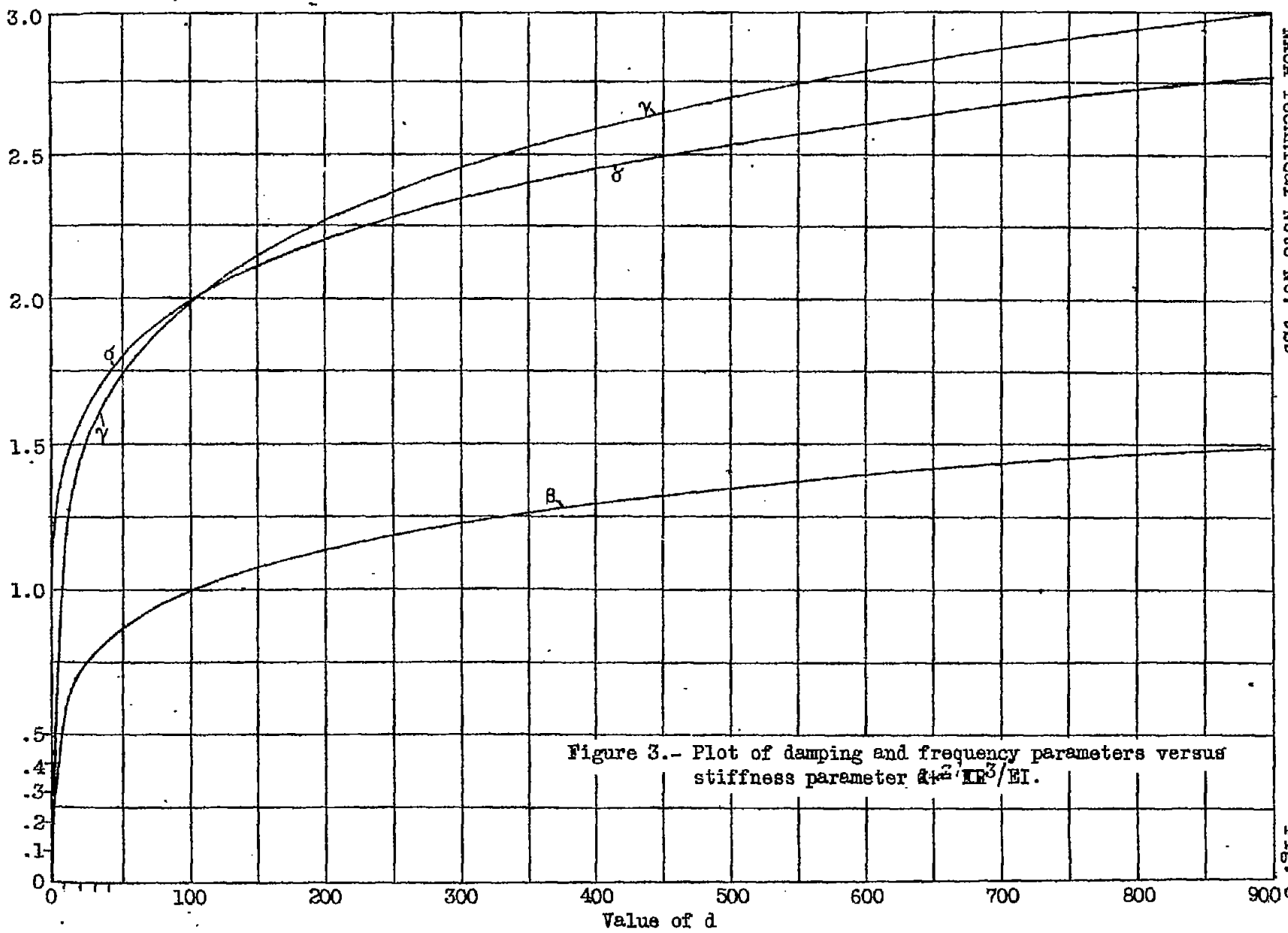

Figure 3.- Plot of damping and frequency parameters versus stiffness parameter $d^2\sqrt{\rho/EI}$.

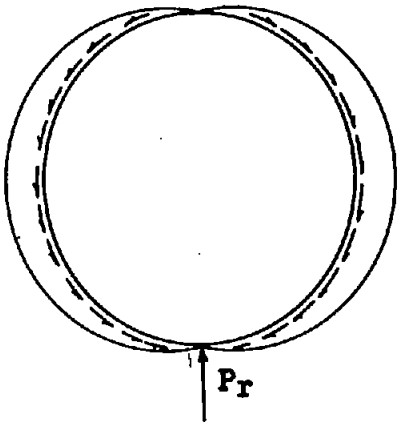

Figure 5

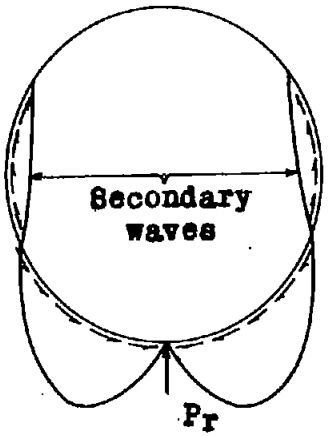

Figure 7

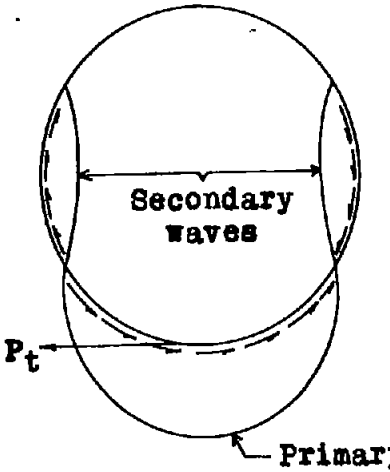

Figure 9

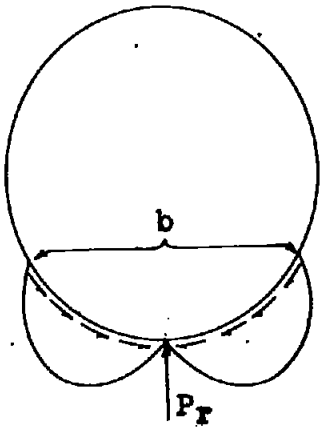

Figure 6

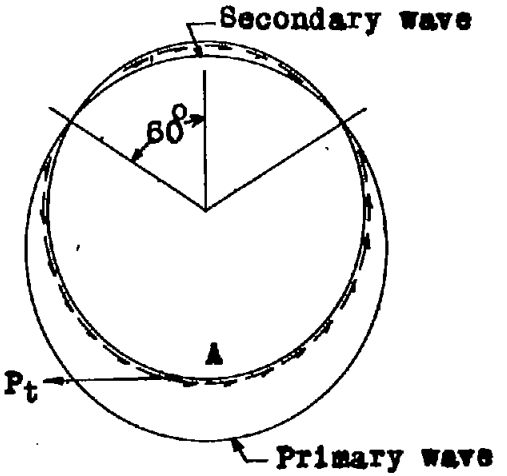

Figure 8

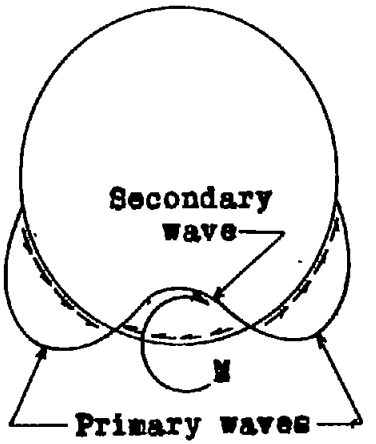

Figure 10

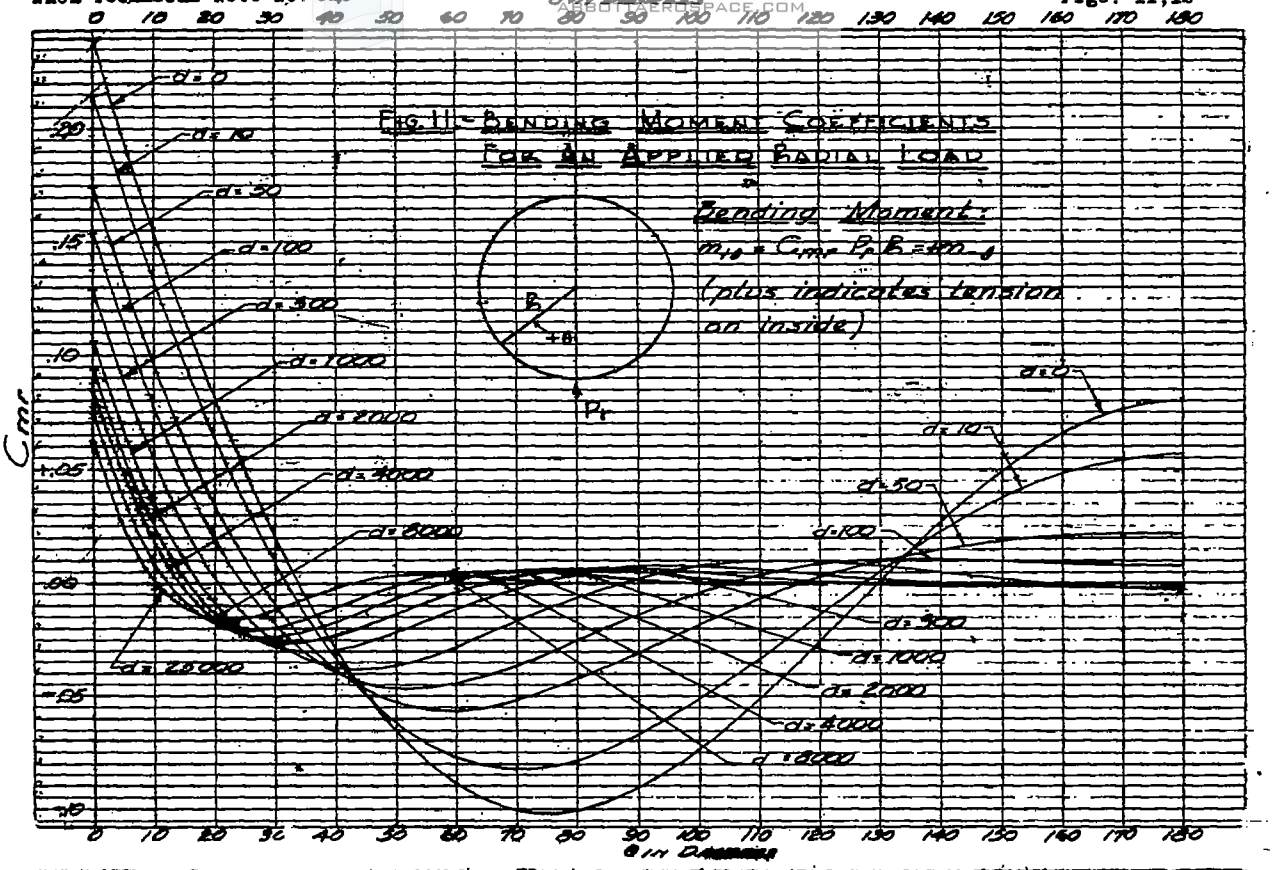

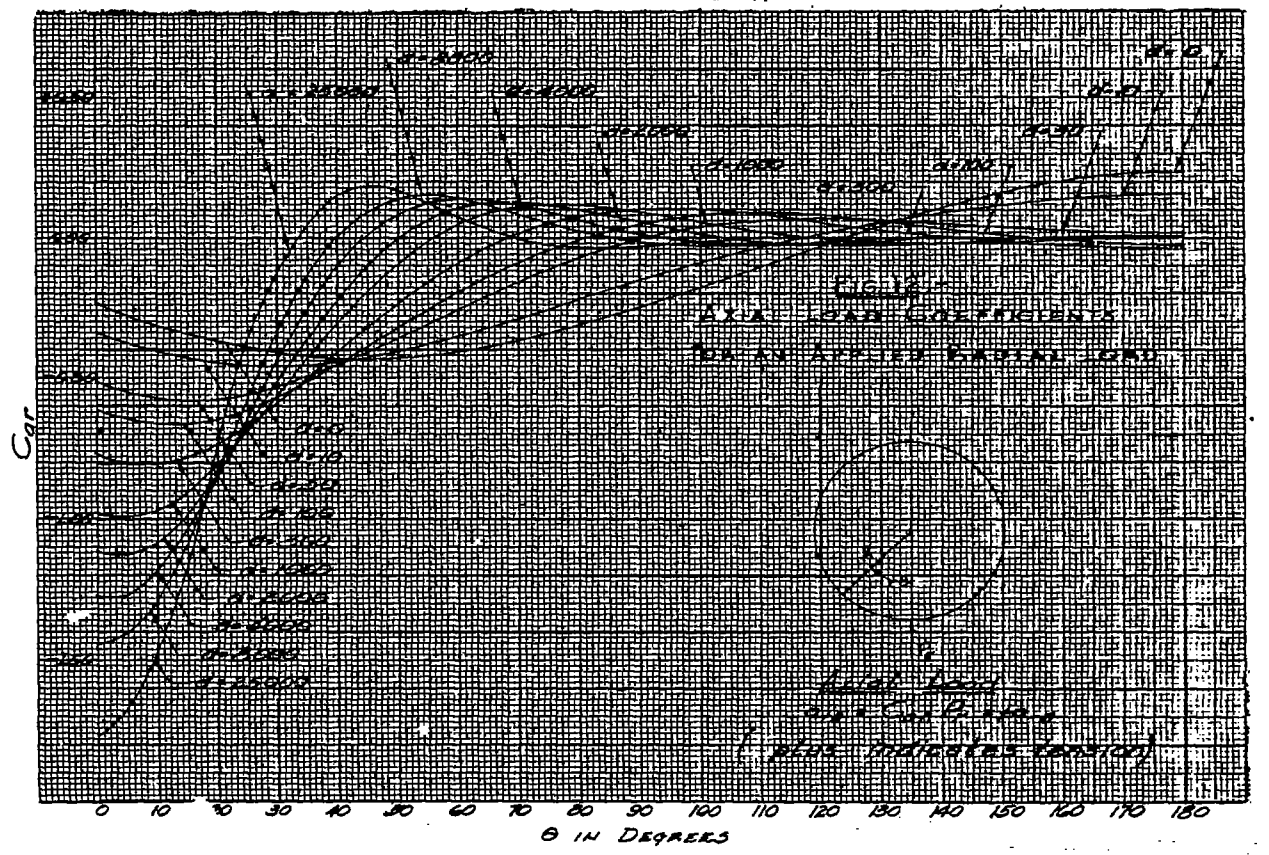

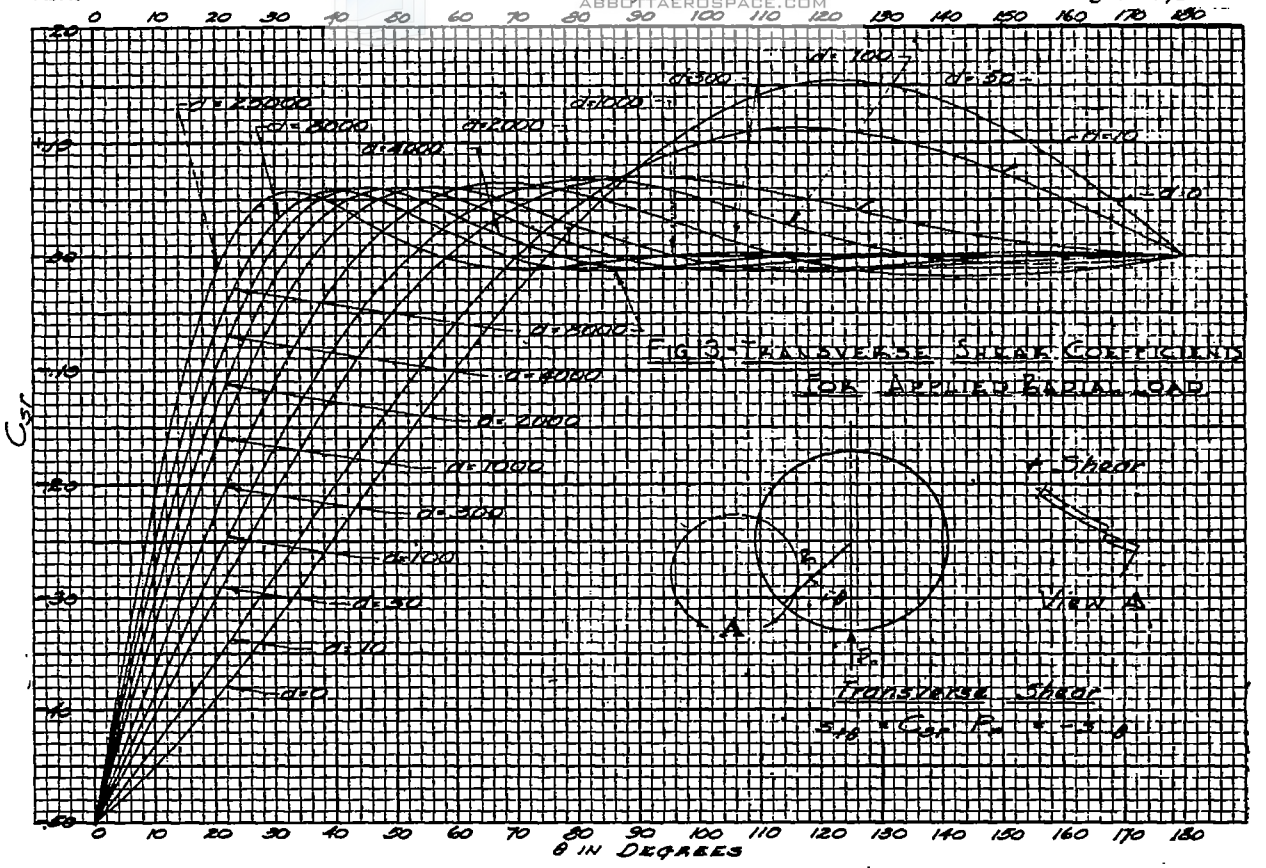

FIG 13.- TRANSVERSE SHEAR COEFFICIENTS FOR APPLIED RADIAL LOAD

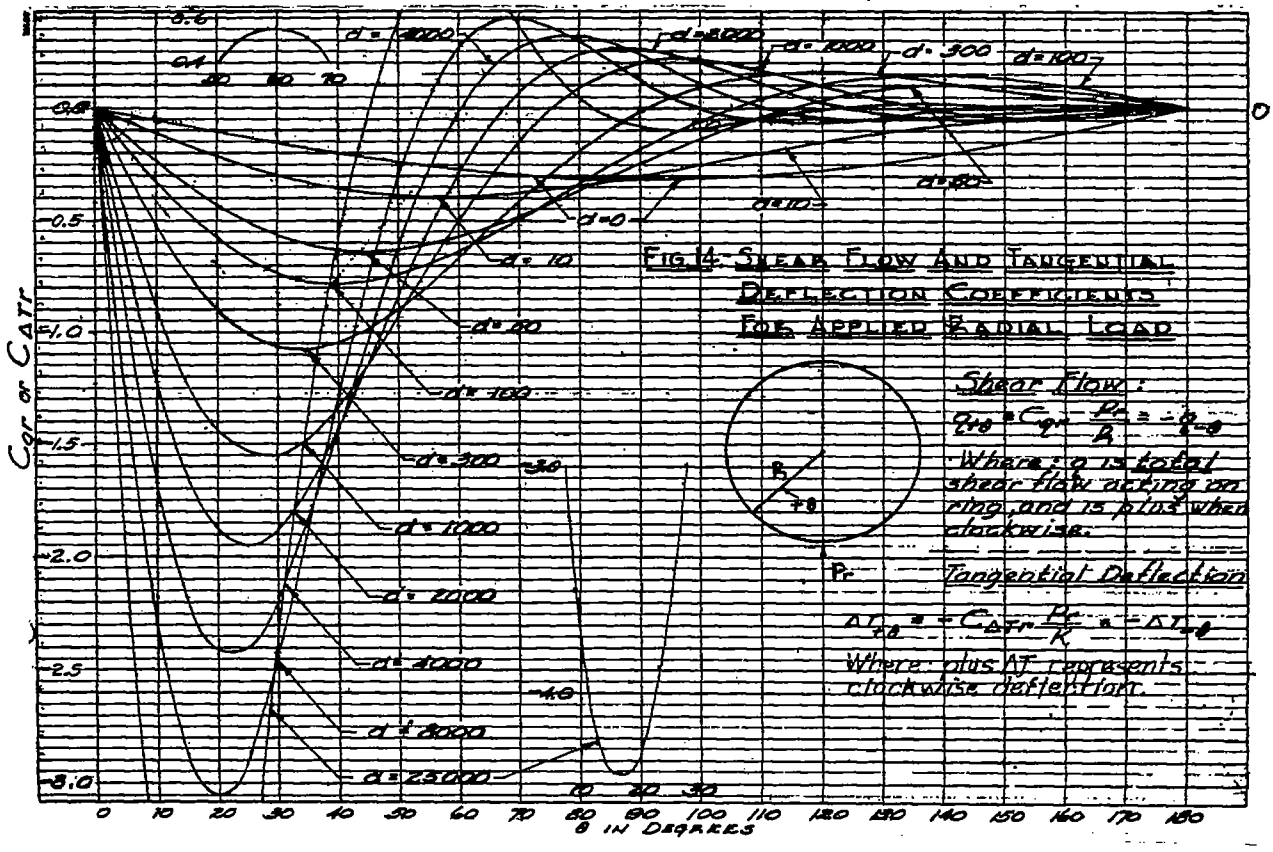

FIG 14.- SHEAR FLOW AND TANGENTIAL DEFLECTION COEFFICIENTS FOR APPLIED RADIAL LOAD

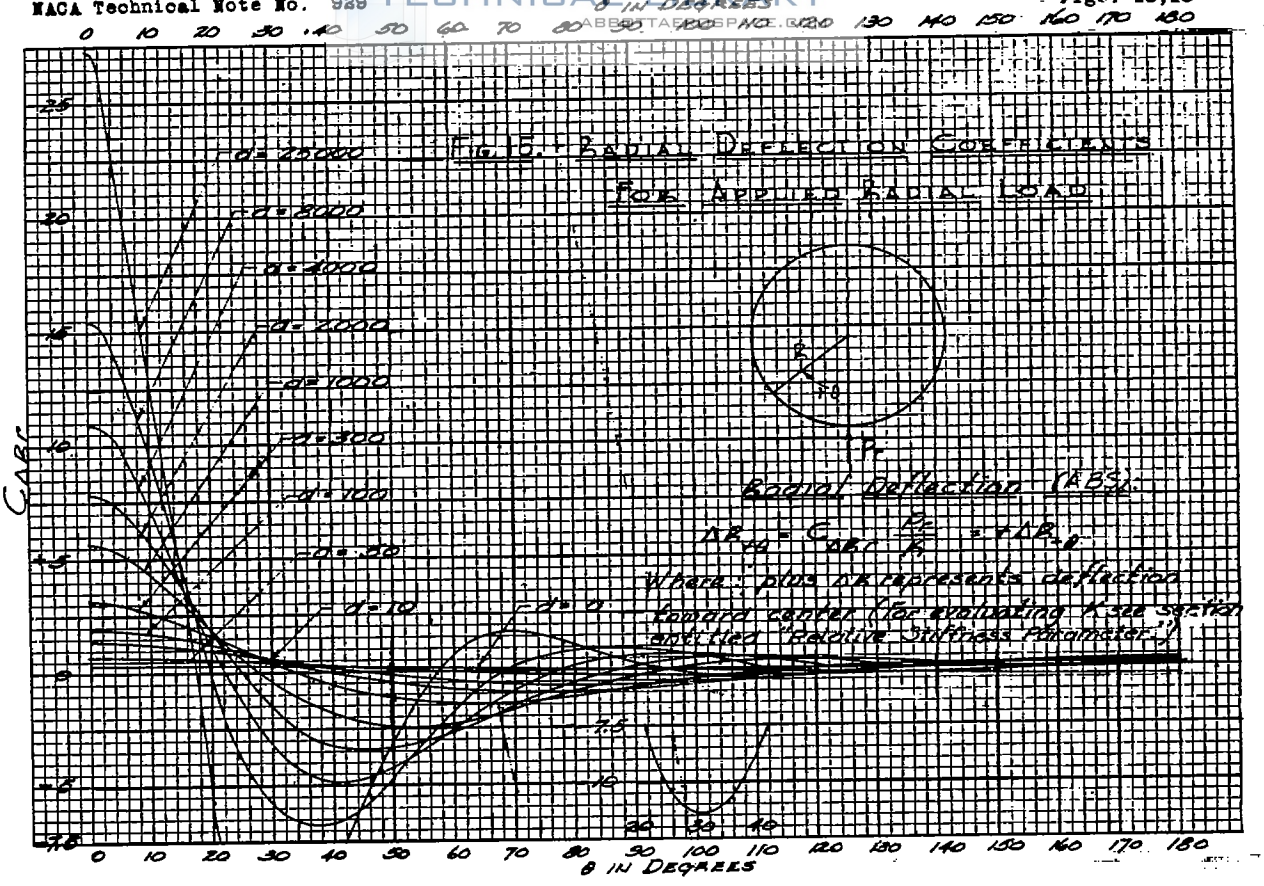

Fig. 15. Radial Deflection Coefficients for Applied Radial Load

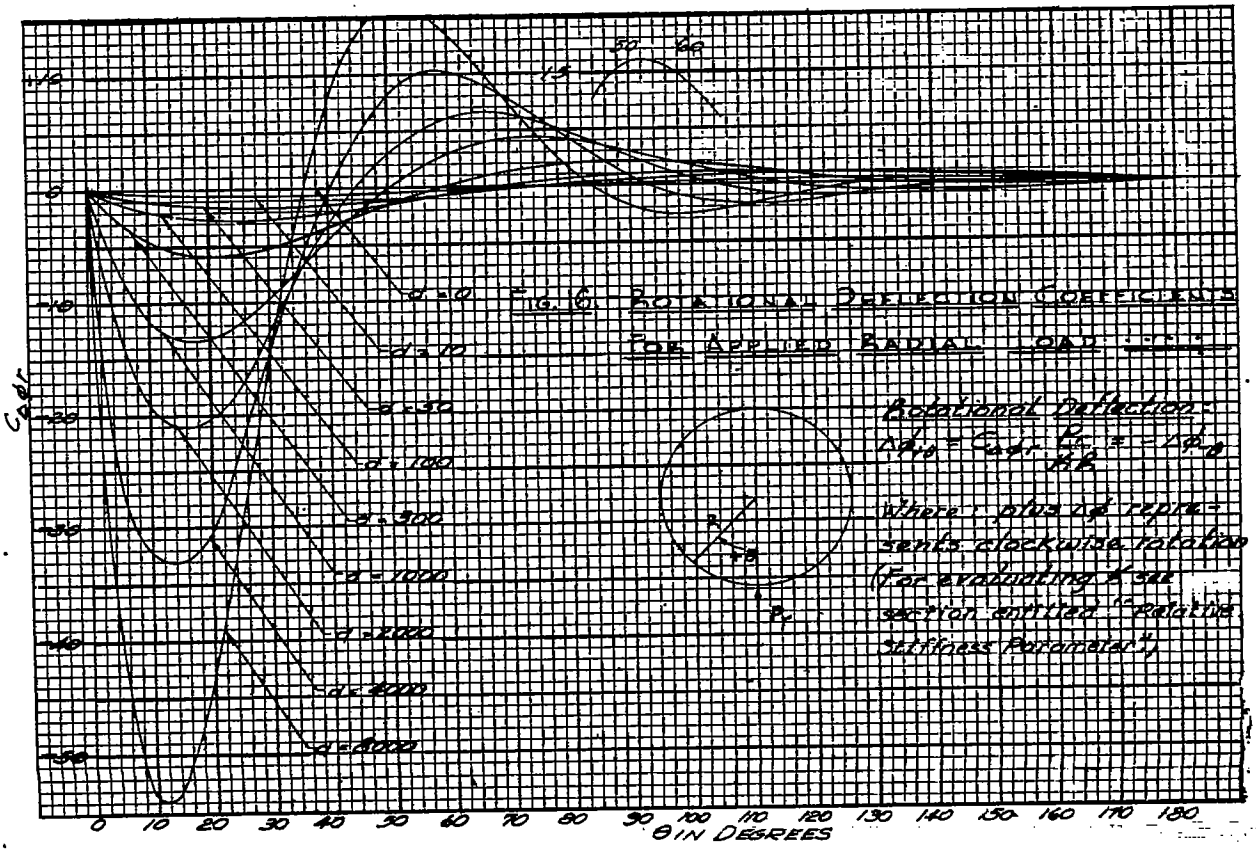

Fig. 16. Rotational Deflection Coefficients for Applied Radial Load

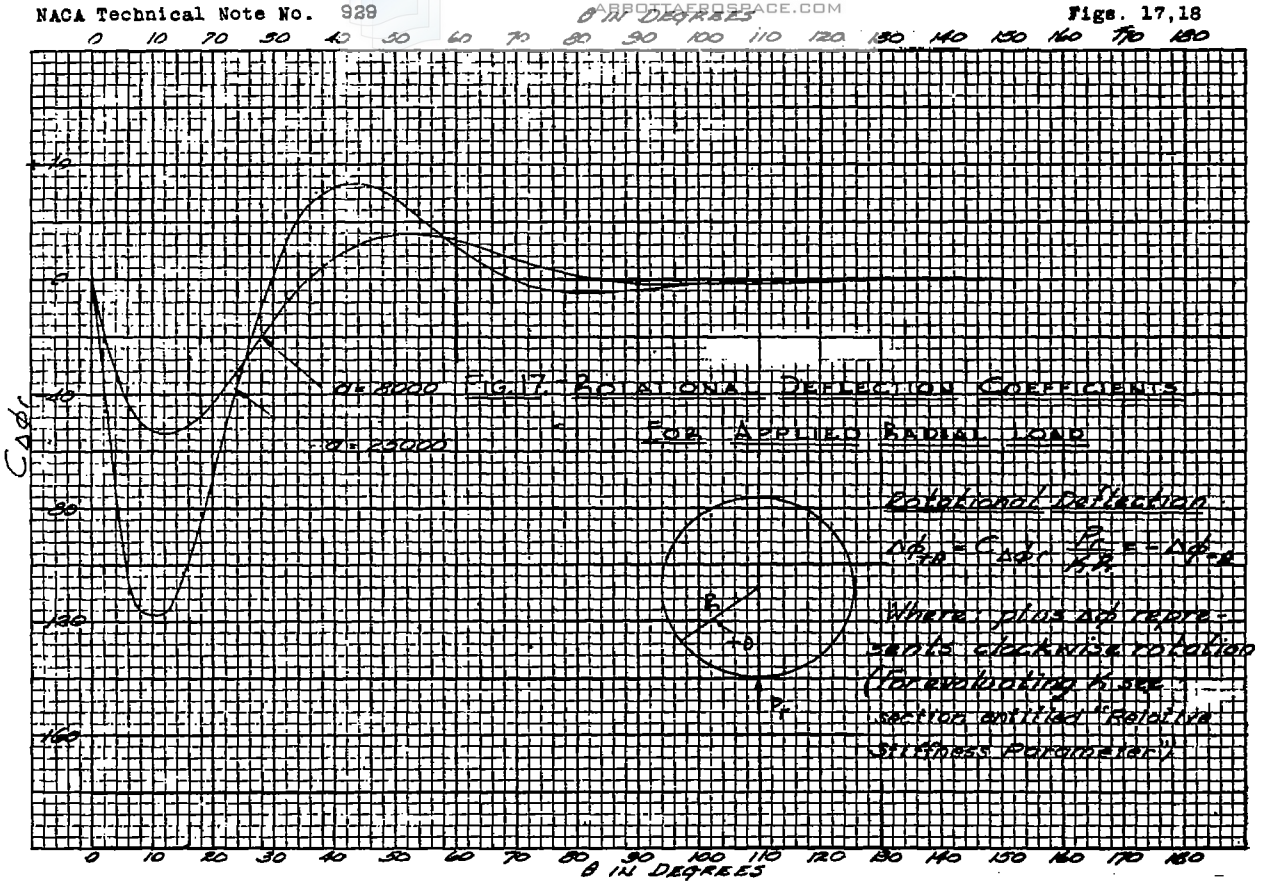

FIG. 17.- ROTATIONAL DEFLECTION COEFFICIENTS FOR AN APPLIED RADIAL LOAD

Rotational Deflection

$$\Delta\phi_{+\theta} = C_{\Delta\phi r} \frac{P_r}{E} \left(\frac{R}{k}\right)^2 = -\Delta\phi_{-\theta}$$

Where plus $\Delta\phi$ represents clockwise rotation (for evaluating k see section entitled "Relative Stiffness Parameter").

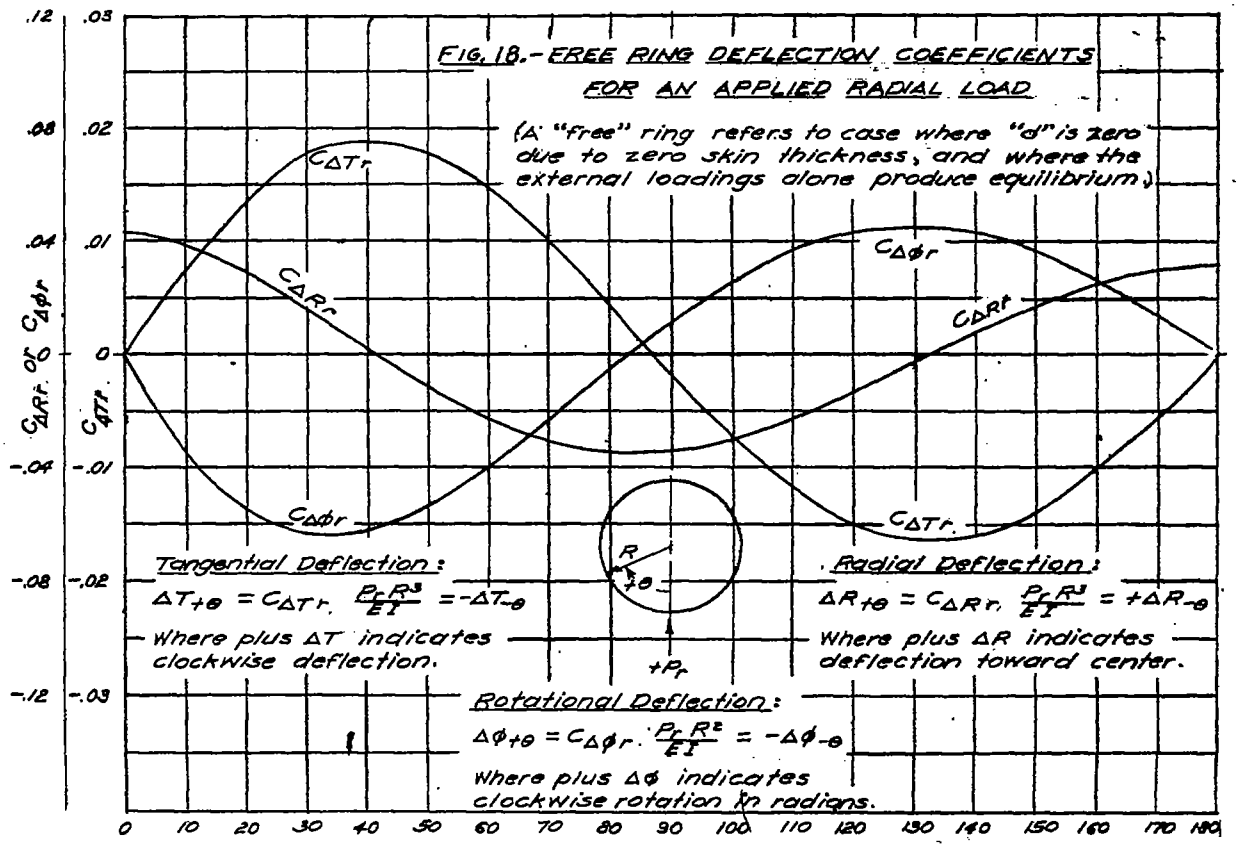

FIG. 18.- FREE RING DEFLECTION COEFFICIENTS FOR AN APPLIED RADIAL LOAD

(A "free" ring refers to case where "d" is zero due to zero skin thickness, and where the external loadings alone produce equilibrium.)

Tangential Deflection:

$$\Delta T_{+\theta} = C_{\Delta Tr} \frac{P_r R^3}{EI} = -\Delta T_{-\theta}$$

Where plus ΔT indicates clockwise deflection.

Radial Deflection:

$$\Delta R_{+\theta} = C_{\Delta Rr} \frac{P_r R^3}{EI} = +\Delta R_{-\theta}$$

Where plus ΔR indicates deflection toward center.

Rotational Deflection:

$$\Delta\phi_{+\theta} = C_{\Delta\phi r} \frac{P_r R^2}{EI} = -\Delta\phi_{-\theta}$$

Where plus $\Delta\phi$ indicates clockwise rotation in radians.

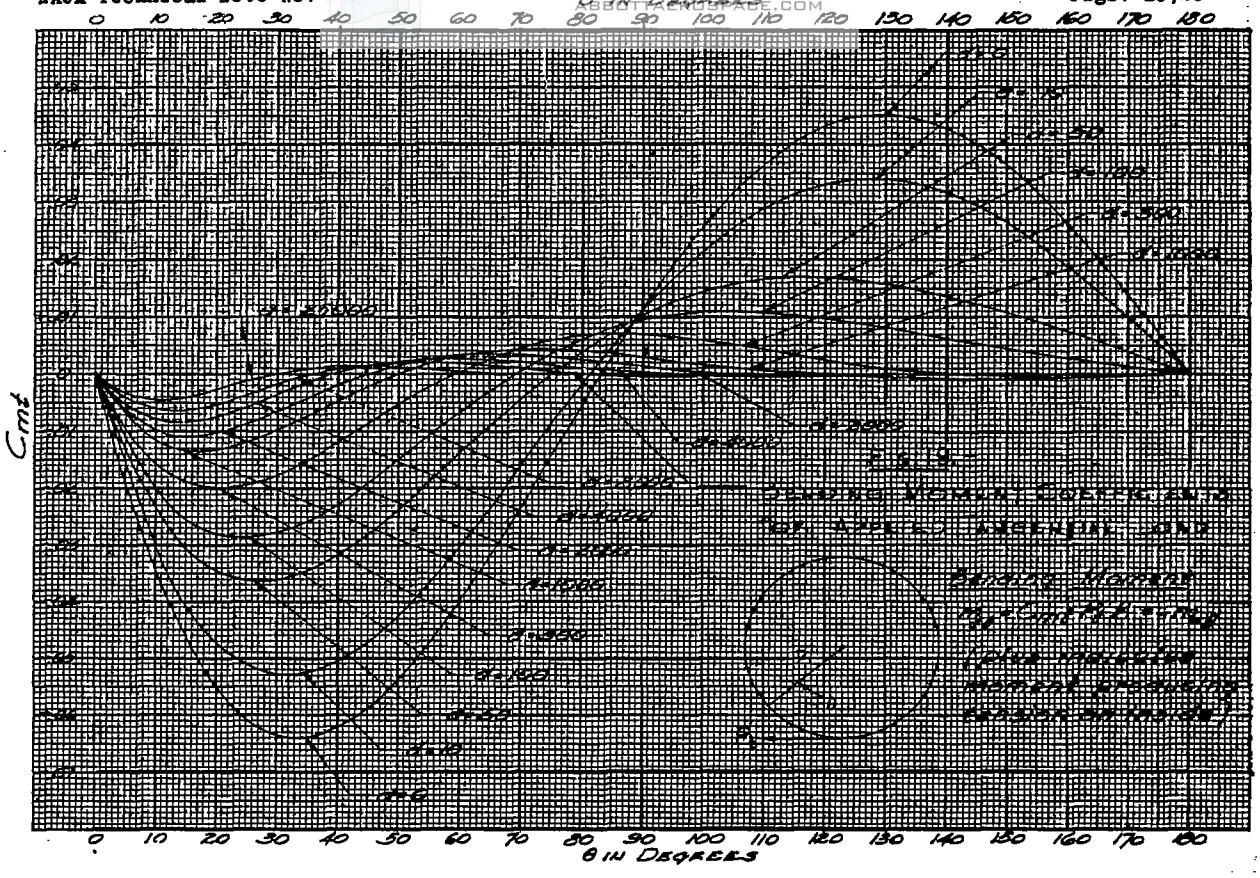

Fig. 19.- Bending moment coefficients for applied tangential load.

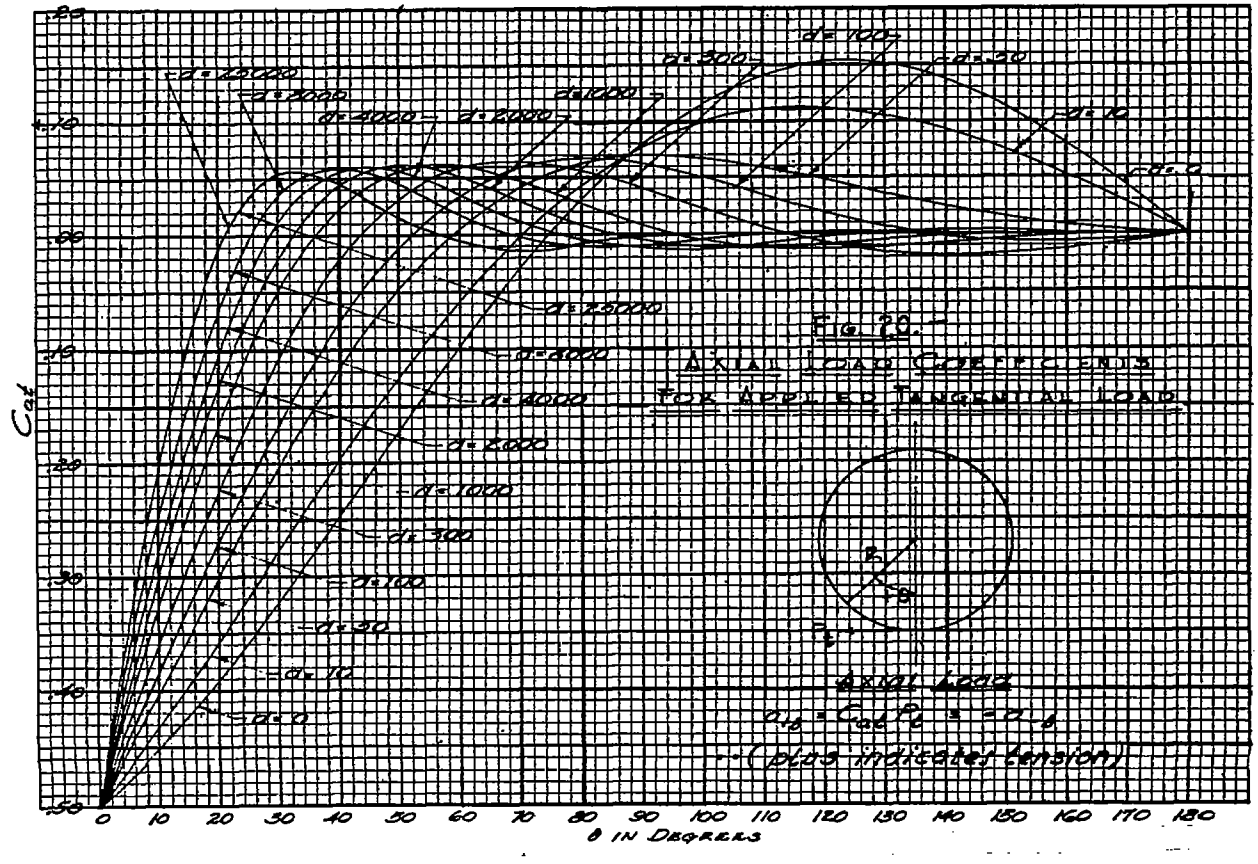

Fig. 20.- Axial load coefficients for applied tangential load.

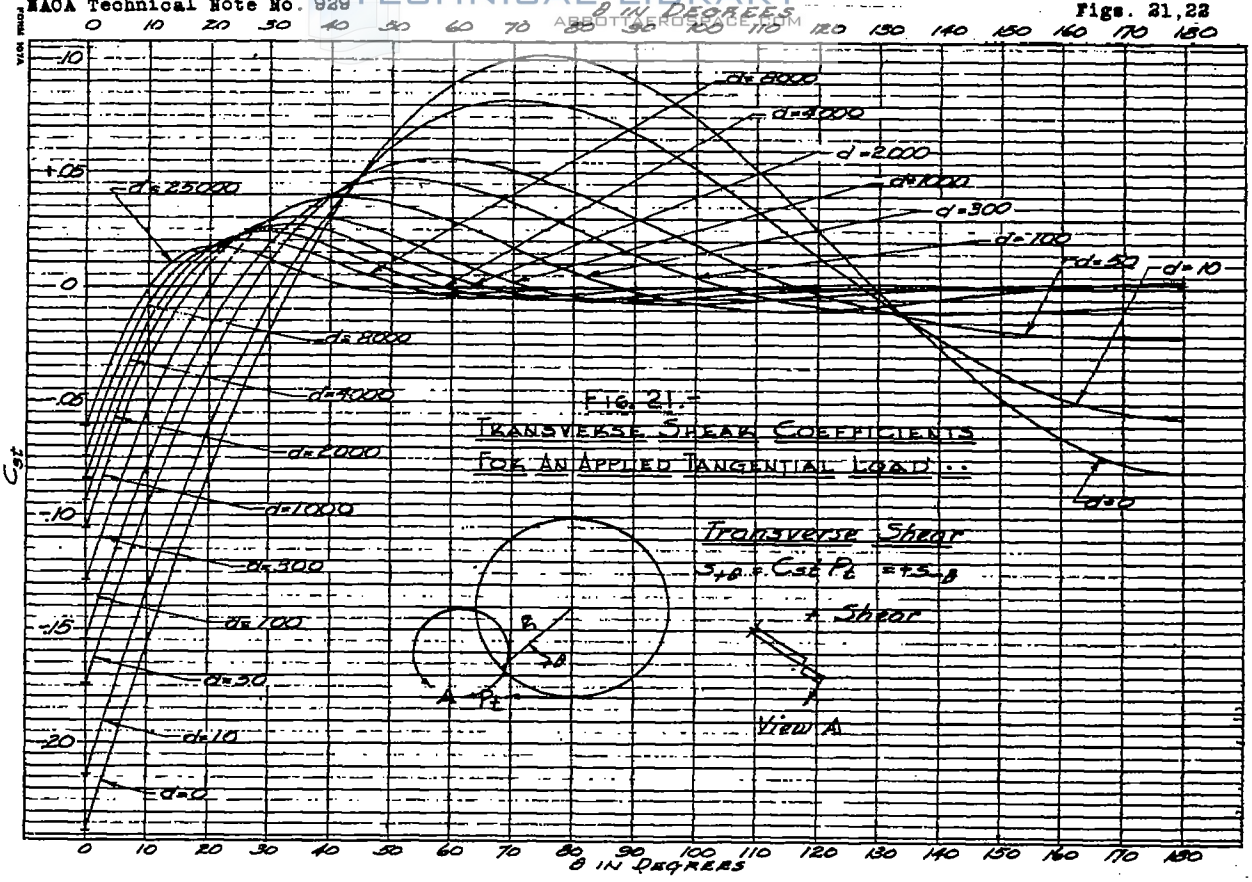

FIG. 21.- TRANSVERSE SHEAR COEFFICIENTS FOR AN APPLIED TANGENTIAL LOAD.

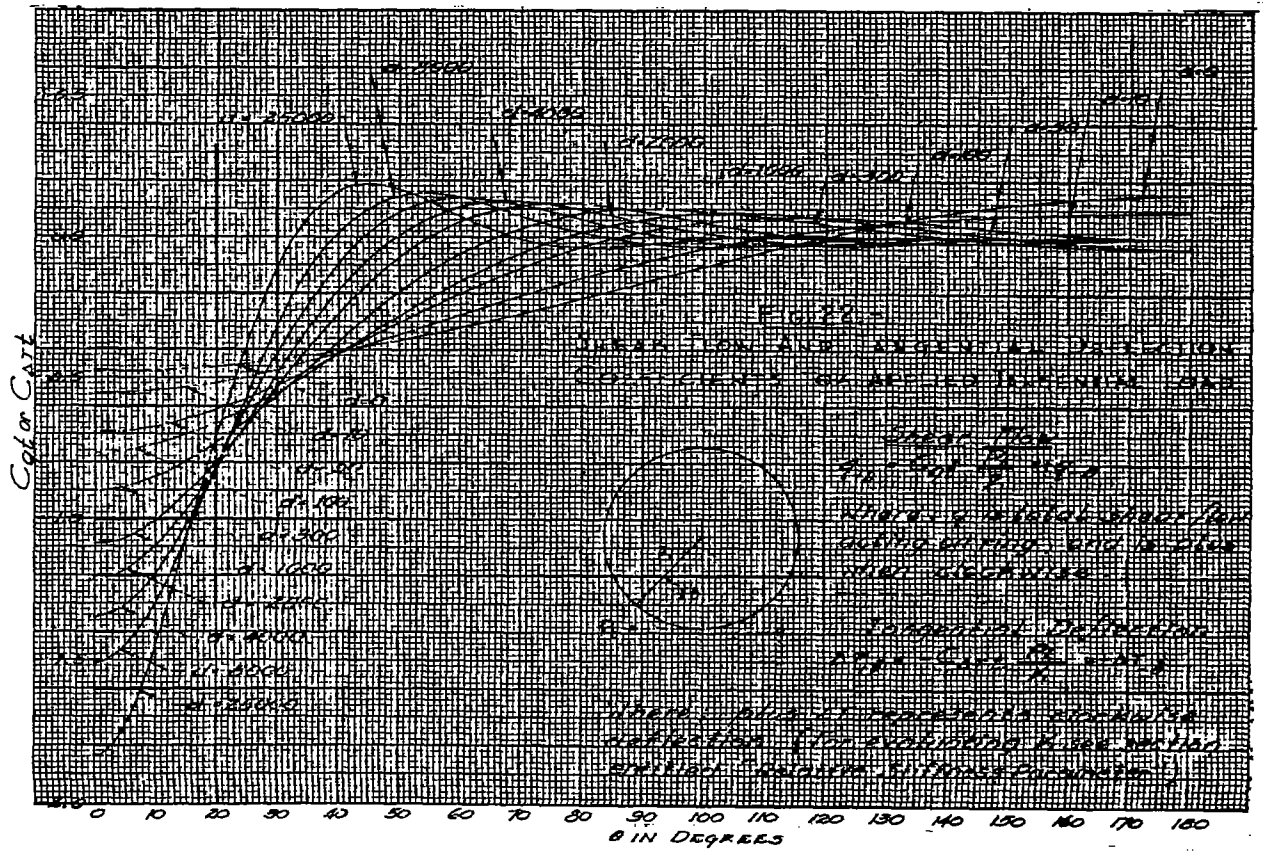

FIG. 22.- SHEAR FLOW AND RADIAL DEFLECTION COEFFICIENTS OF APPLIED TANGENTIAL LOAD

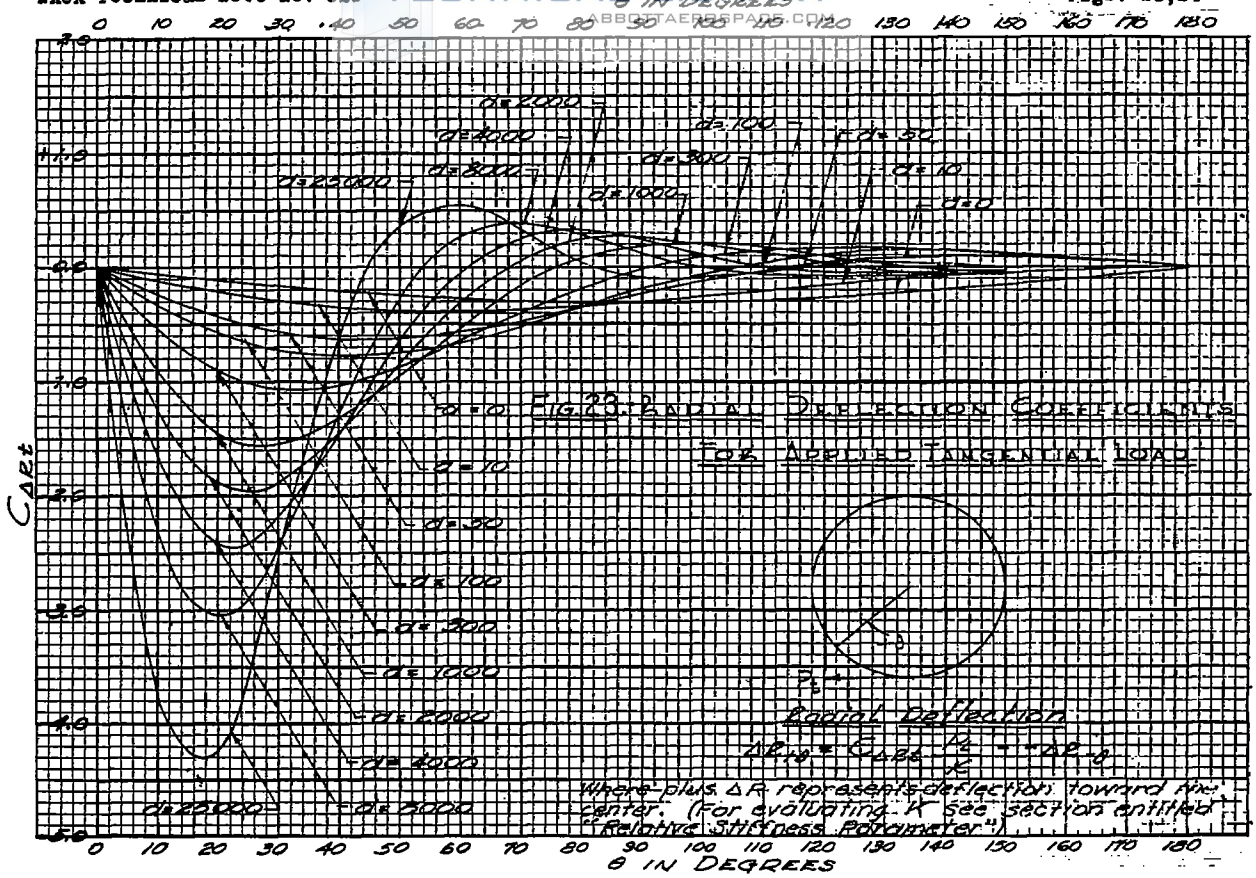

FIG. 23. RADIAL DEFLECTION COEFFICIENTS FOR APPLIED TANGENTIAL LOAD

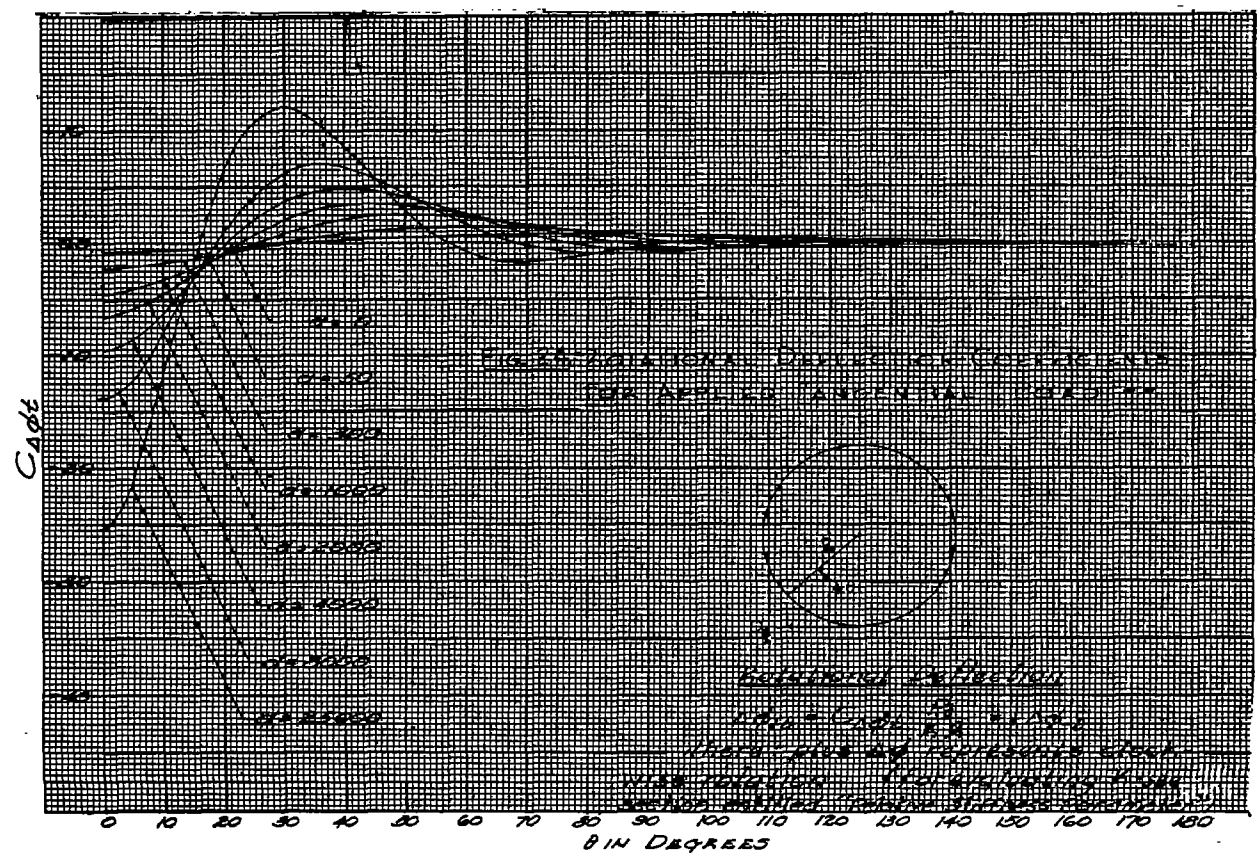

FIGS. 24. TANGENTIAL DEFLECTION COEFFICIENTS FOR APPLIED TANGENTIAL LOAD

FIG. 25.- FREE RING DEFLECTION COEFFICIENTS FOR AN APPLIED TANGENTIAL LOAD

(A "free" ring refers to case where "d" is zero due to zero skin thickness, and where the external loadings alone produce equilibrium.)

$C_{\Delta Tt}$, $C_{\Delta Rt}$ or $C_{\Delta\phi t}$

$C_{\Delta Tt}$

$C_{\Delta Rt}$

$C_{\Delta\phi t}$

Tangential Deflection:

$\Delta T_{+\theta} = C_{\Delta Tt} \frac{P_t R^3}{EI} = +\Delta T_{-\theta}$

Where plus ΔT indicates clockwise deflection.

Radial Deflection:

$\Delta R_{+\theta} = C_{\Delta Rt} \frac{P_t R^3}{EI} = -\Delta R_{-\theta}$

Where plus ΔR indicates deflection toward center.

Rotational Deflection:

$\Delta\phi_{+\theta} = C_{\Delta\phi t} \frac{P_t R^2}{EI} = +\Delta\phi_{-\theta}$

Where plus $\Delta\phi$ indicates clockwise rotation in radians.

$+P_t$, R, $+\theta$

θ IN DEGREES

FIG. 26.- BENDING MOMENT COEFFICIENTS FOR APPLIED MOMENT LOAD

C_{mm}

$+M$, $+\theta$

Bending Moment

$m_{+\theta} = C_{mm} M = m_{-\theta}$

(Plus indicates moment producing tension on inside)

d=0, d=10, d=30, d=100, d=300, d=1000, d=3000, d=10000, d=30000, d=100000

θ IN DEGREES

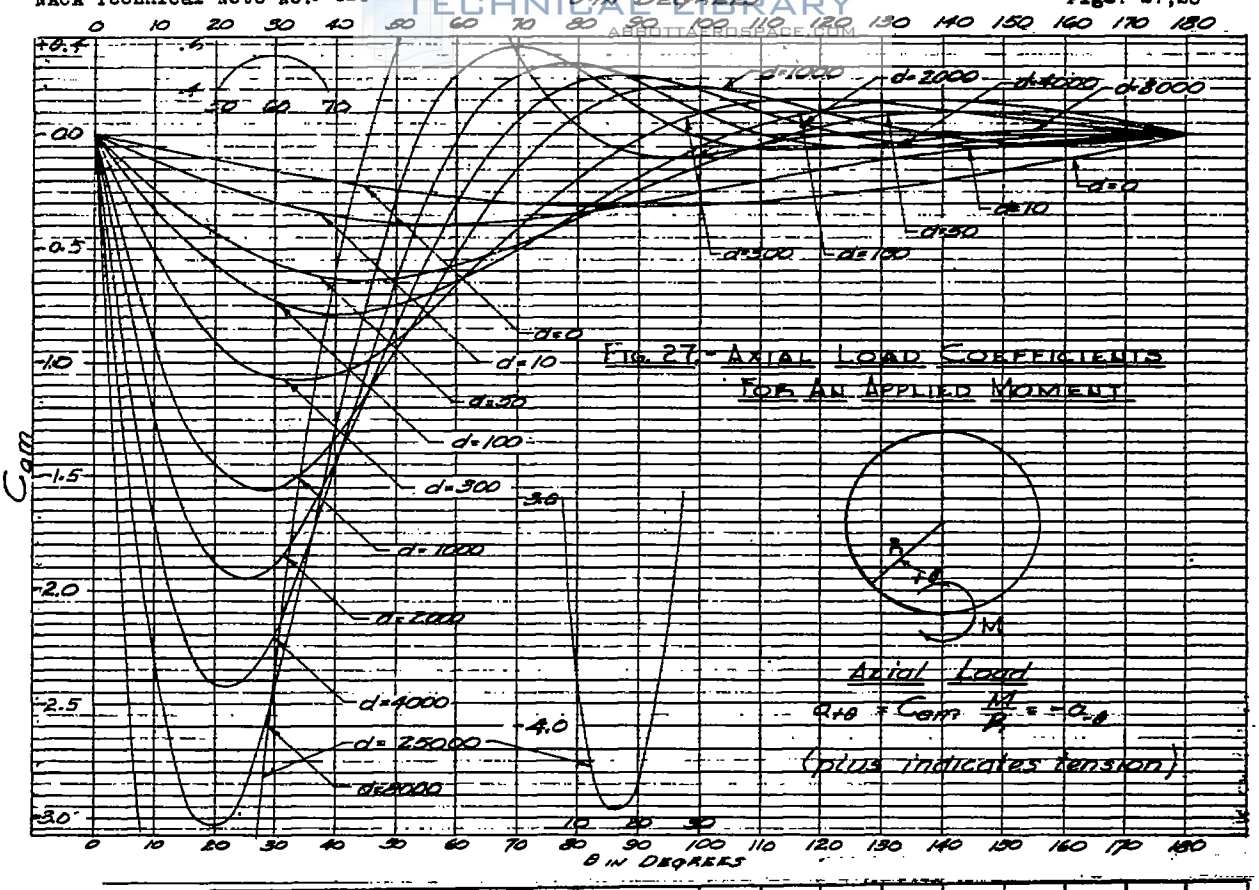

FIG. 27.- AXIAL LOAD COEFFICIENTS FOR AN APPLIED MOMENT

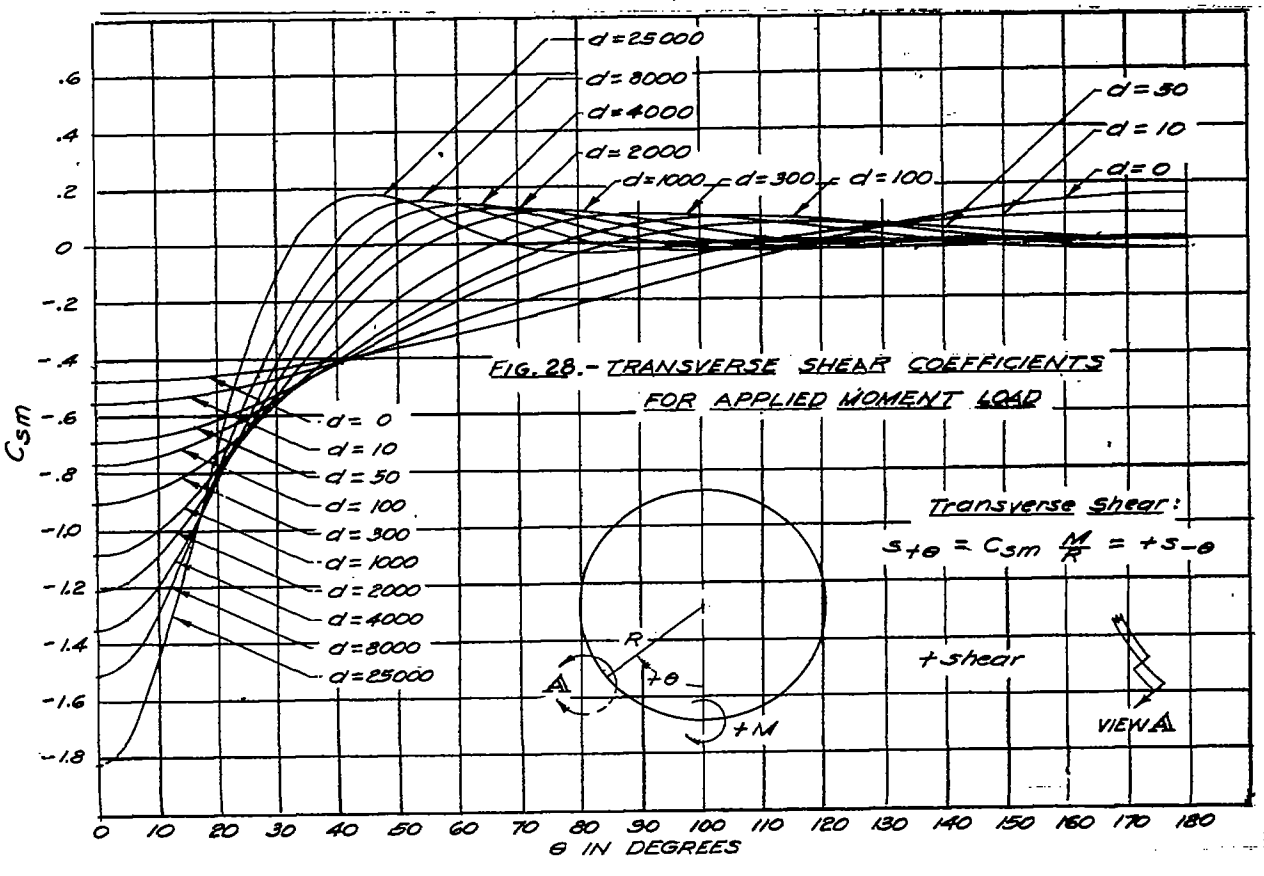

FIG. 28.- TRANSVERSE SHEAR COEFFICIENTS FOR APPLIED MOMENT LOAD

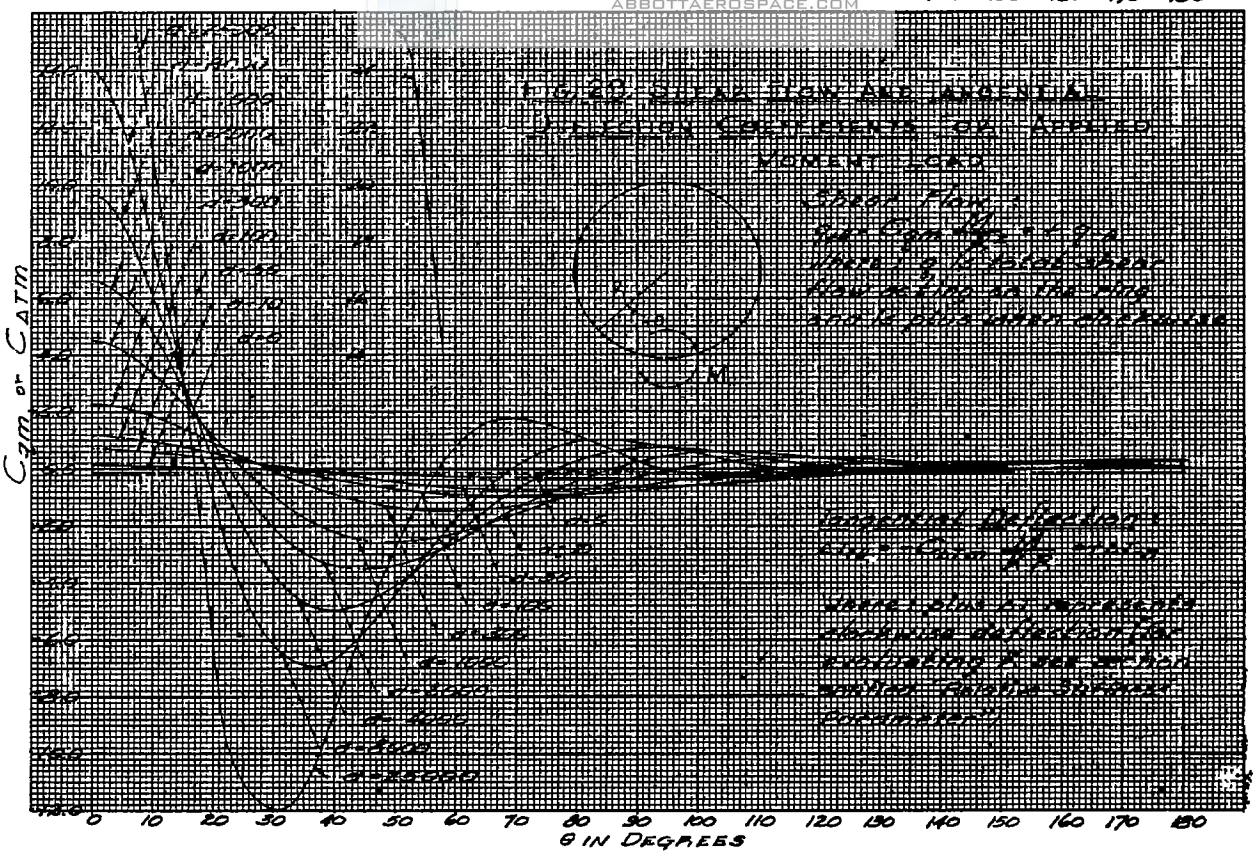

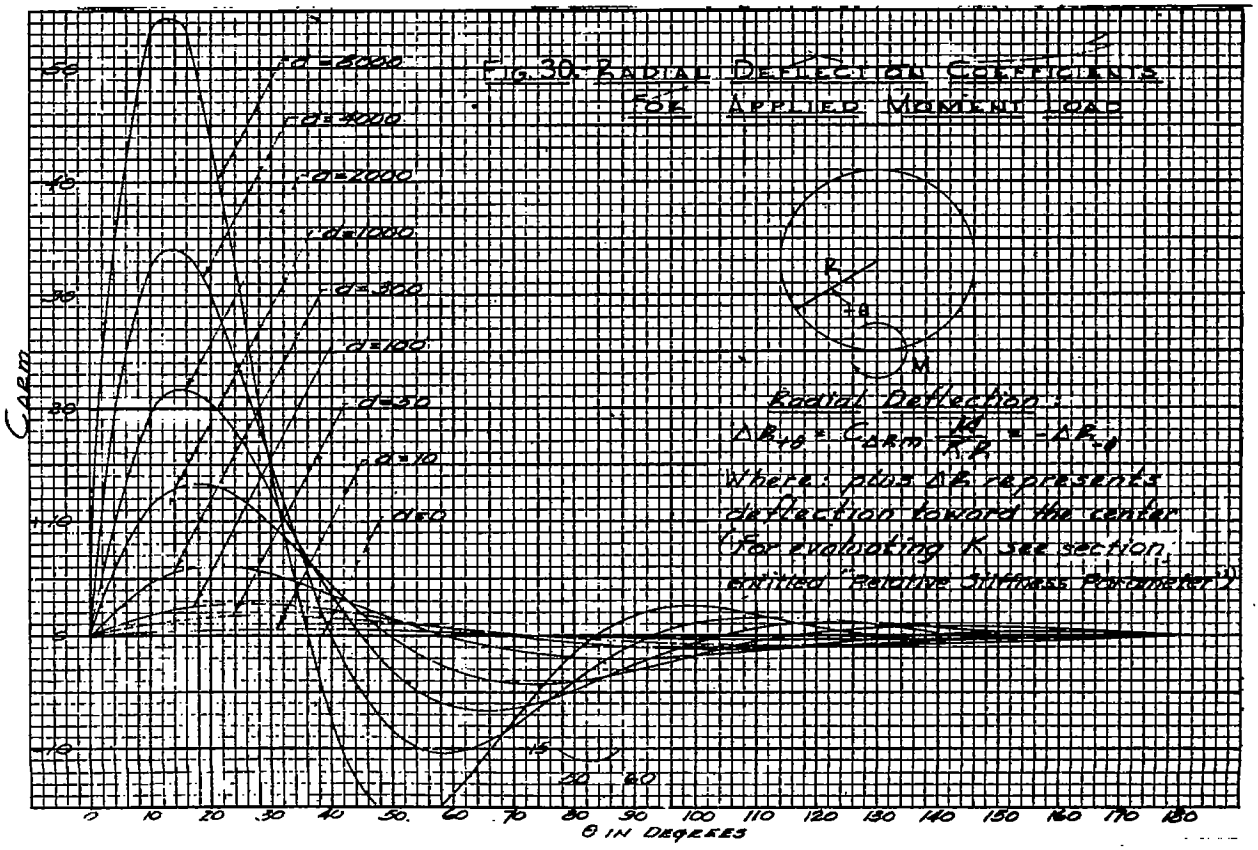

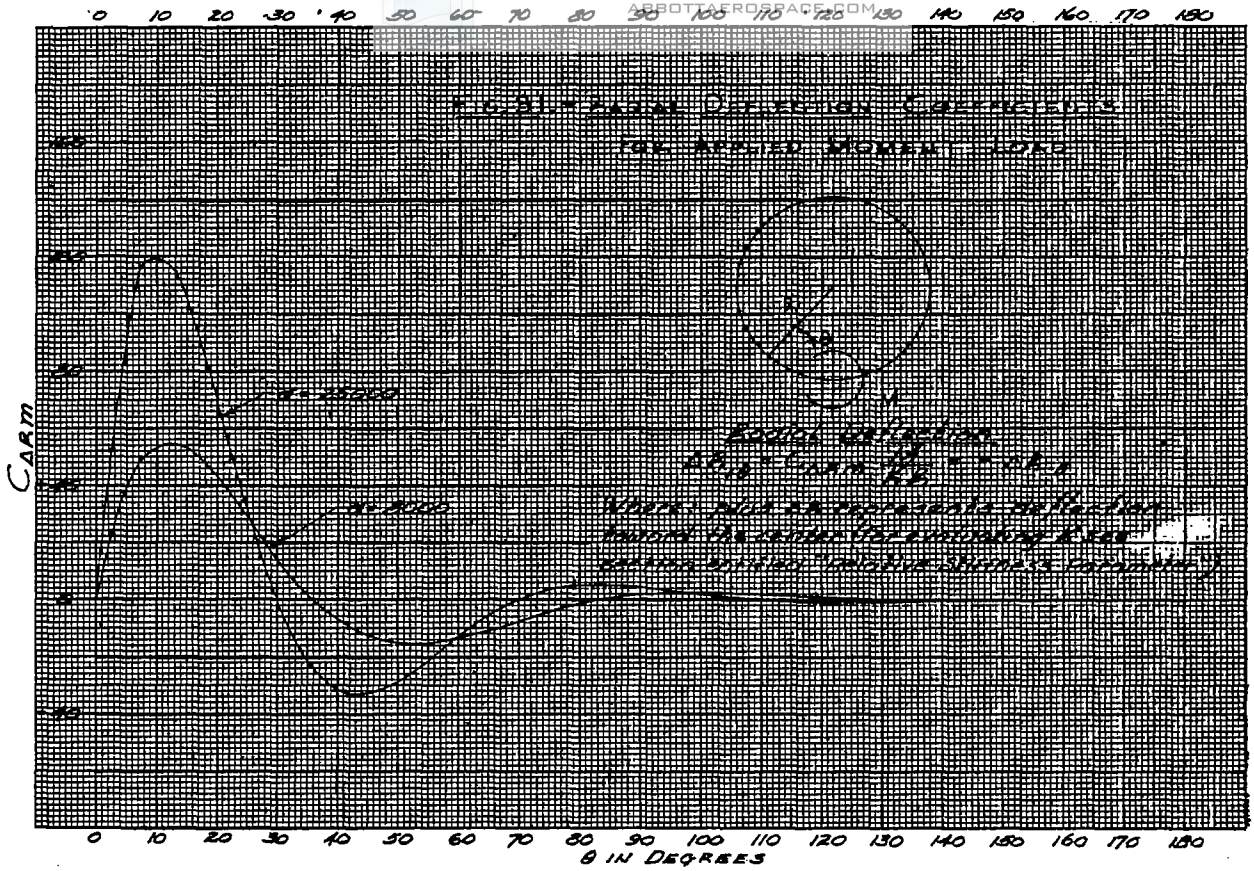

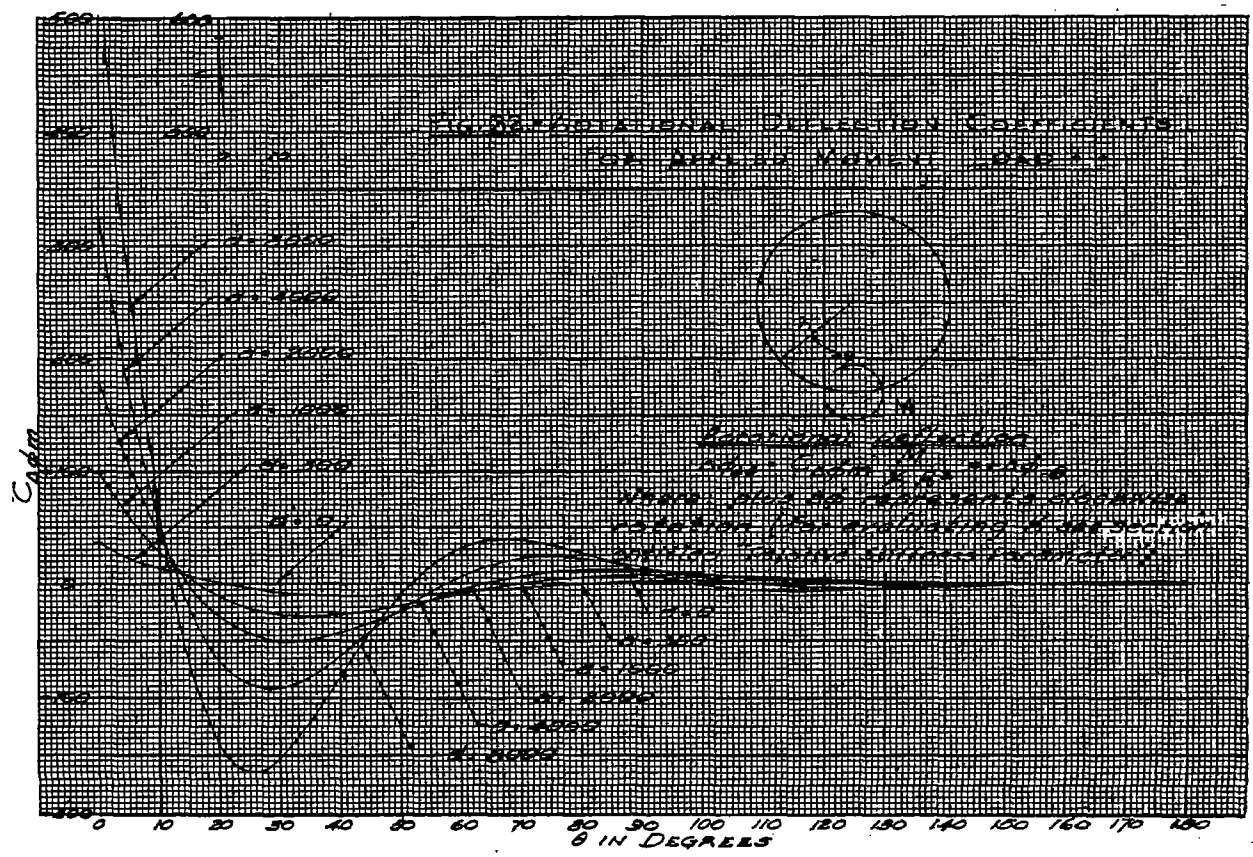

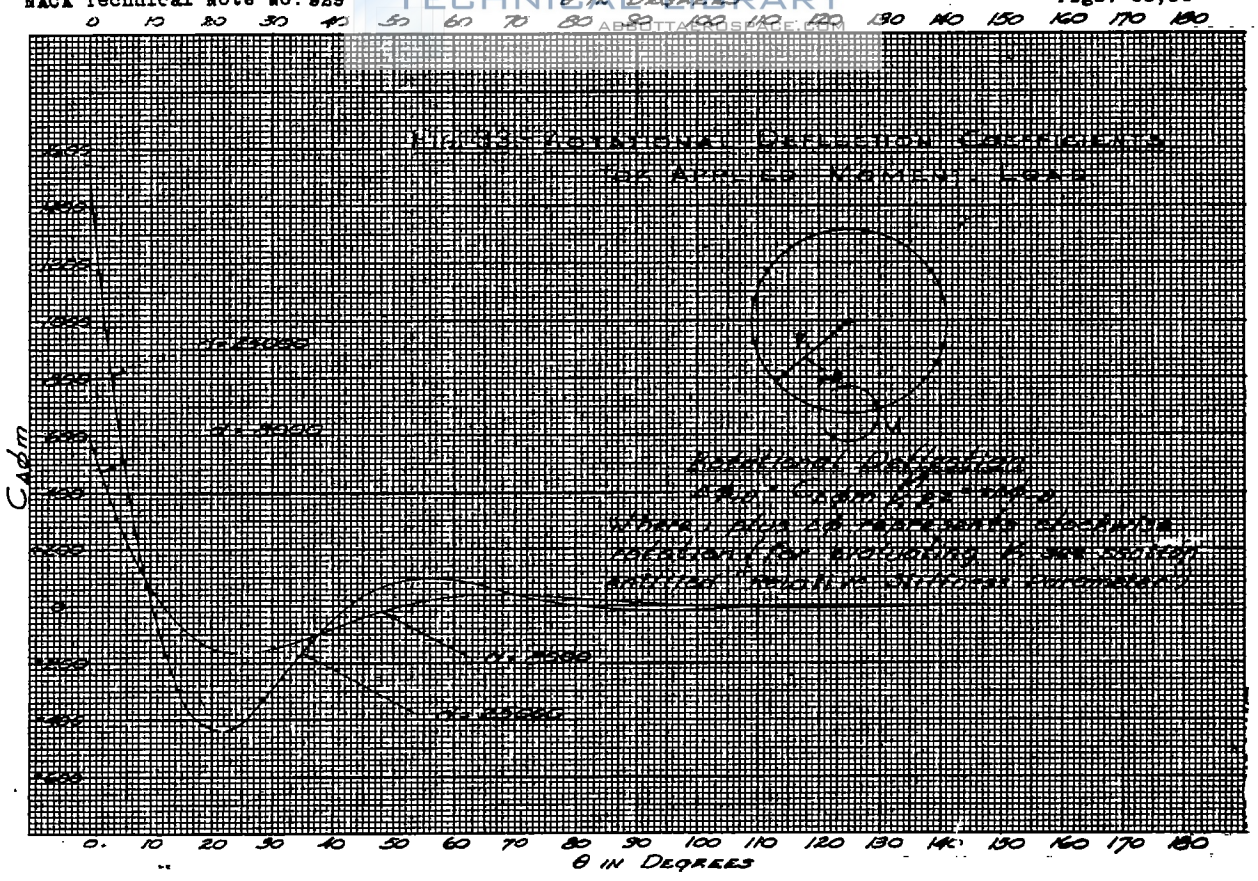

FIG. 33.- FIXED END DEFLECTION COEFFICIENTS FOR AN APPLIED MOMENT LOAD

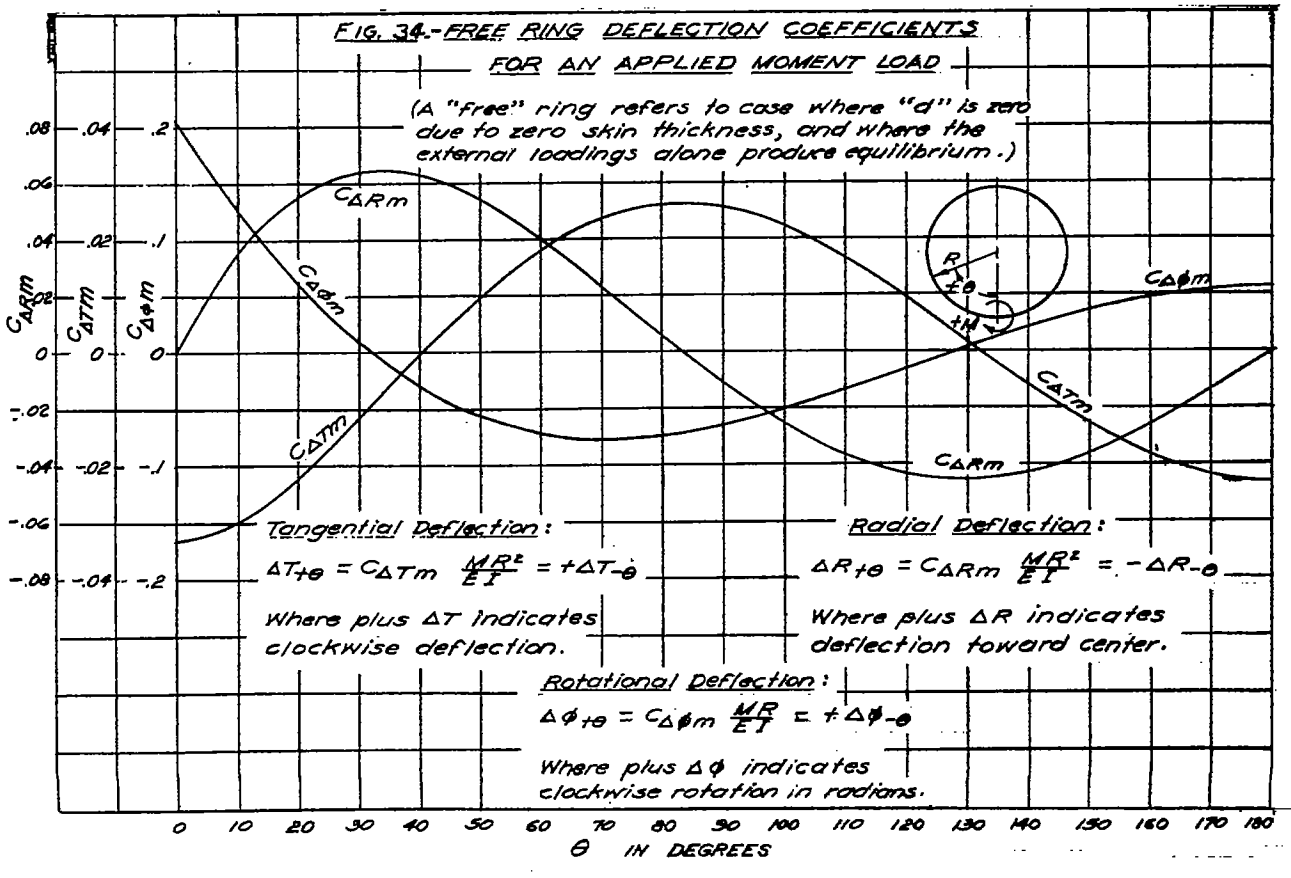

FIG. 35. - BENDING MOMENT COEFFICIENTS FOR SYMMETRICALLY APPLIED ROTATION

$\phi = 180°$

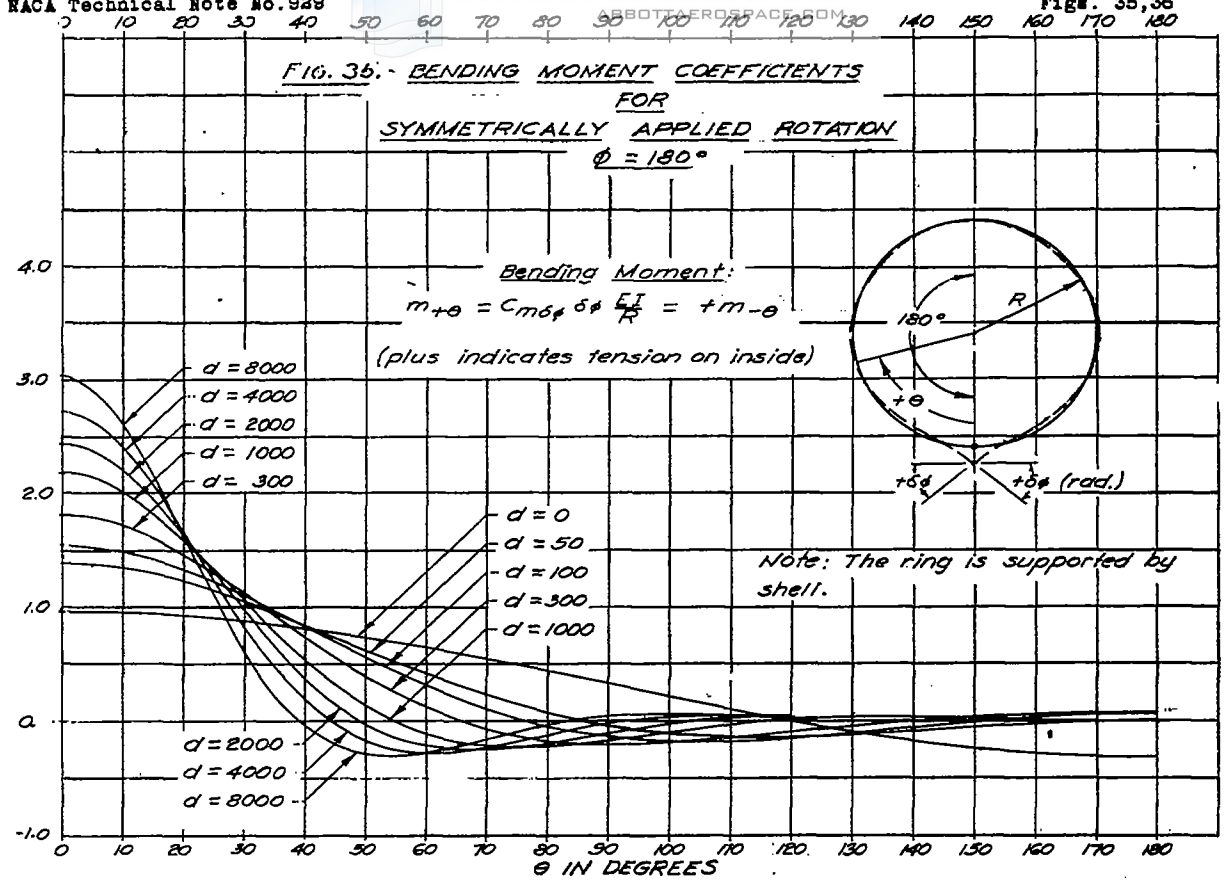

FIG. 36. - AXIAL LOAD COEFFICIENTS FOR SYMMETRICALLY APPLIED ROTATION

$\phi = 180°$

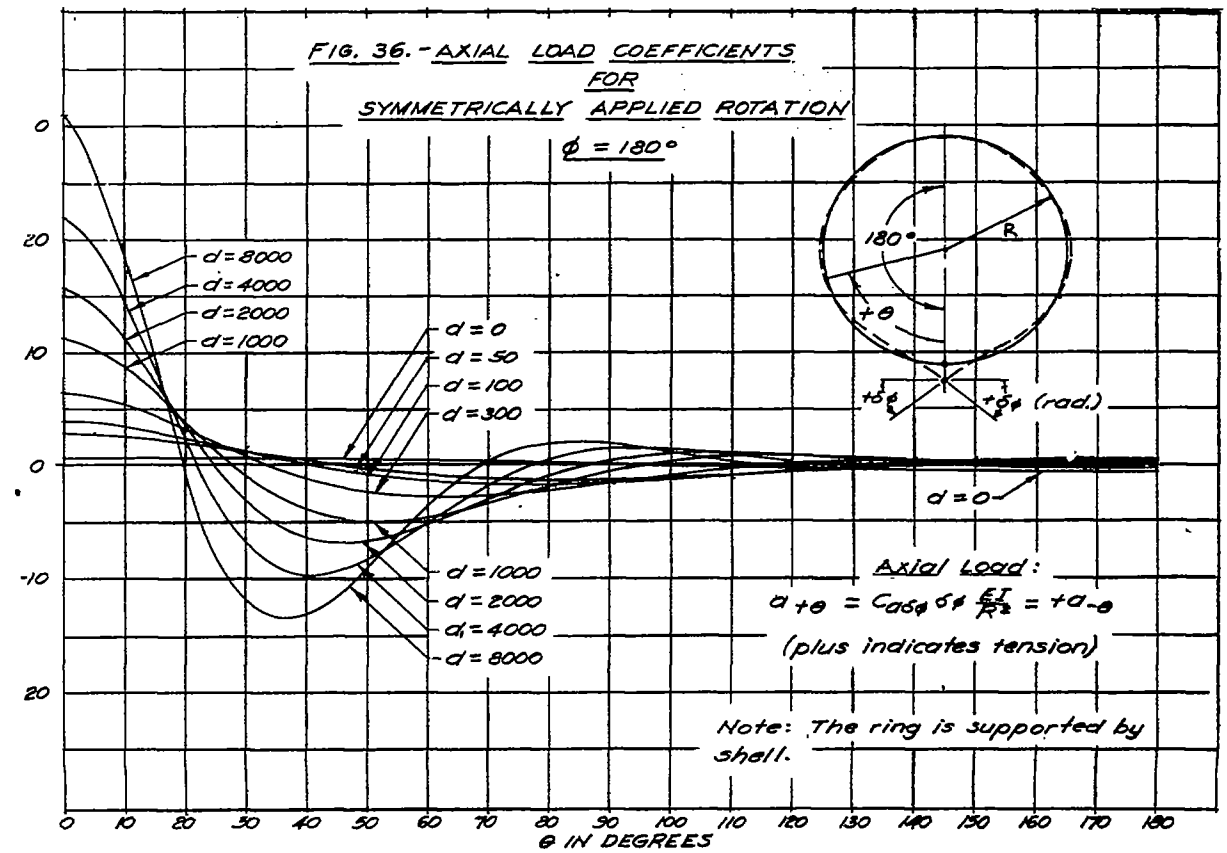

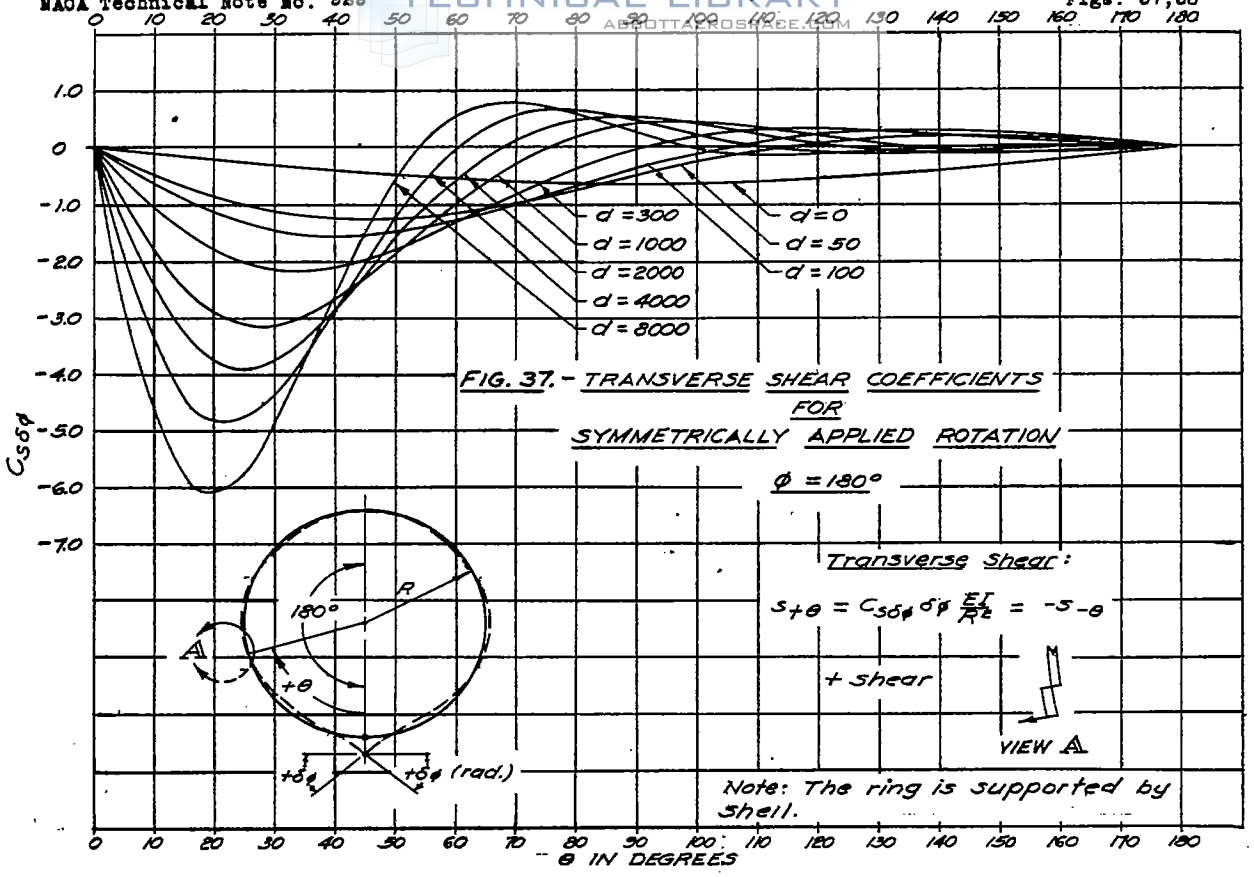

FIG. 37.- TRANSVERSE SHEAR COEFFICIENTS FOR SYMMETRICALLY APPLIED ROTATION

$\phi = 180°$

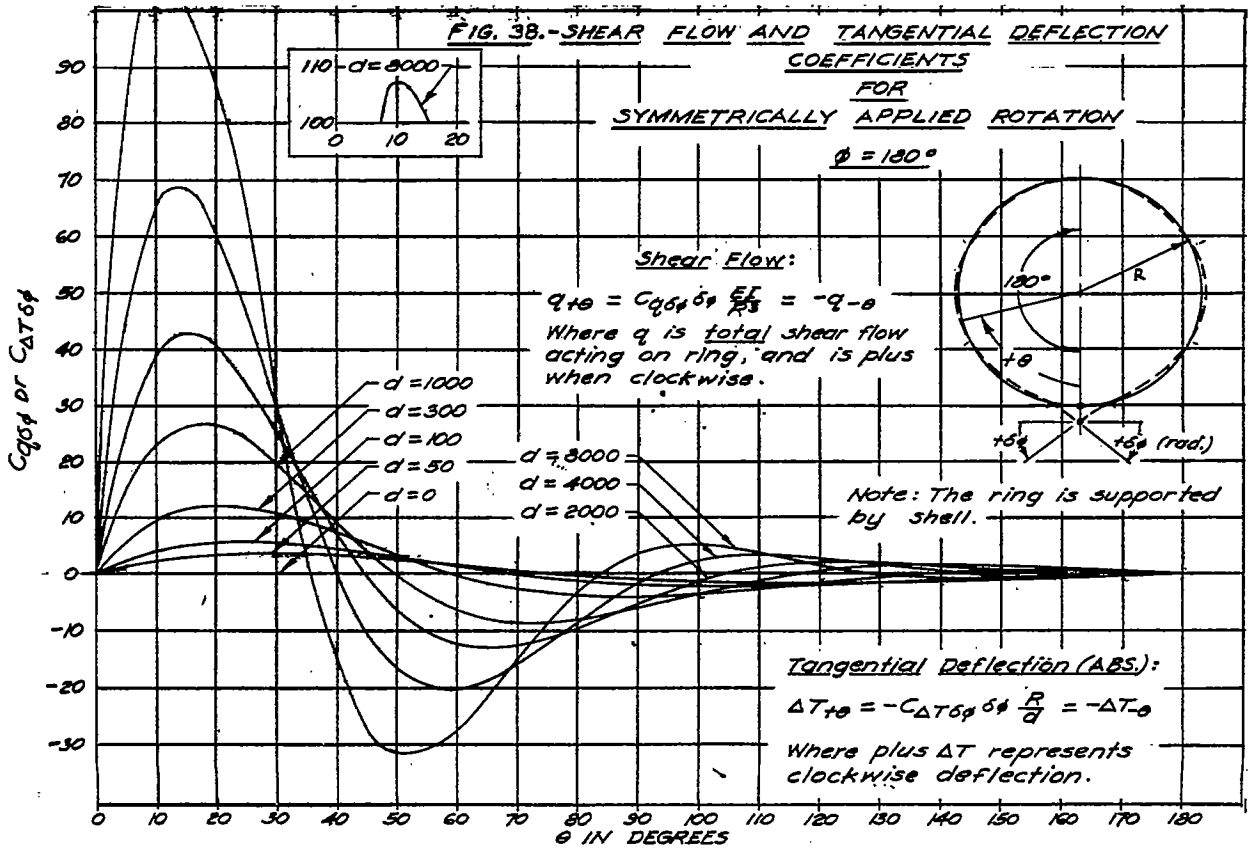

FIG. 38.- SHEAR FLOW AND TANGENTIAL DEFLECTION COEFFICIENTS FOR SYMMETRICALLY APPLIED ROTATION

$\phi = 180°$

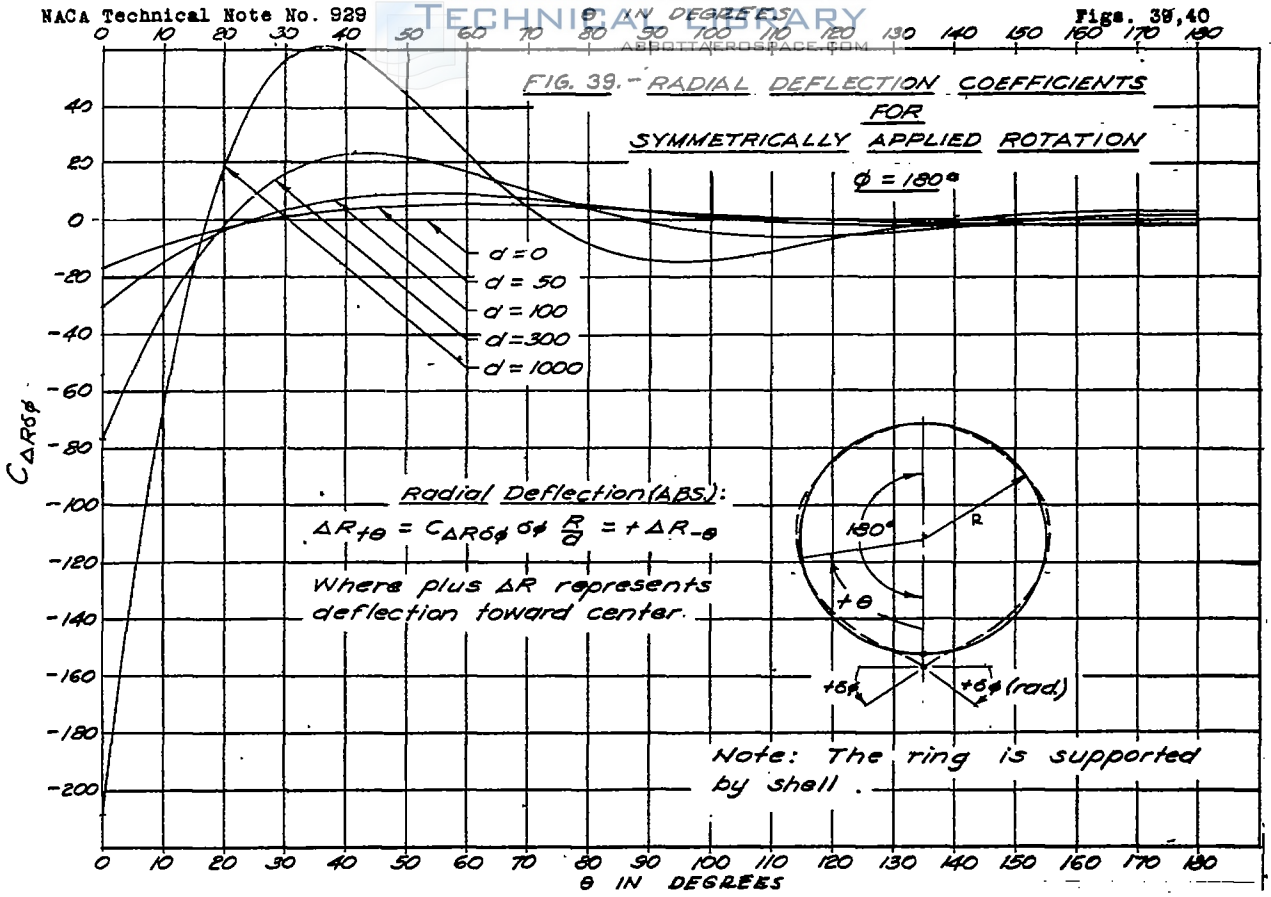

FIG. 39.- RADIAL DEFLECTION COEFFICIENTS FOR SYMMETRICALLY APPLIED ROTATION

$\phi = 180°$

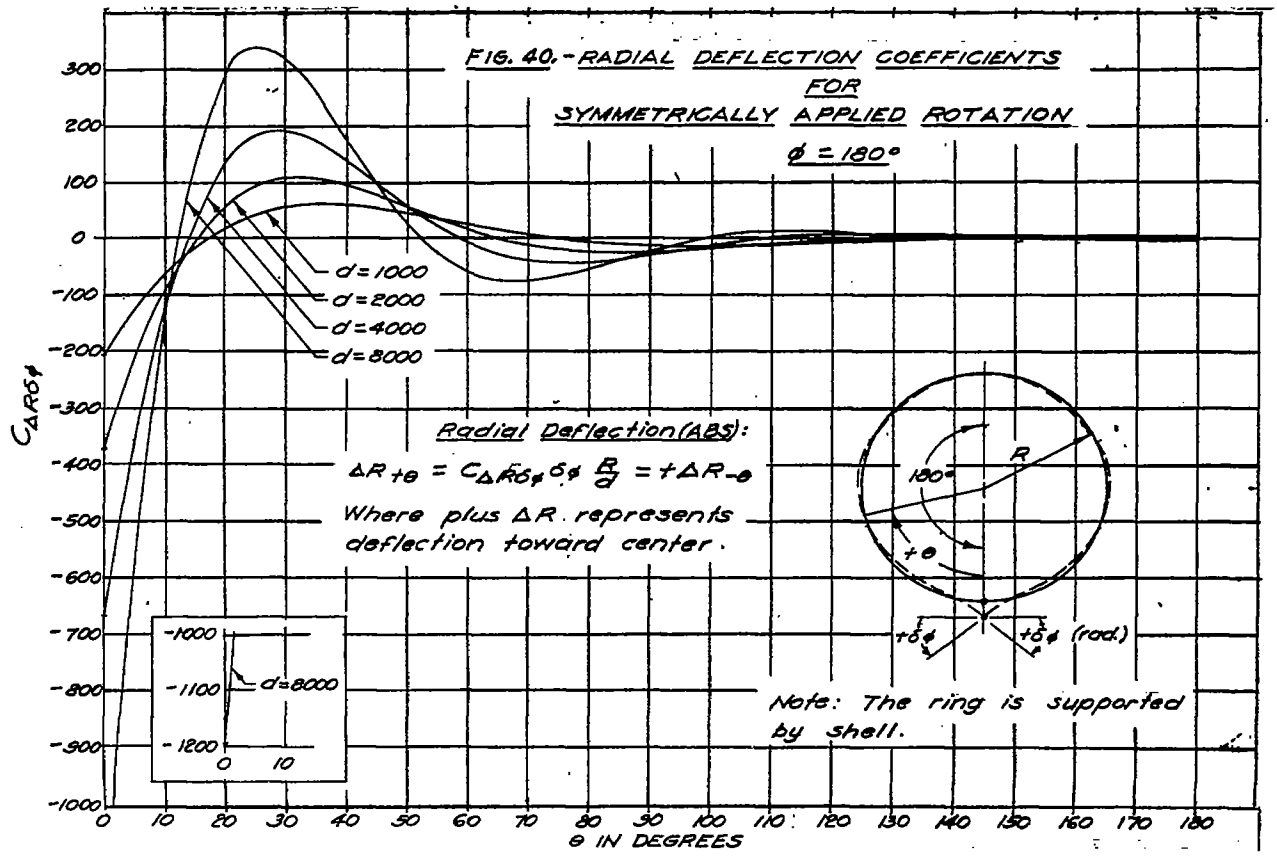

FIG. 40.- RADIAL DEFLECTION COEFFICIENTS FOR SYMMETRICALLY APPLIED ROTATION

$\phi = 180°$

FIG. 41.- ROTATIONAL DEFLECTION COEFFICIENTS FOR SYMMETRICALLY APPLIED ROTATION

$\phi = 180°$

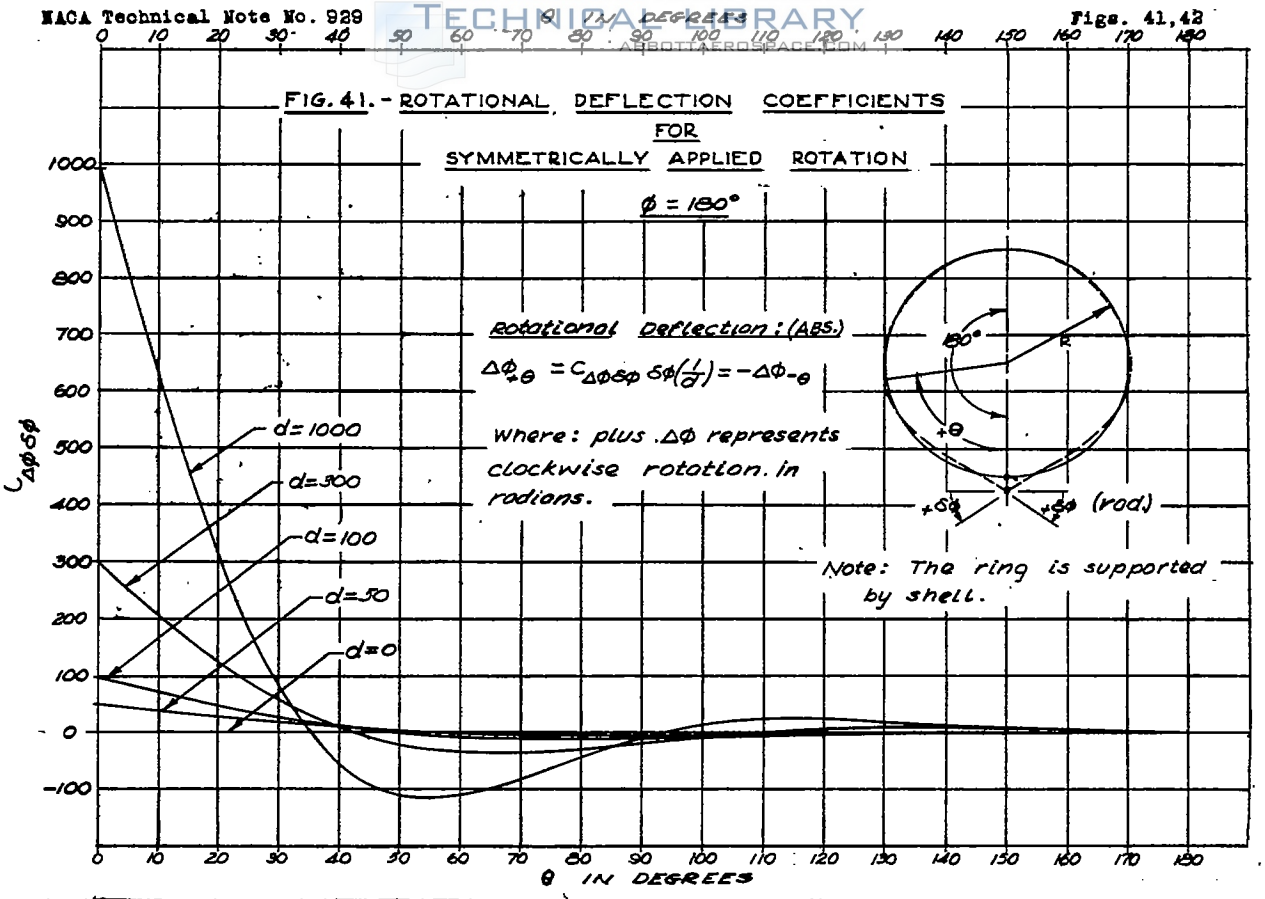

FIG. 42.- ROTATIONAL DEFLECTION COEFFICIENTS FOR SYMMETRICALLY APPLIED ROTATION

$\phi = 180°$

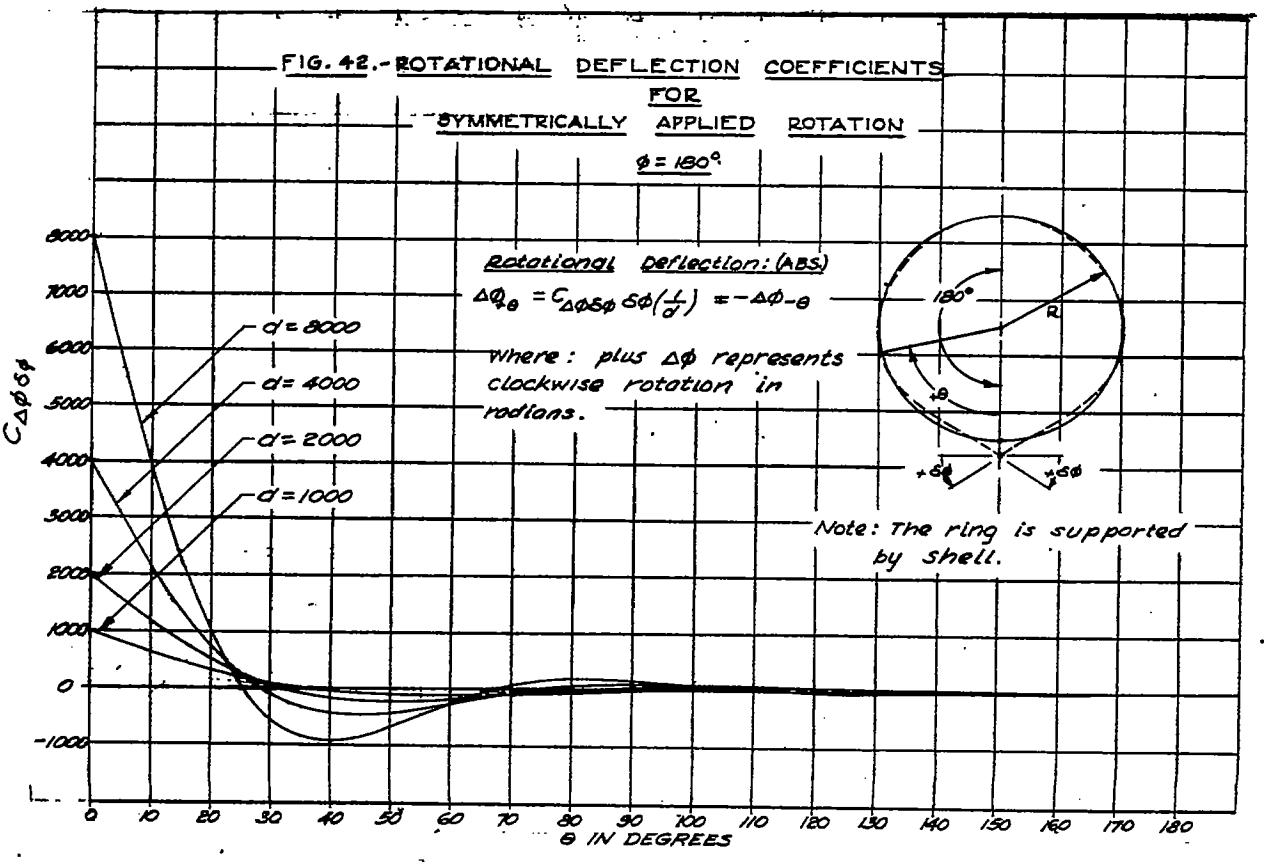

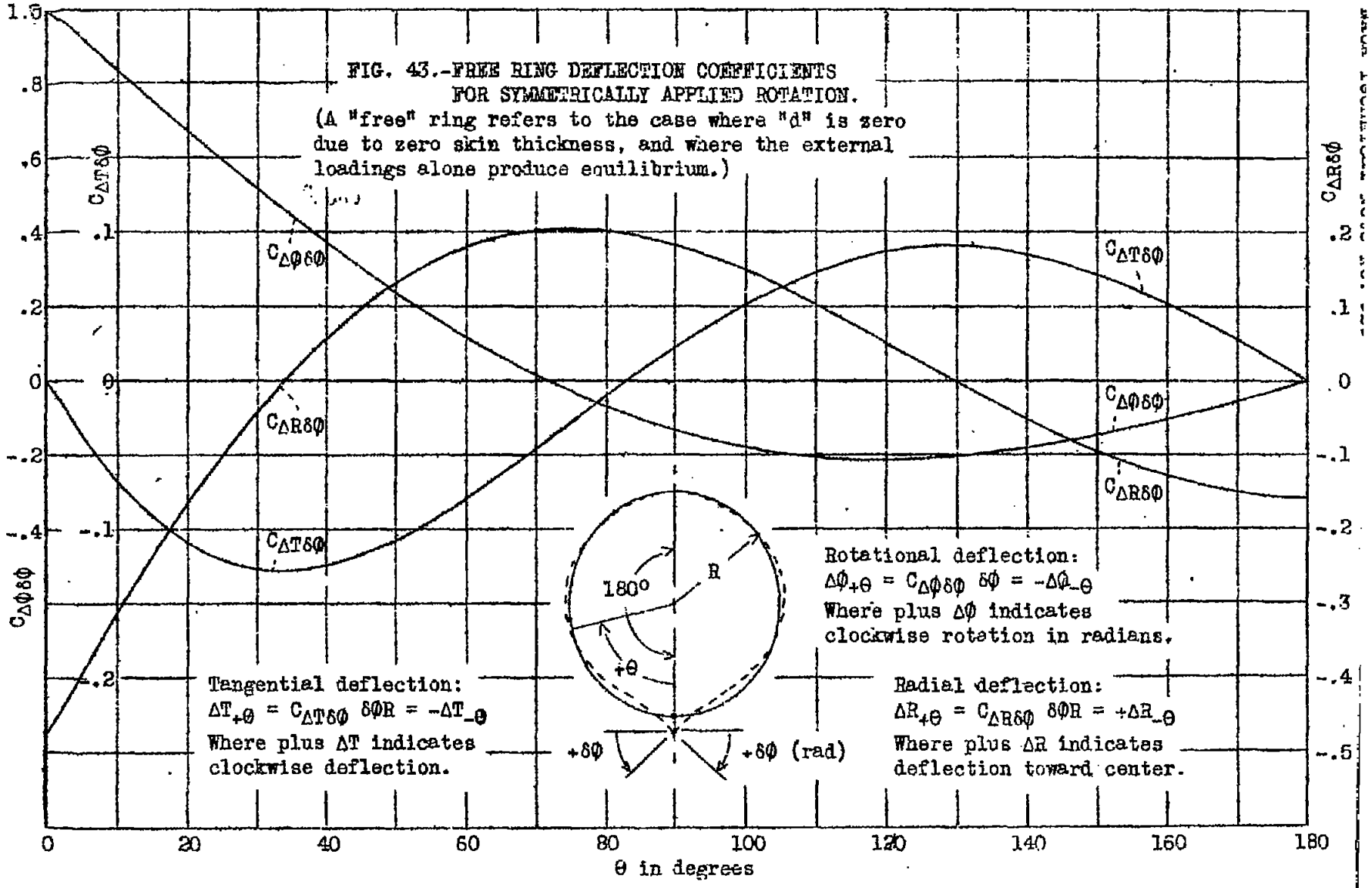

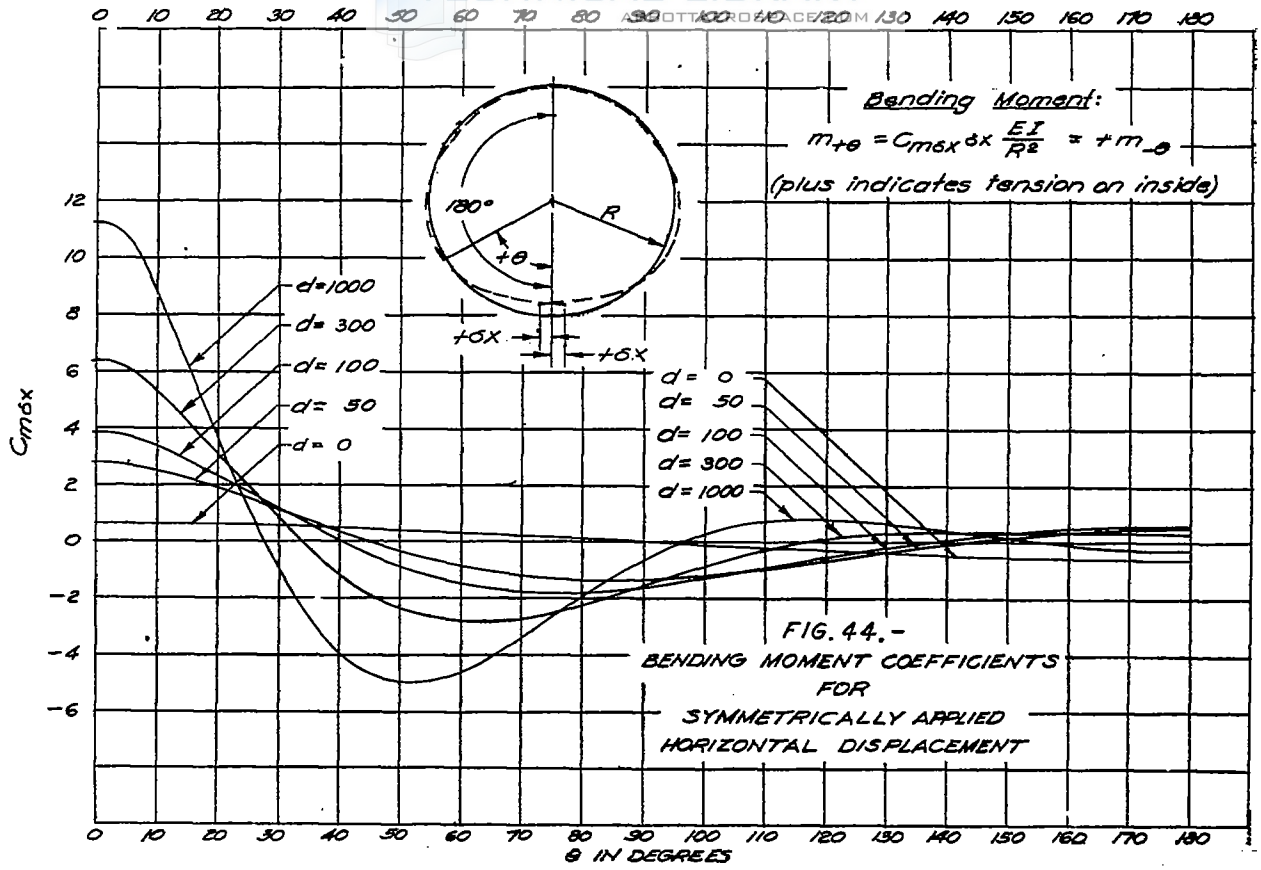

FIG. 44.- BENDING MOMENT COEFFICIENTS FOR SYMMETRICALLY APPLIED HORIZONTAL DISPLACEMENT

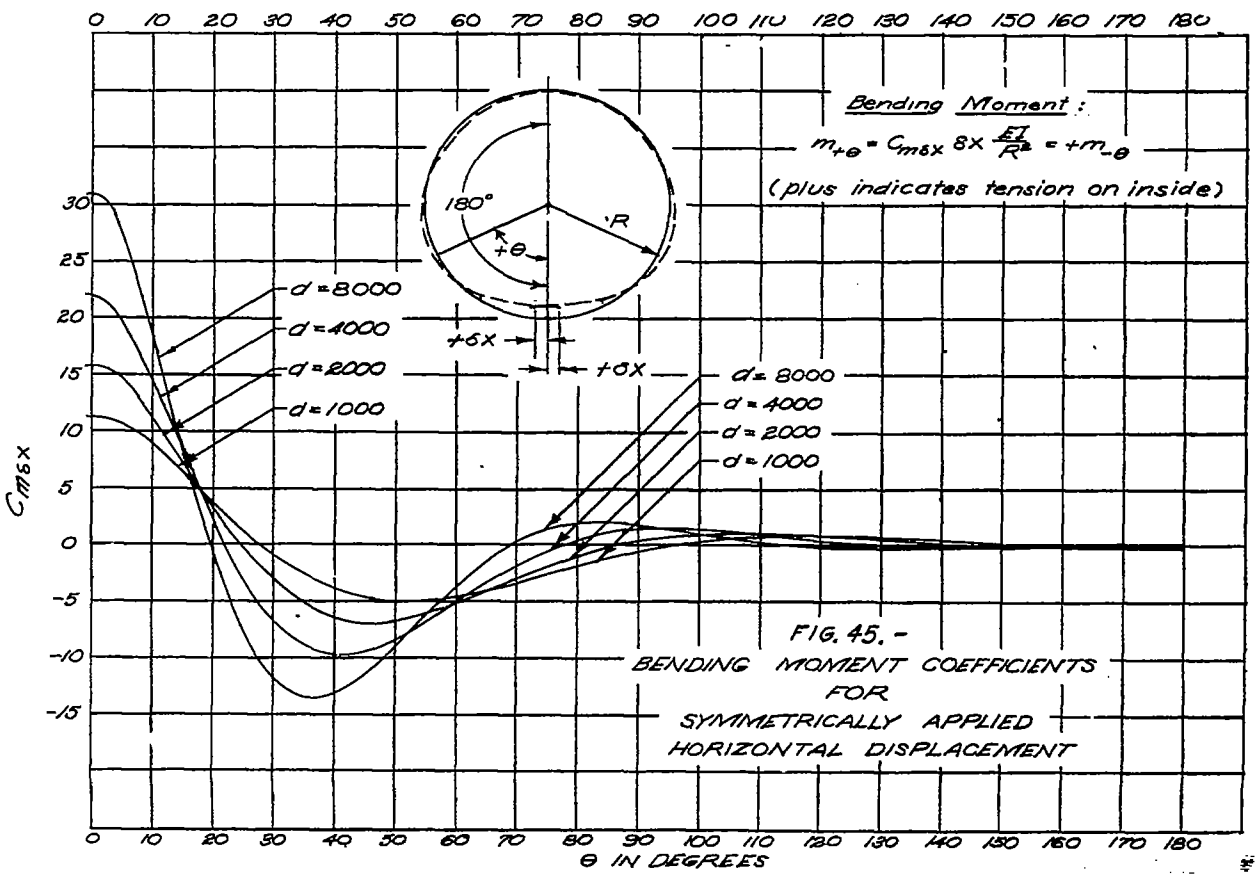

FIG. 45.- BENDING MOMENT COEFFICIENTS FOR SYMMETRICALLY APPLIED HORIZONTAL DISPLACEMENT

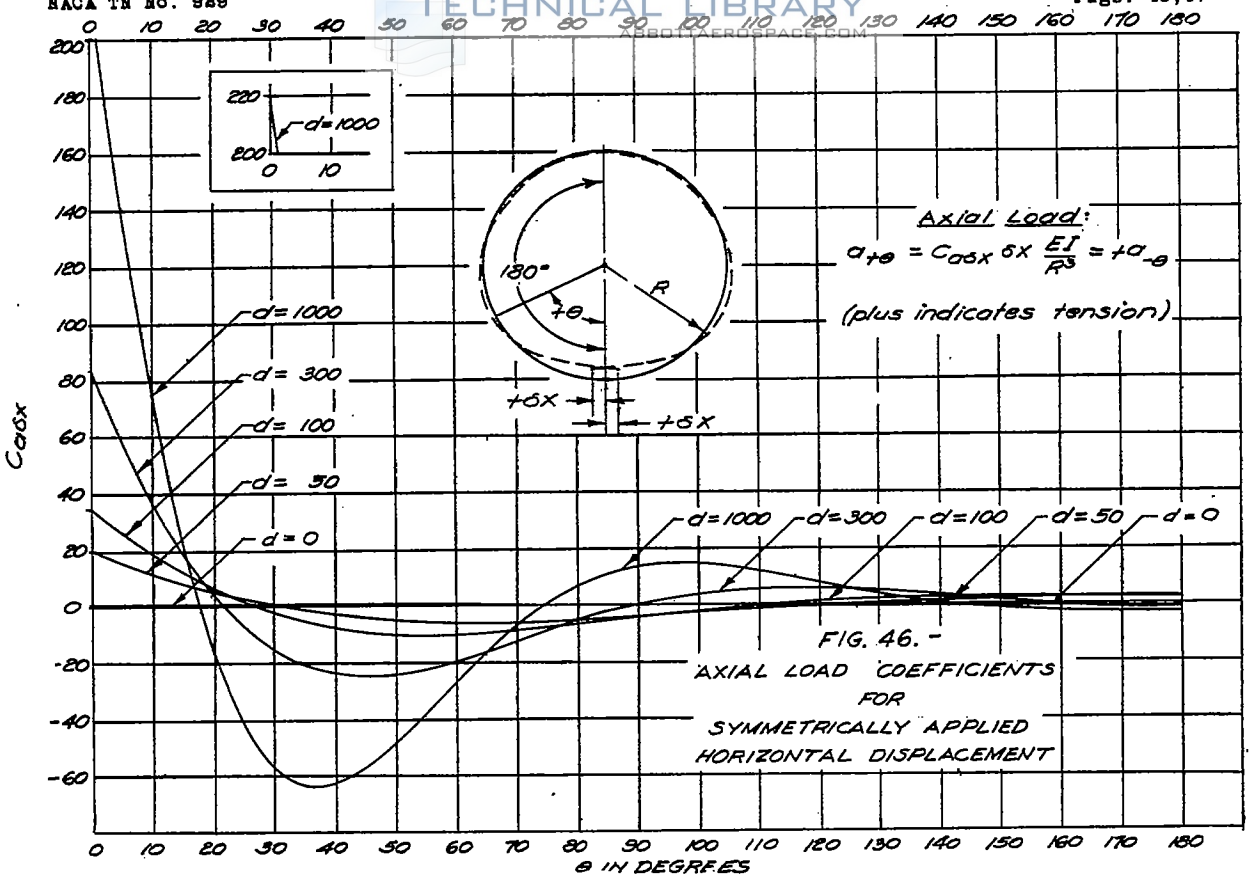

FIG. 46. - AXIAL LOAD COEFFICIENTS FOR SYMMETRICALLY APPLIED HORIZONTAL DISPLACEMENT

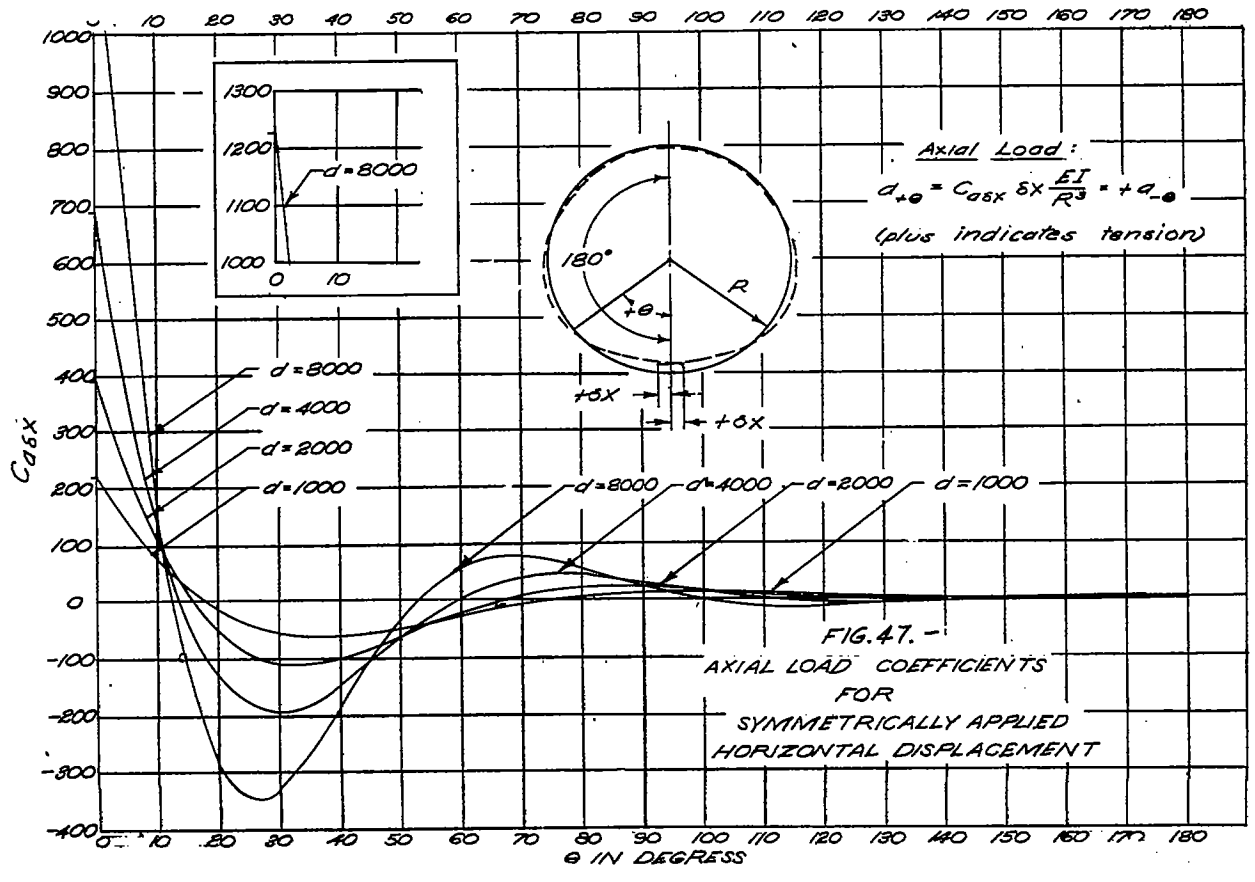

FIG. 47. - AXIAL LOAD COEFFICIENTS FOR SYMMETRICALLY APPLIED HORIZONTAL DISPLACEMENT

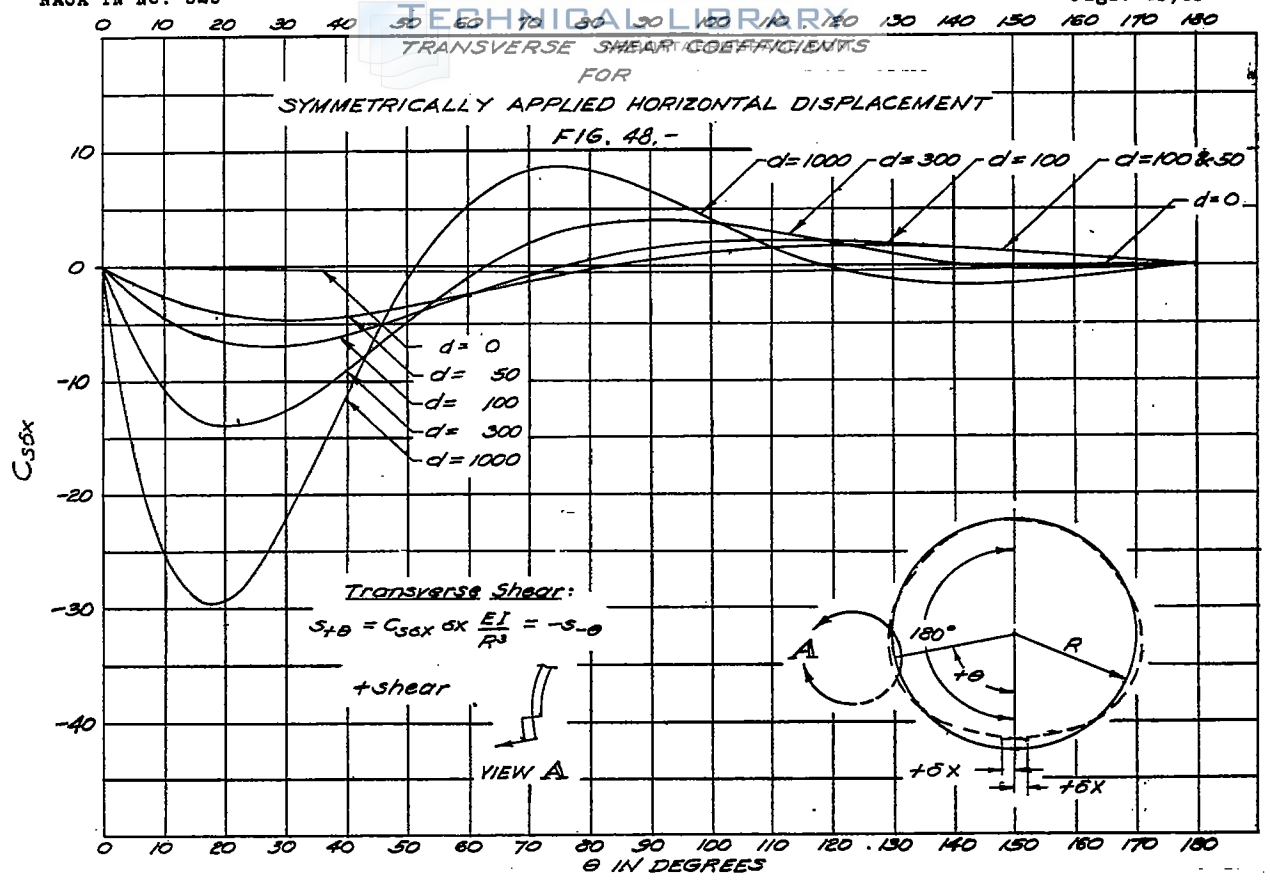

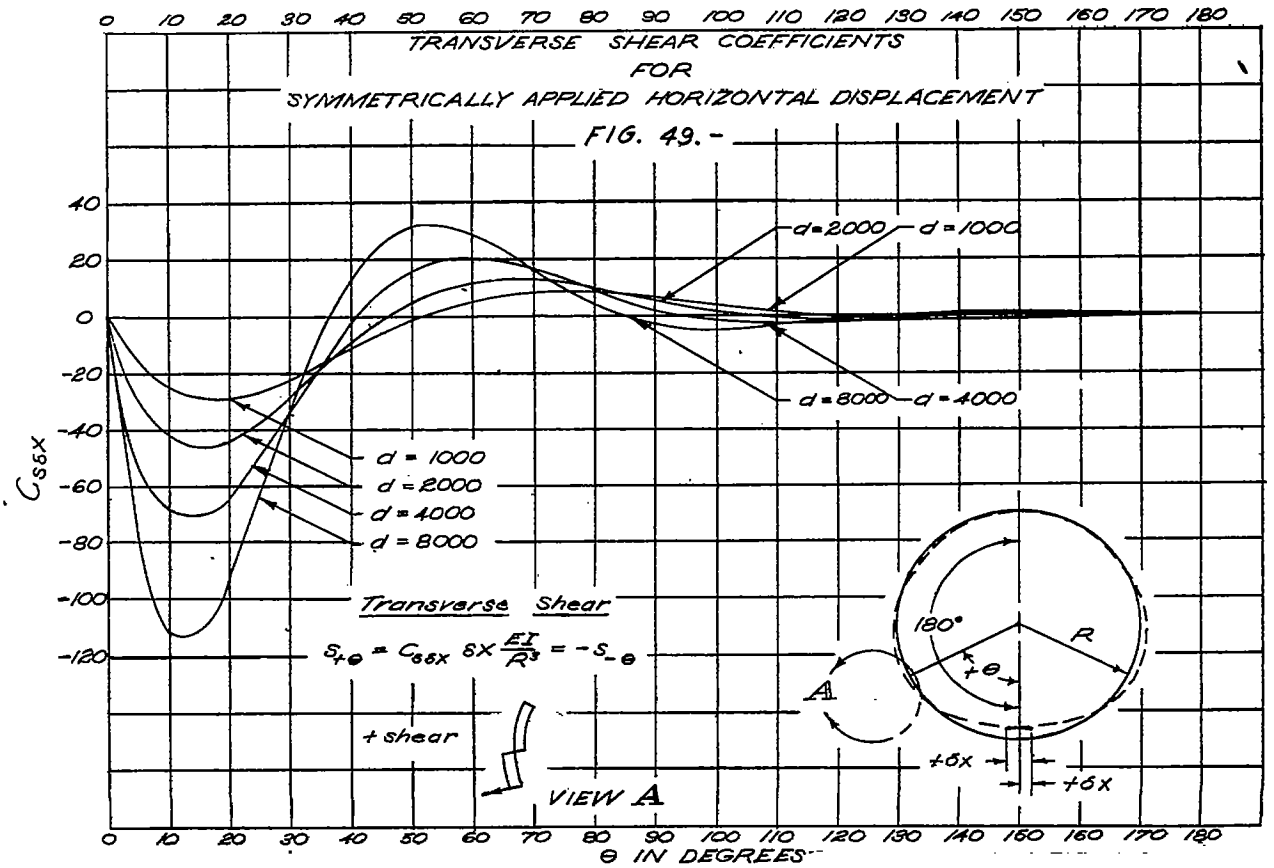

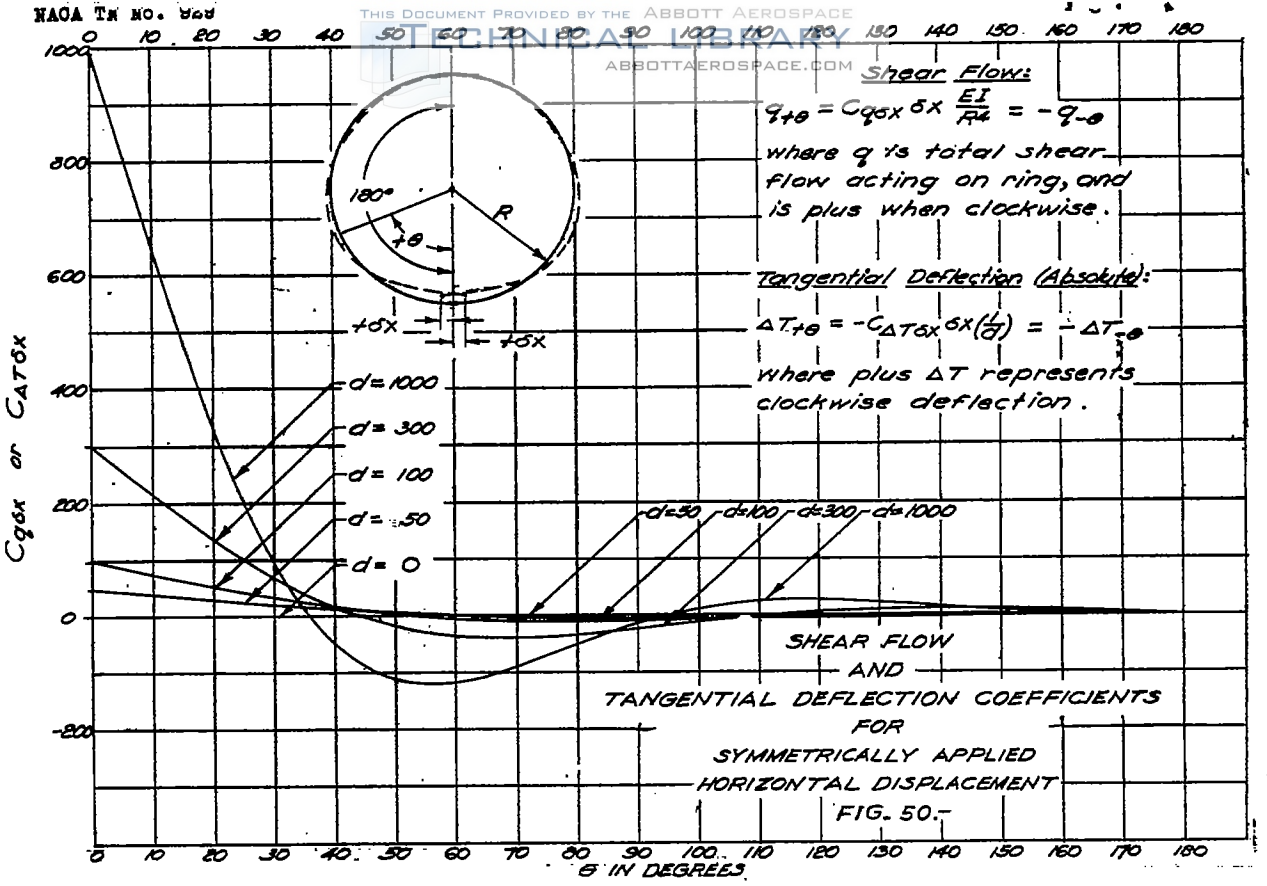

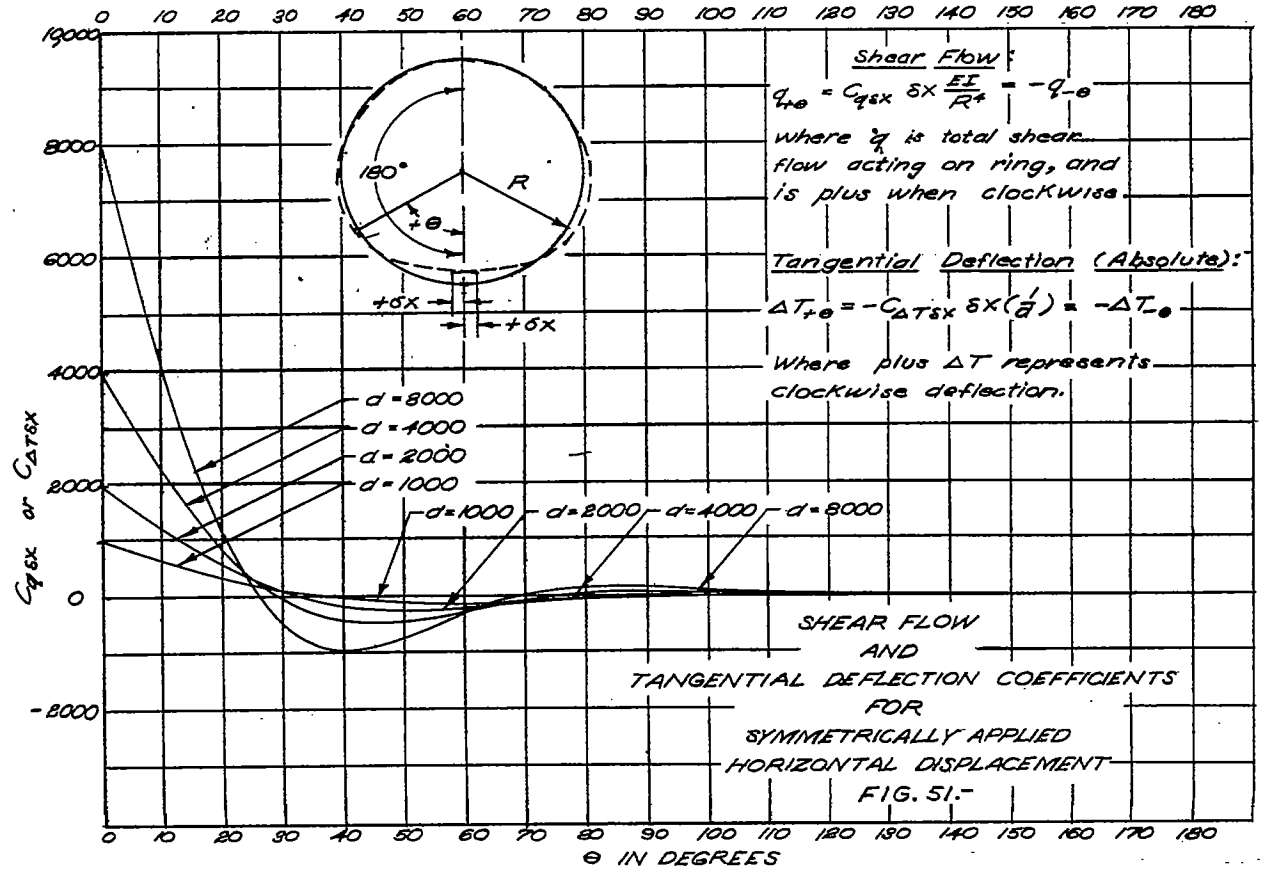

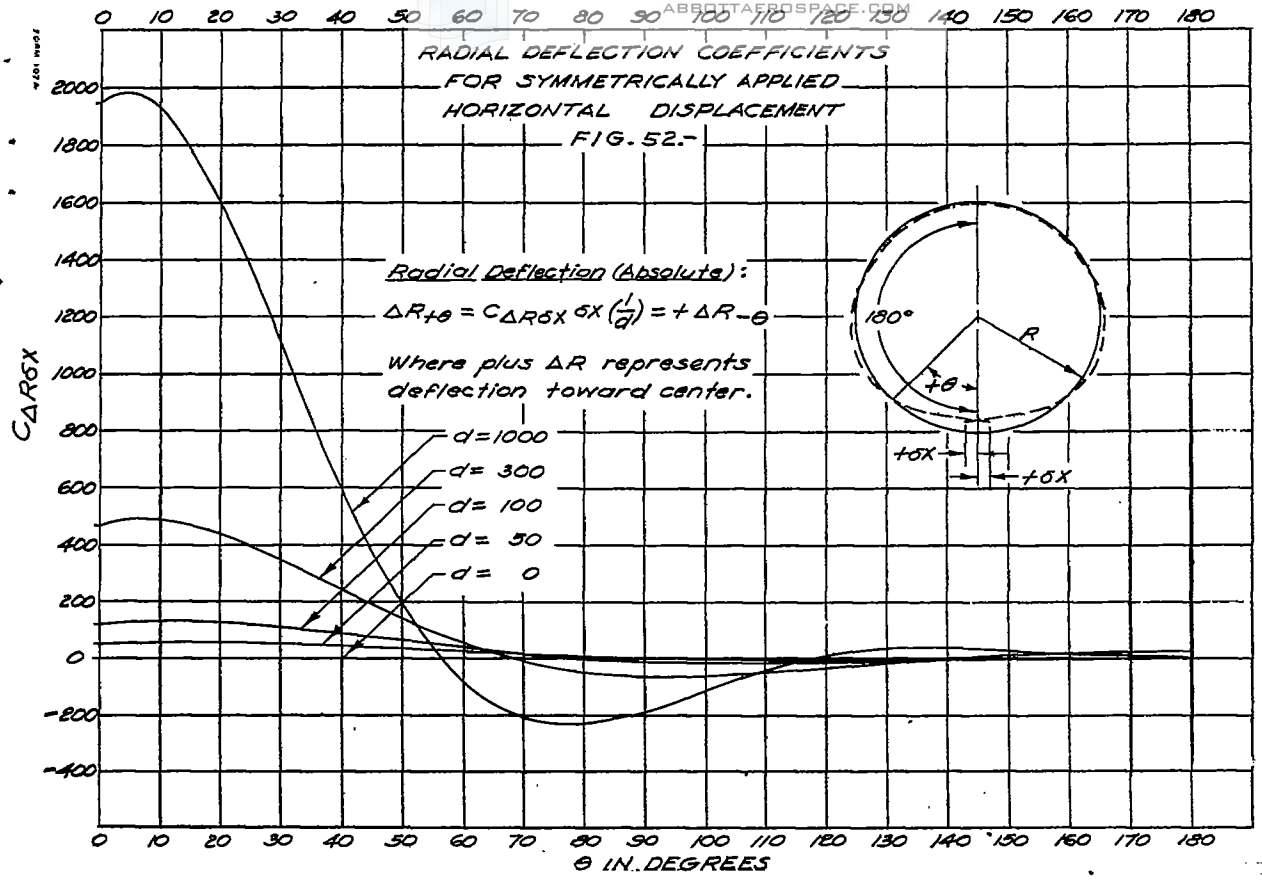

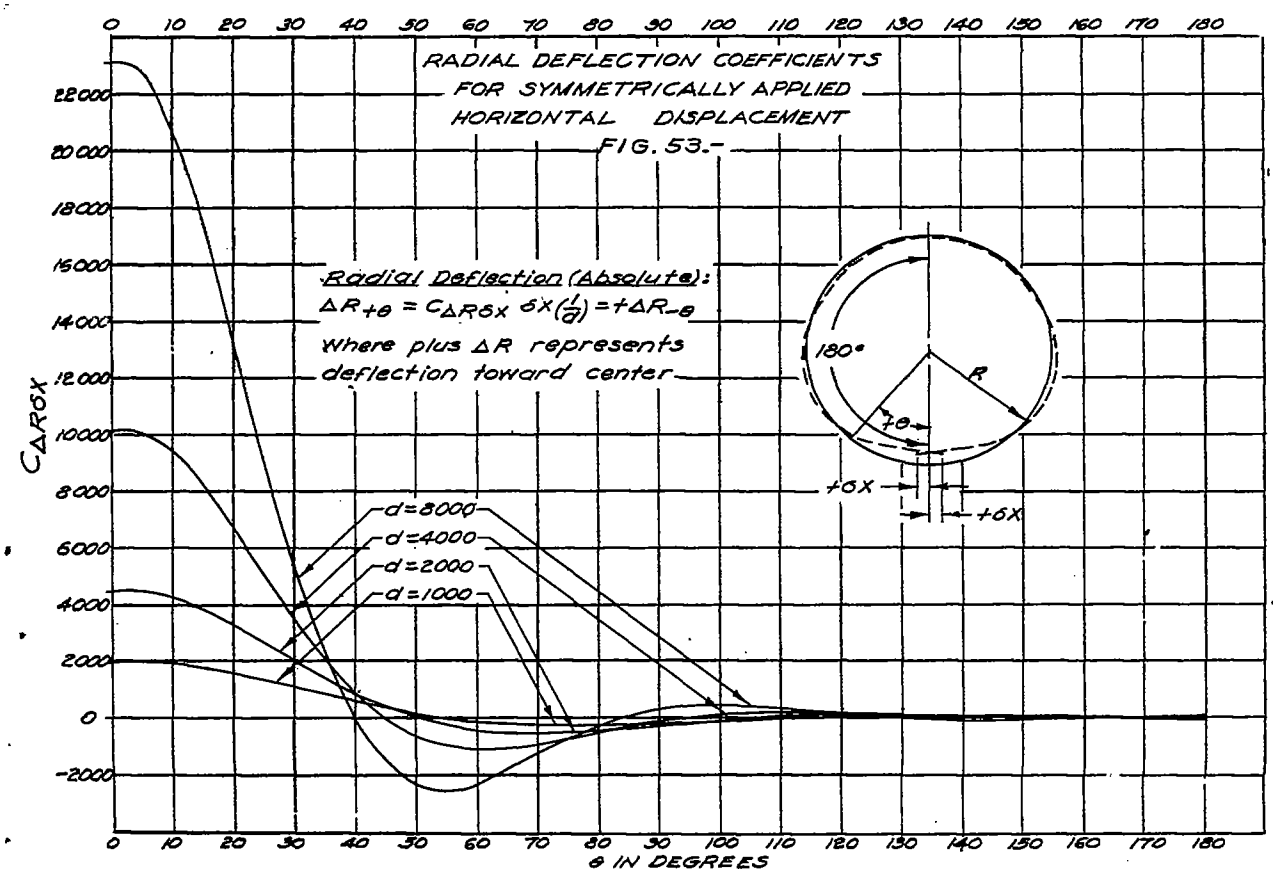

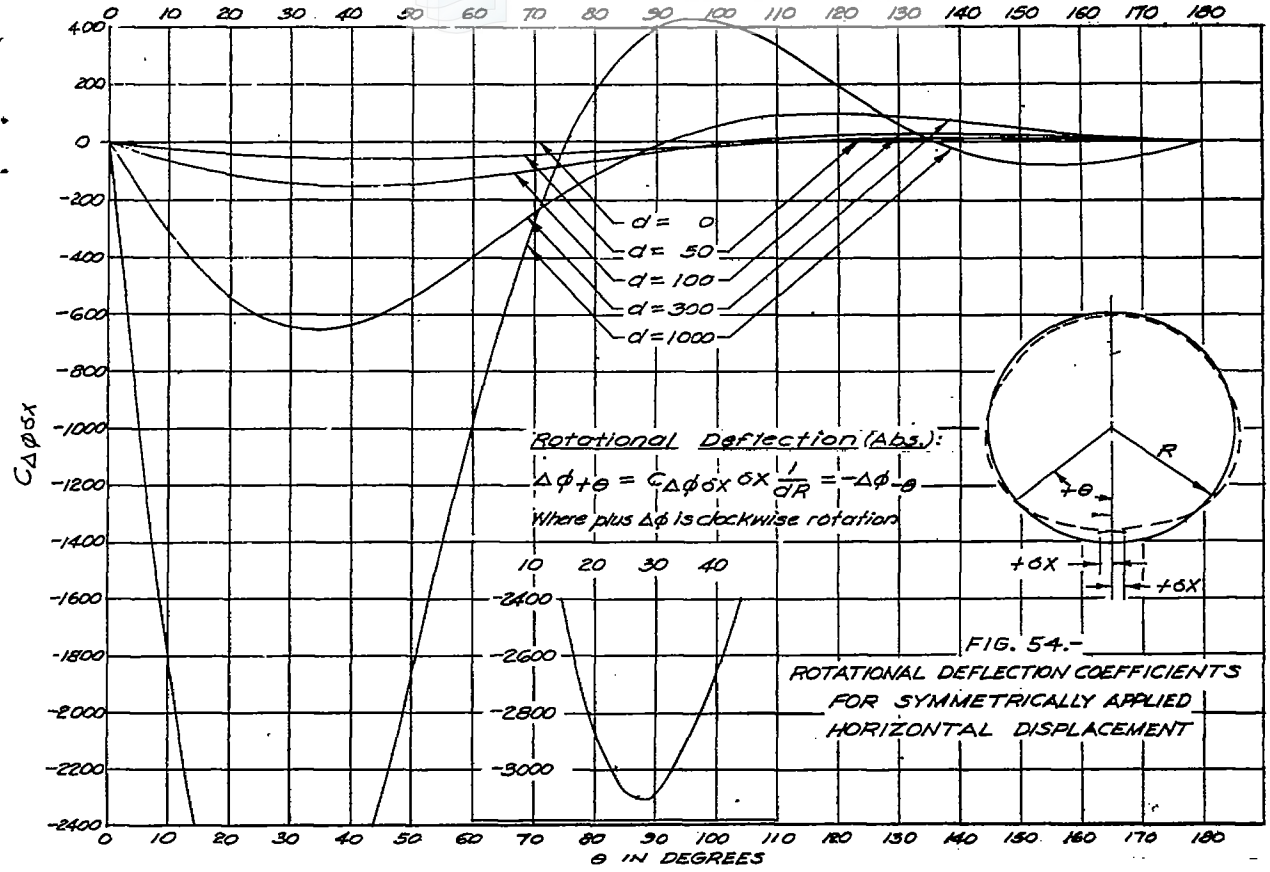

FIG. 54.- ROTATIONAL DEFLECTION COEFFICIENTS FOR SYMMETRICALLY APPLIED HORIZONTAL DISPLACEMENT

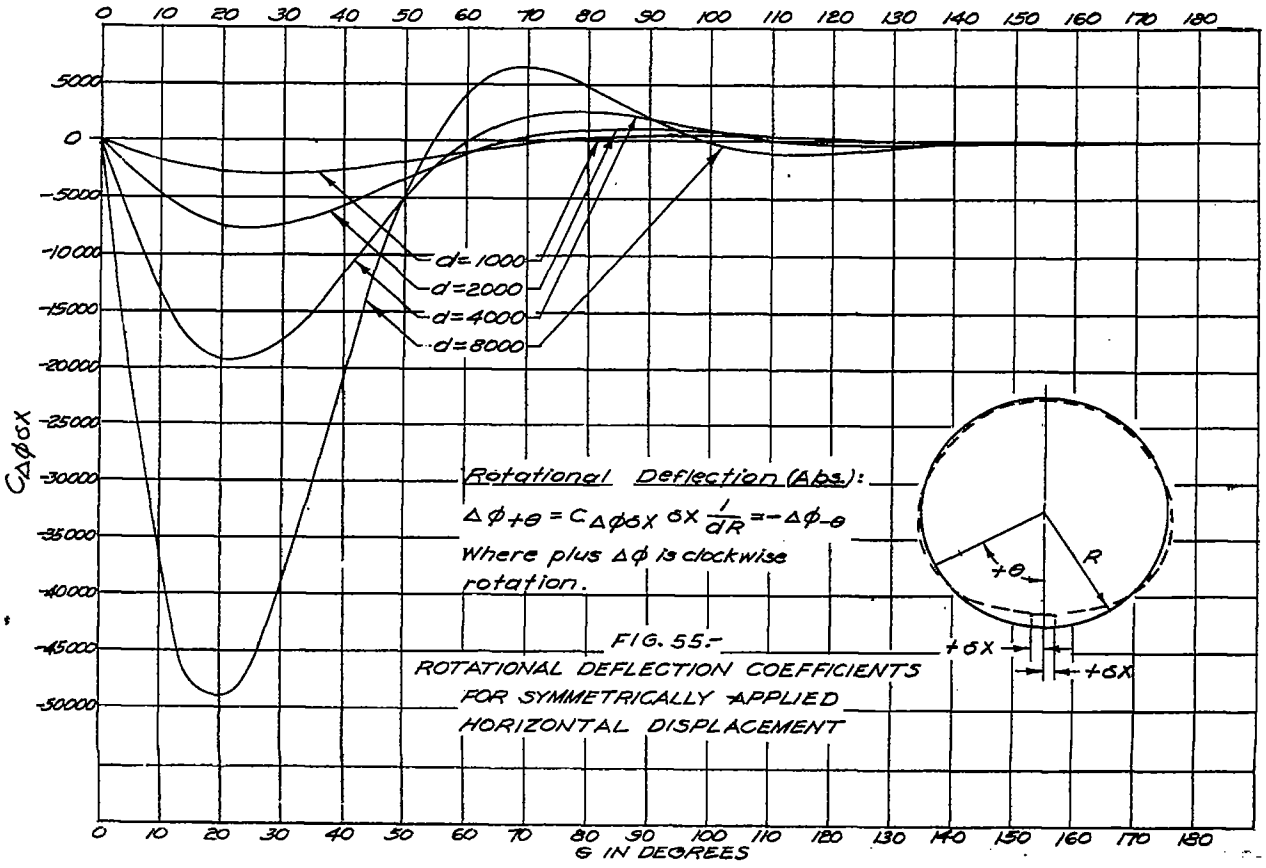

FIG. 55.- ROTATIONAL DEFLECTION COEFFICIENTS FOR SYMMETRICALLY APPLIED HORIZONTAL DISPLACEMENT

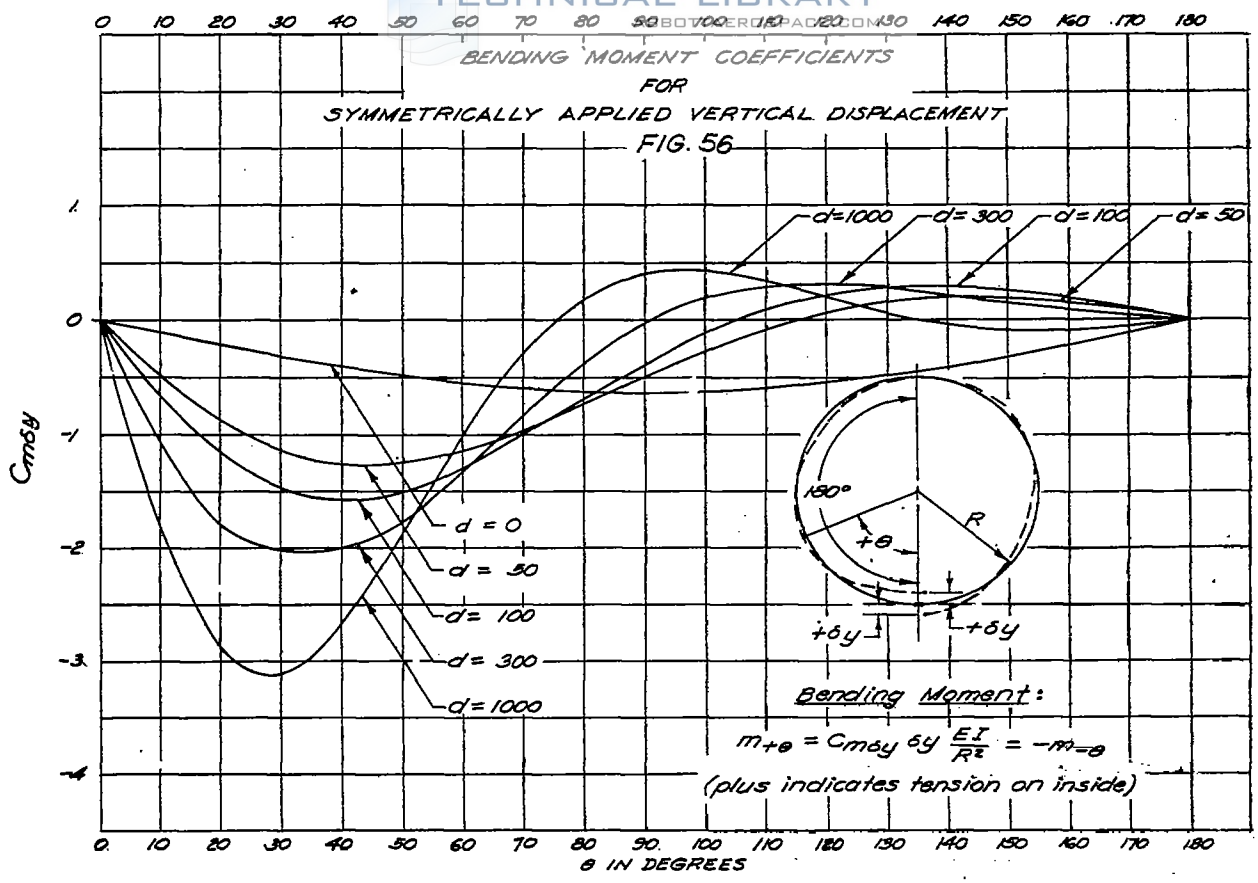

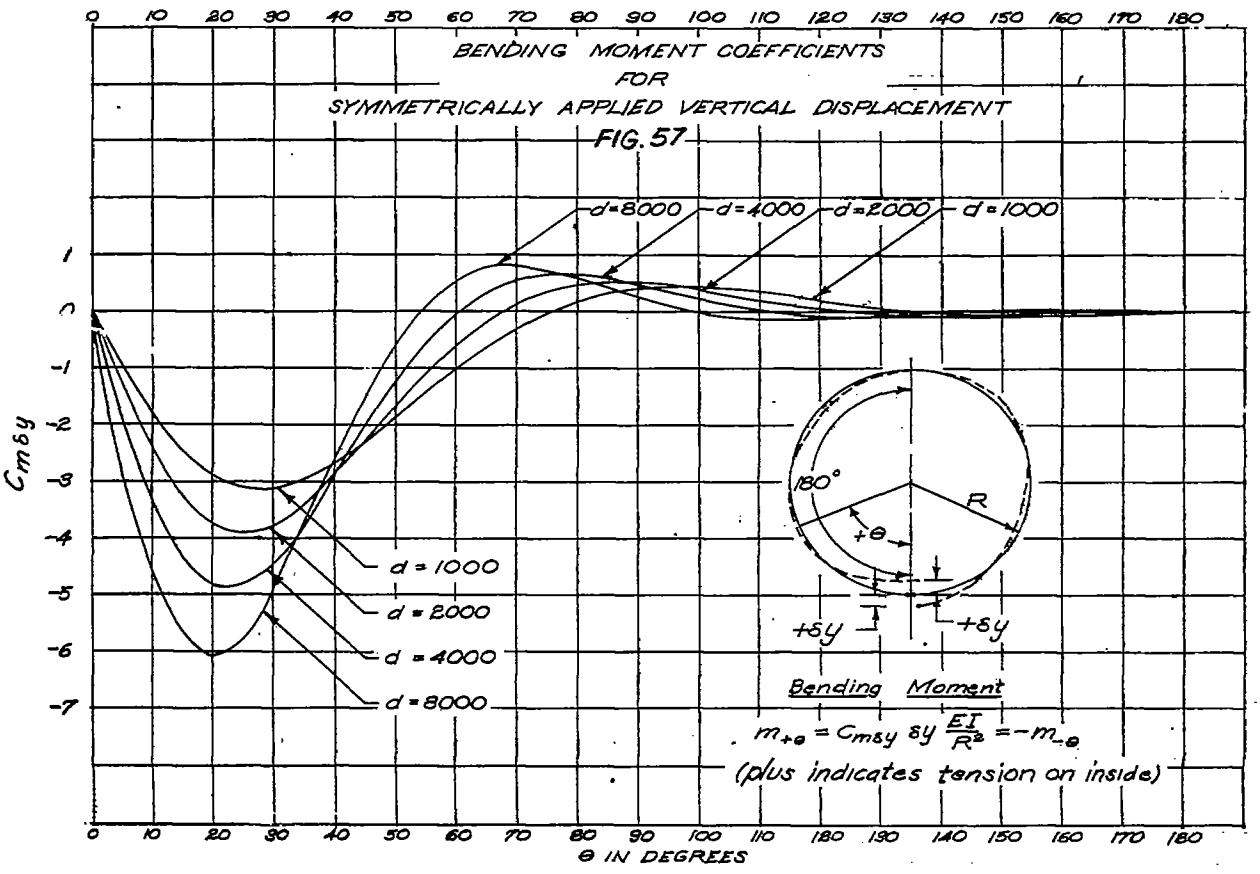

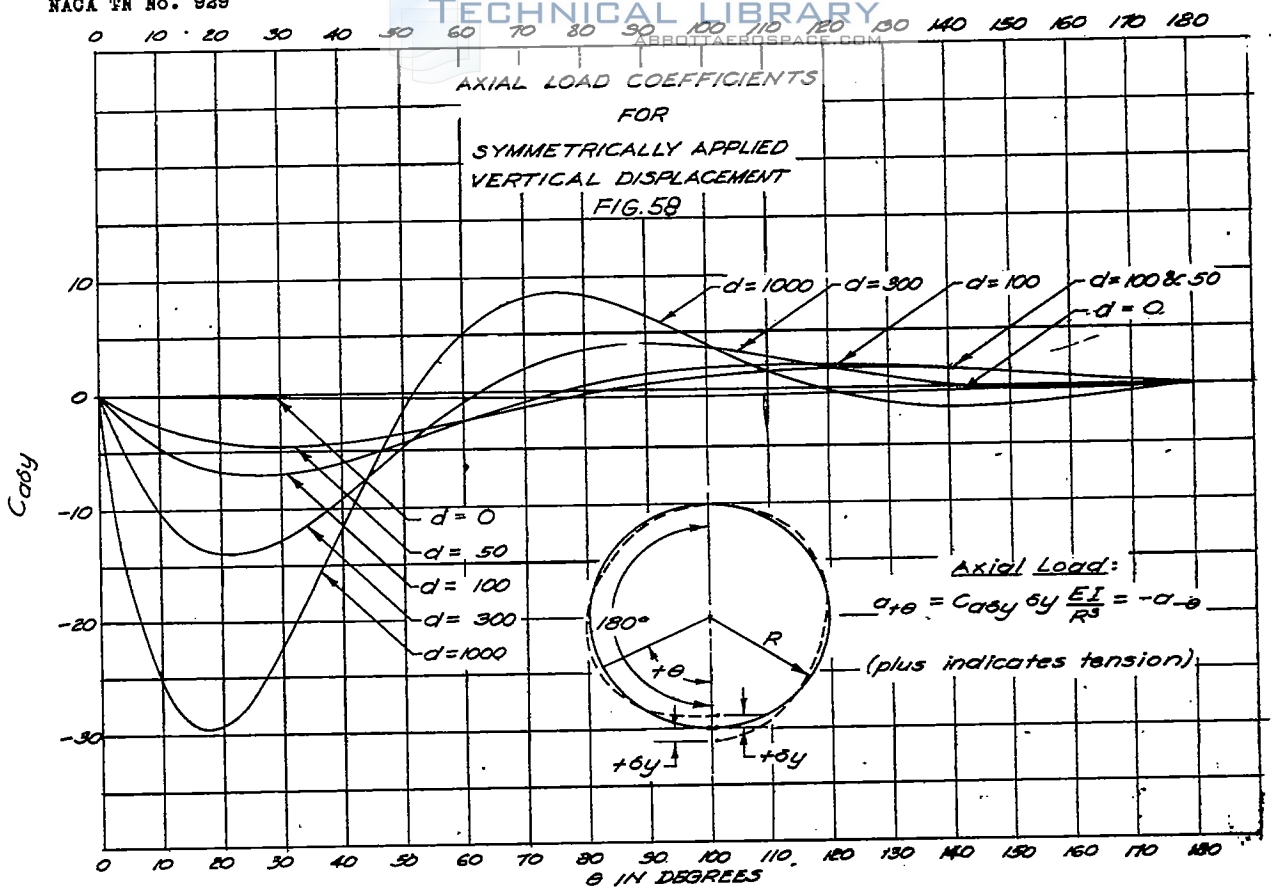

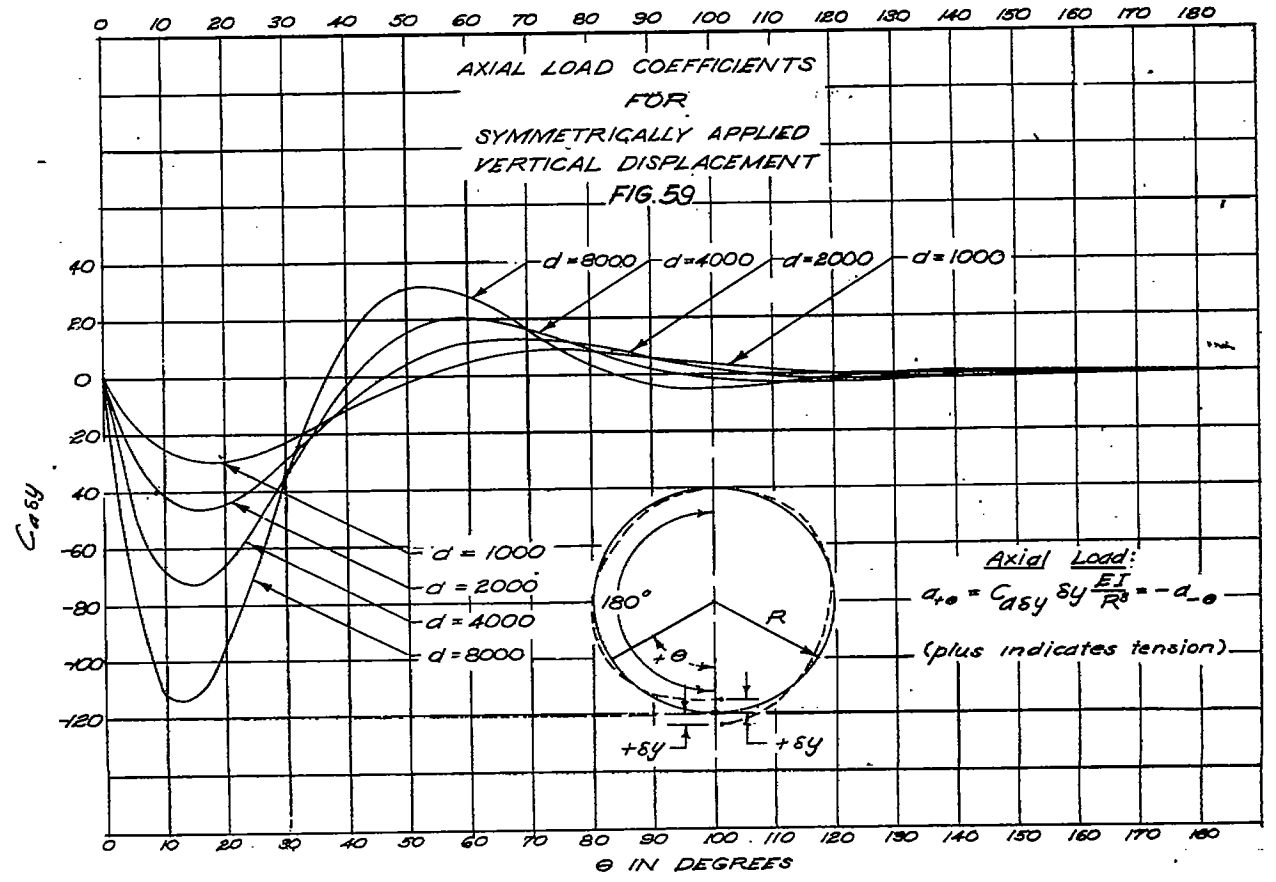

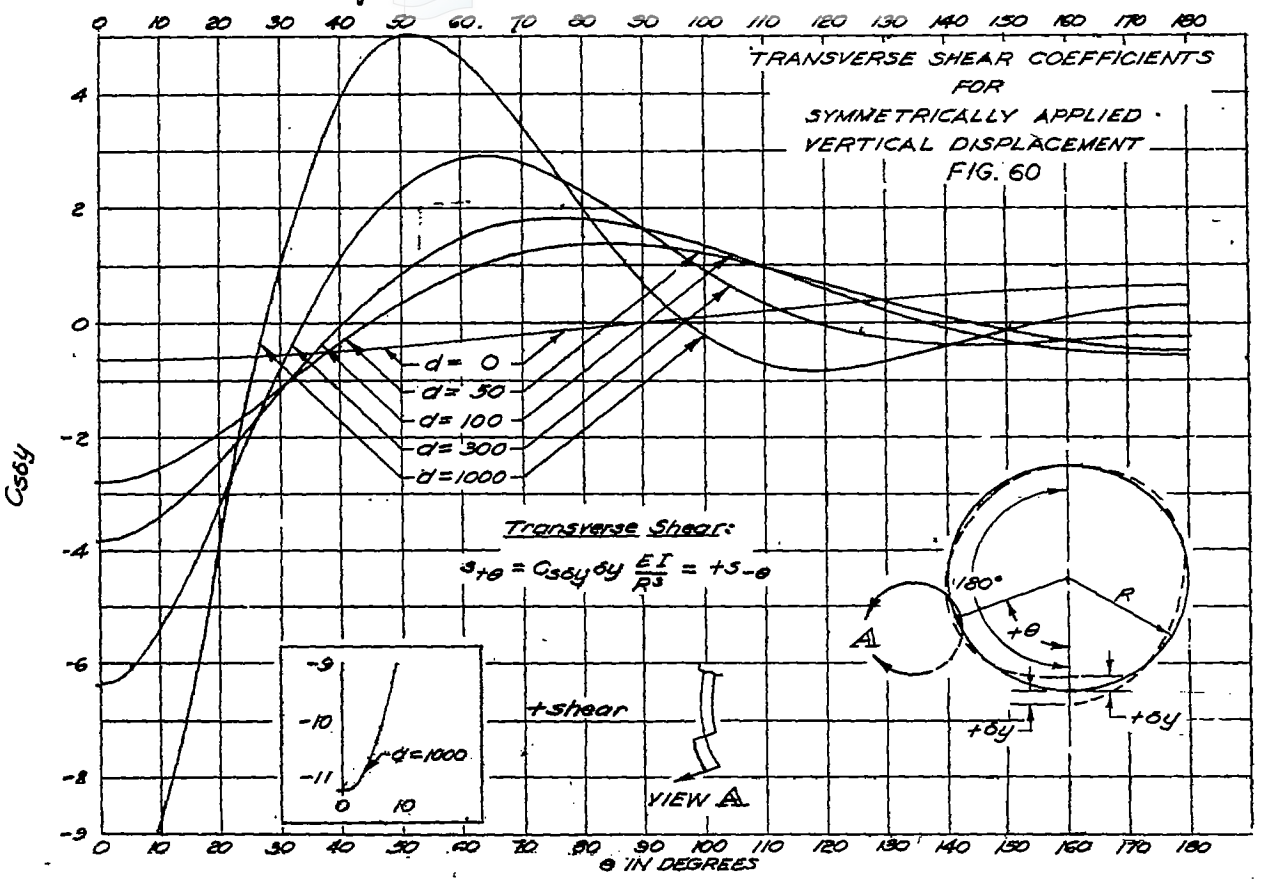

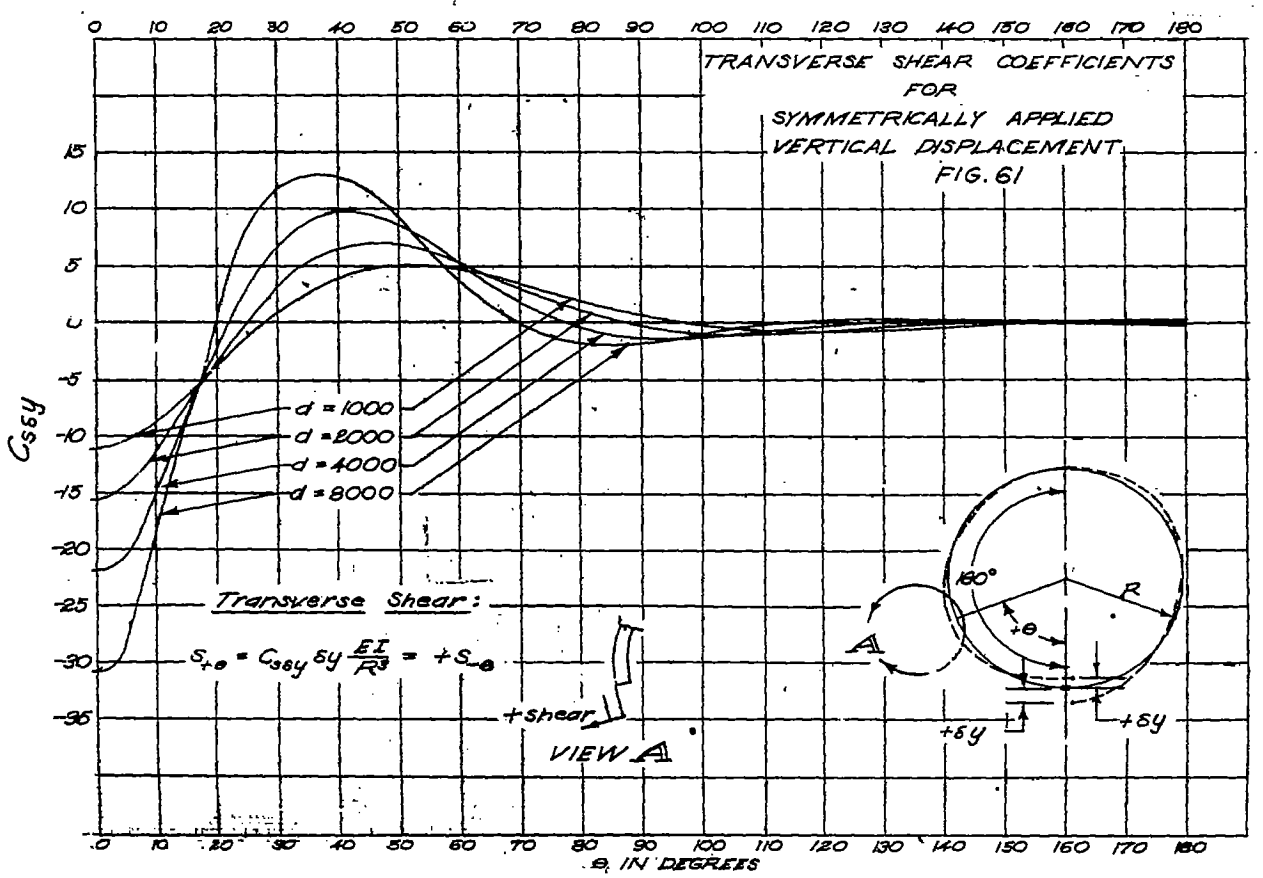

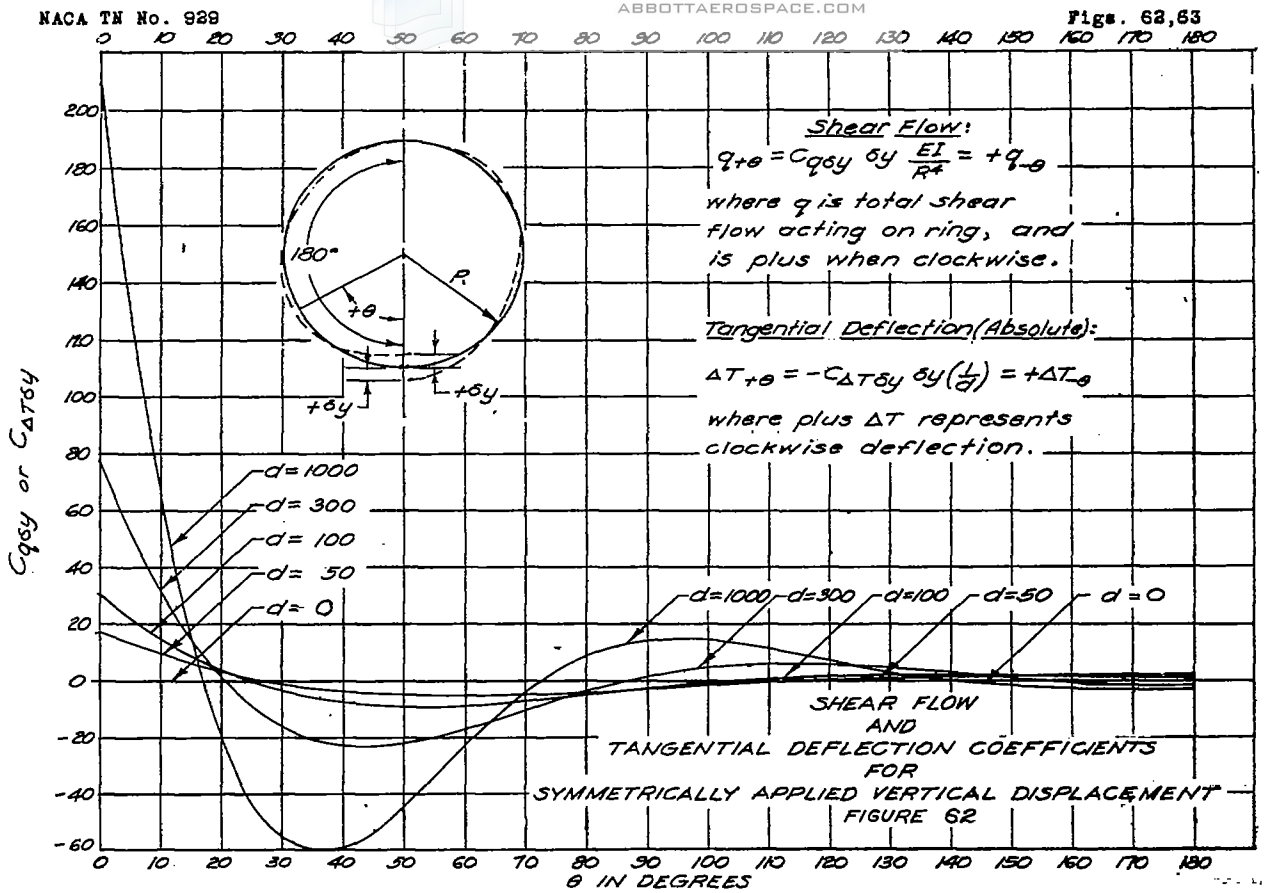

SHEAR FLOW AND TANGENTIAL DEFLECTION COEFFICIENTS FOR SYMMETRICALLY APPLIED VERTICAL DISPLACEMENT
FIGURE 62

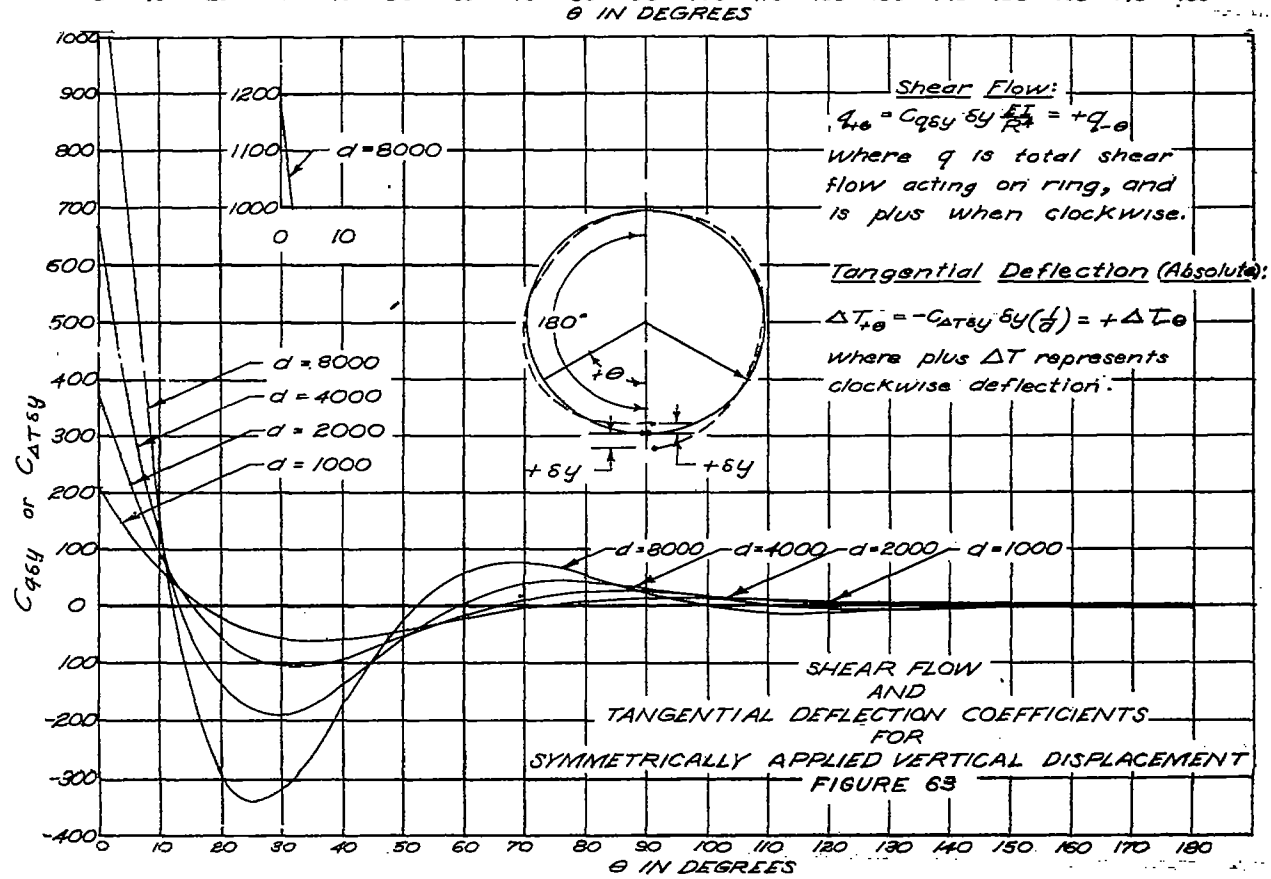

SHEAR FLOW AND TANGENTIAL DEFLECTION COEFFICIENTS FOR SYMMETRICALLY APPLIED VERTICAL DISPLACEMENT
FIGURE 63

RADIAL DEFLECTION COEFFICIENTS
FOR SYMMETRICALLY APPLIED
VERTICAL DISPLACEMENT
FIGURE 64

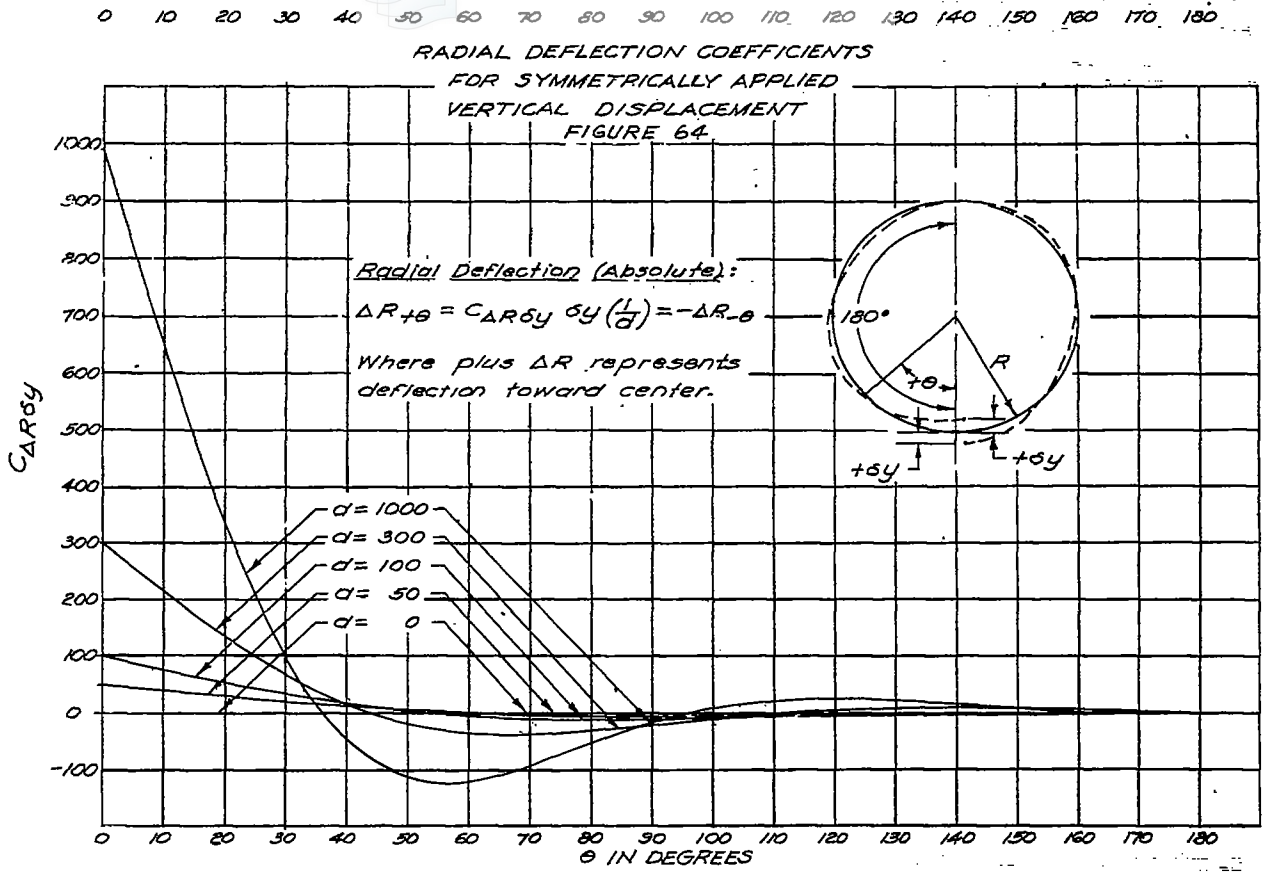

RADIAL DEFLECTION COEFFICIENTS
FOR SYMMETRICALLY APPLIED
VERTICAL DISPLACEMENT
FIGURE 65

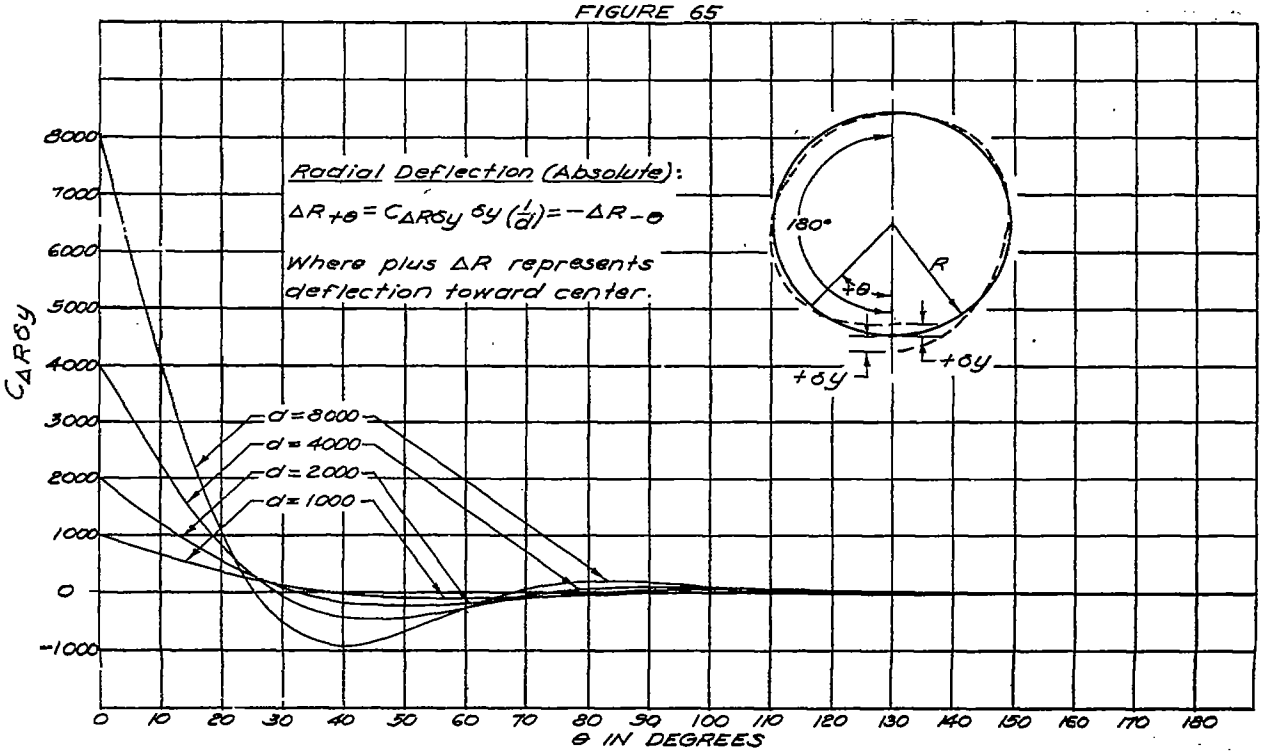

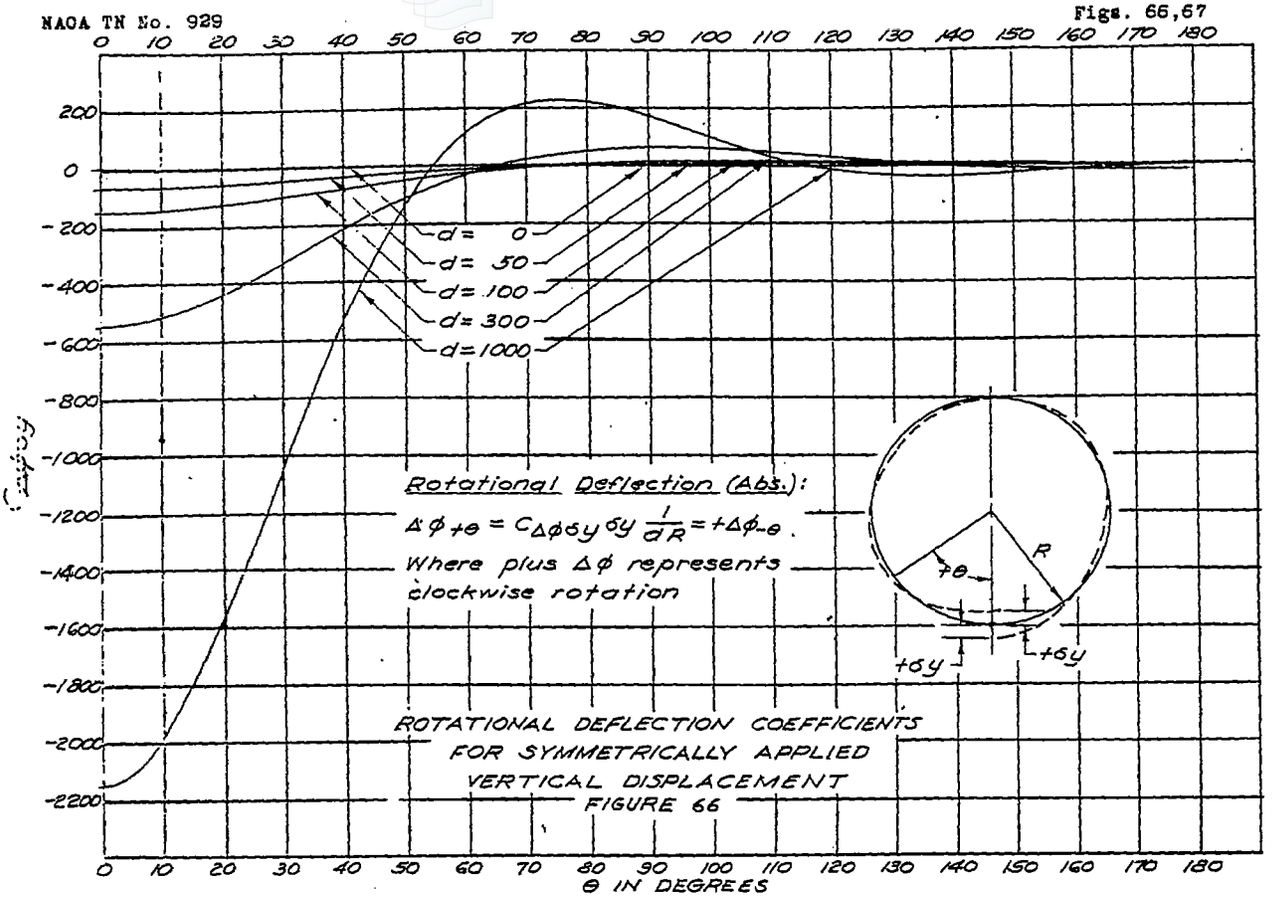

ROTATIONAL DEFLECTION COEFFICIENTS
FOR SYMMETRICALLY APPLIED
VERTICAL DISPLACEMENT
FIGURE 66

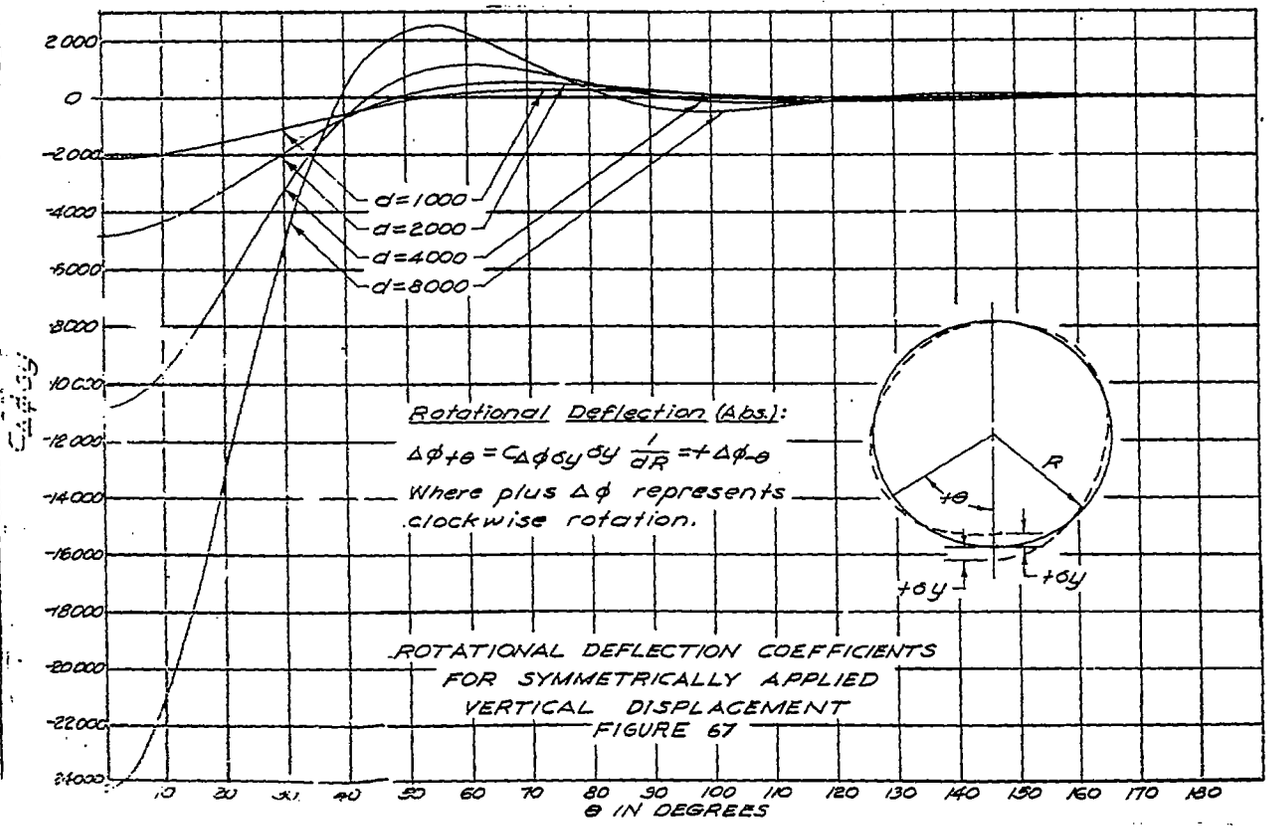

ROTATIONAL DEFLECTION COEFFICIENTS
FOR SYMMETRICALLY APPLIED
VERTICAL DISPLACEMENT
FIGURE 67